

HYDROGEN PRODUCTION FROM SORPTION ENHANCED CHEMICAL LOOPING STEAM  
ETHANOL REFORMING USING CALCIUM OXIDE/ COPPER OXIDE/ NICKEL OXIDE  
MULTIFUNCTIONAL CATALYST



A Thesis Submitted in Partial Fulfillment of the Requirements  
for the Degree of Master of Engineering in Chemical Engineering

Department of Chemical Engineering

Faculty of Engineering

Chulalongkorn University

Academic Year 2018

Copyright of Chulalongkorn University

การผลิตไฮโดรเจนด้วยการปฏิรูปเอทานอลด้วยไอน้ำแบบเคมีคอลลูบปิงที่ส่งเสริมด้วยการดูดซับโดย  
ตัวเร่งปฏิกิริยาหลายหน้าที่แคลเซียมออกไซด์/คอปเปอร์ออกไซด์/นิกเกิลออกไซด์



วิทยานิพนธ์นี้เป็นส่วนหนึ่งของการศึกษาตามหลักสูตรปริญญาวิศวกรรมศาสตรมหาบัณฑิต  
สาขาวิชาวิศวกรรมเคมี ภาควิชาวิศวกรรมเคมี  
คณะวิศวกรรมศาสตร์ จุฬาลงกรณ์มหาวิทยาลัย  
ปีการศึกษา 2561  
ลิขสิทธิ์ของจุฬาลงกรณ์มหาวิทยาลัย



ชลิตา นิมมาศ : การผลิตไฮโดรเจนด้วยการปฏิรูปเอทานอลด้วยไอน้ำแบบเคมีคอลลูปปีงที่ส่งเสริม  
ด้วยการดูดซับโดยตัวเร่งปฏิกิริยาหลายหน้าที่แคลเซียมออกไซด์/คอปเปอร์ออกไซด์/นิกเกิลออกไซด์.  
( HYDROGEN PRODUCTION FROM SORPTION ENHANCED CHEMICAL LOOPING STEAM  
ETHANOL REFORMING USING CALCIUM OXIDE/ COPPER OXIDE/ NICKEL OXIDE  
MULTIFUNCTIONAL CATALYST) อ.ที่ปรึกษาหลัก : ศ. ดร.สุทธิชัย อัสสะบํารุงรัตน์, อ.ที่ปรึกษา  
ร่วม : ผศ. ดร.สุวิมล วงศ์สกุลเกษัช

ตัวเร่งปฏิกิริยาหลายหน้าที่ถูกนำมาประยุกต์ใช้ในกระบวนการดูดซับเพื่อผลิตแก๊สไฮโดรเจน  
แคลเซียมอะซิเตท แคลเซียมคลอไรด์ ได้นำมาทดสอบสำหรับใช้เป็นสารตั้งต้นแคลเซียม ส่วนโซเดียมคาร์บอเนต  
ยูเรีย เป็นสารตั้งต้นของคาร์บอเนต โดยตัวเร่งปฏิกิริยาหลายหน้าที่ใช้ตัวดูดซับที่เตรียมจากแคลเซียมอะซิเตท  
และยูเรียแสดงความสามารถในการดูดซับคาร์บอนไดออกไซด์นานที่สุด (60 นาที) และให้ความบริสุทธิ์ของ  
ไฮโดรเจนร้อยละ 88 ที่อัตราส่วนเอทานอลต่อไอน้ำเท่ากับ 4 อุณหภูมิ 600 องศาเซลเซียส นอกจากนี้ความ  
เสถียรของตัวเร่งปฏิกิริยาหลายหน้าที่ ( $\text{NiO}/\text{CaO}_{\text{Ac-Urea}}\text{-Ca}_{12}\text{Al}_{14}\text{O}_{33}$ ) ถูกทดสอบ 10 รอบ พบว่ามีความเสถียร  
ตลอดการทดสอบ จากการศึกษาเปรียบเทียบวิธีการสังเคราะห์ของตัวเร่งปฏิกิริยาหลายหน้าที่ตัวเร่งปฏิกิริยาที่เตรียม  
ด้วยวิธีโซลเมิกซ์กับวิธีโซลเจลพบว่าตัวเร่งปฏิกิริยาที่เตรียมด้วยวิธีโซลเจลสามารถผลิตไฮโดรเจน (ร้อยละ 91) ได้  
สูงกว่าตัวเร่งปฏิกิริยาที่เตรียมด้วยวิธีโซลเมิกซ์ (ร้อยละ 88) การเติมโลหะคอปเปอร์ลงบนตัวเร่งปฏิกิริยาหลาย  
หน้าที่ด้วยวิธีโซลเจลที่แตกต่างกันด้วยรายละเอียดเทคนิคการสังเคราะห์ถูกนำมาประยุกต์ใช้ในกระบวนการดูด  
ซับเพื่อส่งเสริมการปฏิรูปแบบเคมีคอลลูปปีงของเอทานอลเพื่อผลิตแก๊สไฮโดรเจน โดยตัวเร่งปฏิกิริยาหลาย  
หน้าที่ที่เติมโลหะนิกเกิลในขั้นตอนเดียว (Ni-Cu-CA) สามารถผลิตไฮโดรเจนได้ความบริสุทธิ์สูงที่สุดร้อยละ 91  
ตัวเร่งปฏิกิริยาหลายหน้าที่ที่ทำการเติมโลหะคอปเปอร์ภายหลังด้วยวิธีจุ่มชุบ (Cu/(Ni-CA)) สามารถผลิต  
ไฮโดรเจนได้ความบริสุทธิ์ร้อยละ 89 และตัวเร่งปฏิกิริยาทำการเติมโลหะนิกเกิลภายหลังด้วยวิธีจุ่มชุบ(Ni/(Cu -  
CA)) สามารถผลิตไฮโดรเจนได้ความบริสุทธิ์สูงที่สุดร้อยละ 83 ที่อัตราส่วนเอทานอลต่อไอน้ำเท่ากับ 3 อุณหภูมิ  
500 องศาเซลเซียส ความดันบรรยากาศ ตัวเร่งปฏิกิริยาหลายหน้าที่ (Cu/(Ni-CA)) สามารถผลิตไฮโดรเจนได้คงที่  
ร้อยละ 88 เป็นจำนวน 5 รอบ ในขณะที่ตัวเร่งปฏิกิริยา Ni-Cu-CA ลดลงจากร้อยละ 93% ในรอบที่ 1 เหลือร้อย  
ละ 86% ในรอบที่ 5

สาขาวิชา วิศวกรรมเคมี  
ปีการศึกษา 2561

ลายมือชื่อนิสิต .....  
ลายมือชื่อ อ.ที่ปรึกษาหลัก .....  
ลายมือชื่อ อ.ที่ปรึกษาร่วม .....

# # 5970195421 : MAJOR CHEMICAL ENGINEERING

KEYWORD: HYDROGEN PRODUCTION, SORPTION-ENHANCED CHEMICAL LOOPING ETHANOL  
STEAM REFORMING, CAO, NIO, CUO, CARBON DIOXIDE ADSORPTION CAPACITY

Talita Nimmas :

HYDROGEN PRODUCTION FROM SORPTION ENHANCED CHEMICAL LOOPING STEAM  
ETHANOL REFORMING USING CALCIUM OXIDE/ COPPER OXIDE/ NICKEL OXIDE

MULTIFUNCTIONAL CATALYST. Advisor: Prof. SUTTICHA ASSABUMRUNGRAT, Ph.D. Co-  
advisor: Asst. Prof. Suwimol Wongsakulphasatch, Ph.D.

Multifunctional catalyst was developed for hydrogen production via sorption enhanced chemical looping ethanol steam reforming. Calcium acetate ( $\text{Ca}_2\text{Ac}$ ) and calcium chloride ( $\text{CaCl}$ ) were used as calcium precursor. Sodium carbonate ( $\text{Na}_2\text{CO}_3$ ) and urea ( $\text{CO}(\text{NH}_2)_2$ ) were used as carbonate precursor. The  $\text{NiO}/\text{CaO}_{\text{Ac-Urea}}-\text{Ca}_{12}\text{Al}_{14}\text{O}_{33}$  showed the longest pre-breakthrough period of 60 min and 88% of hydrogen purity at steam to ethanol molar ratio (S/E) of 4:1, temperature  $600^\circ\text{C}$ . Stability of  $\text{NiO}/\text{CaO}_{\text{Ac-Urea}}-\text{Ca}_{12}\text{Al}_{14}\text{O}_{33}$  was tested over 10 cycles and the results showed hydrogen purity can be maintained at 90% during pre-breakthrough period. The effect of synthesis method: sol-mixing and sol-gel, on hydrogen production was compared and the result found that sol-gel method produced hydrogen purity (91%) higher than sol-mixing method (88%). The copper addition into multifunctional catalyst by sol-gel method was studied with different strategies. The preparation method in one-pot synthesis Ni-Cu-CA offered the highest hydrogen purity ca. 93% for 60 min, while, the impregnation synthesis of Cu into Ni-CA (Cu/(Ni-CA)) produced hydrogen purity ca. 89%, and Ni/(Cu-CA) showed hydrogen purity ca. 83%. The stability of Cu/(Ni-CA) can be maintained at ca. 88%, whereas Ni-Cu-CA slightly decreased from 93% to 87% after 5 cycles.

Field of Study: Chemical Engineering

Student's Signature .....

Academic Year: 2018

Advisor's Signature .....

Co-advisor's Signature .....

## ACKNOWLEDGEMENTS

I really appreciate and would like to express my sincere thanks to my thesis advisor, Professor Suttichai Assabumrungrat and my co-advisor, Assistant Professor Suwimol wongsakulphasatch for their guidances and suggestions that are useful to this thesis. I would like to thank the joint project “The National Research Council of Thailand (NRCT) and The National Natural Science Foundation of China (NSFC)”, National Science and Technology Development Agency (NSTDA) and Chulalongkorn University for financial support and I would also be grateful to Associate Professor Kasidit Nootong as the chairman, Dr. Rungthiwa Methaapanon and Assistant Professor Worapon Kiatkittipongas as the members of the thesis committee, for their useful comments and suggestions. In addition, I am grateful to the scientists, my seniors, my friend, who are the members of Center of excellence on catalysis and catalytic reaction engineering, Chulalongkorn University and Research Center of Catalysis, for assistance, guideline and others. Especially, I would like to give my special thanks to Suwimol Wongsakulphasatch who always suggests everything which is beneficial throughout this thesis. Finally, I most gratefully acknowledge my parents for consistent support and encourage me throughout the period of this research.

จุฬาลงกรณ์มหาวิทยาลัย  
CHULALONGKORN UNIVERSITY

Talita Nimmas

## TABLE OF CONTENTS

	Page
ABSTRACT (THAI).....	iii
ABSTRACT (ENGLISH).....	iv
ACKNOWLEDGEMENTS .....	v
TABLE OF CONTENTS .....	vi
CHAPTER I.....	7
INTRODUCTION.....	7
1.1 Rationale.....	7
1.2 Objective.....	8
1.3 Scope of work.....	8
CHAPTER 2.....	11
THEORY.....	11
2.1 Hydrogen production process.....	11
2.1.1 Electrochemical process.....	12
2.1.2 Biological process.....	13
2.1.3 Thermochemical process.....	15
2.1.3.1 Partial oxidation.....	15
2.1.3.2 Steam reforming.....	15
2.1.3.3 Autothermal reforming.....	16
2.2 Hydrocarbon feedstock.....	16
2.2.1 Bioethanol.....	16
2.3 Ethanol steam reforming process (ESR).....	18

2.4 Sorption enhanced ethanol steam reforming (SER).....	22
2.5 Sorption enhanced chemical looping ethanol steam reforming (SECLSR) .....	22
2.6 Properties of materials involved hydrogen production process .....	24
2.6.1 Hydrogen (H <sub>2</sub> ).....	24
2.6.2 Carbon dioxide (CO <sub>2</sub> ).....	25
2.6.3 Carbon monoxide (CO).....	26
2.6.4 Methane (CH <sub>4</sub> ).....	27
2.6.5 Calcium oxide (CaO).....	27
2.6.6 Aluminum oxide (Al <sub>2</sub> O <sub>3</sub> ).....	29
2.6.7 Calcium aluminate cements (Ca <sub>12</sub> Al <sub>14</sub> O <sub>33</sub> ).....	29
CHAPTER 3.....	31
LITERATURE REVIEW .....	31
3.1 Catalyst.....	31
3.2 Sorbent.....	34
3.3 Multifunctional material .....	37
3.4 Oxygen carrier (metal oxide).....	41
CHAPTER 4.....	45
EXPERIMENTAL .....	45
4.1 Material.....	45
4.2 Multifunctional material preparation .....	45
4.3 Characterization of material.....	48
4.3.1 X-ray diffraction technique .....	48
4.3.2 N <sub>2</sub> adsorption/desorption isotherm .....	49
4.3.3 Scanning electron microscope.....	49



4.3.4 Thermogravimetric Analysis (TGA) .....	50
4.4 Hydrogen production .....	51
4.5 The single cycle for sorption enhanced steam ethanol reforming chemical looping .....	52
CHAPTER 5.....	54
RESULTS AND DISCUSSION.....	54
5.1 Influence of calcium oxide precursor on hydrogen production from sorption enhanced ethanol steam reforming .....	54
5.1.1 Characteristic of multifunctional material .....	54
5.1.2 Effect of CaO precursors on hydrogen production via sorption enhanced ethanol steam reforming. ....	60
5.1.3 Stability test of multifunctional catalysts.....	65
5.2 Effect of multifunctional material preparation method on sorption enhanced ethanol steam reforming.....	67
5.2.1 Characterization .....	67
5.2.2 Hydrogen production .....	70
5.2.3 Coke deposition in catalyst .....	72
5.3 The effect of copper addition and preparation method of multifunctional material on hydrogen production from sorption enhanced steam reforming chemical looping process .....	73
5.3.1 Characterization .....	73
5.3.2 Hydrogen production .....	79
5.3.3 Single cycle for sorption enhanced chemical looping ethanol steam reforming process.....	86
5.3.5 Stability of multifunctional catalyst.....	89
CHAPTER 6.....	94

CONCLUSION AND RECOMMENDATIONS.....	94
6.1 Conclusion.....	94
6.2 Recommendations.....	95
REFERENCES.....	96
APPENDIX A.....	104
APPENDIX B.....	105
APPENDIX C.....	106
VITA.....	112



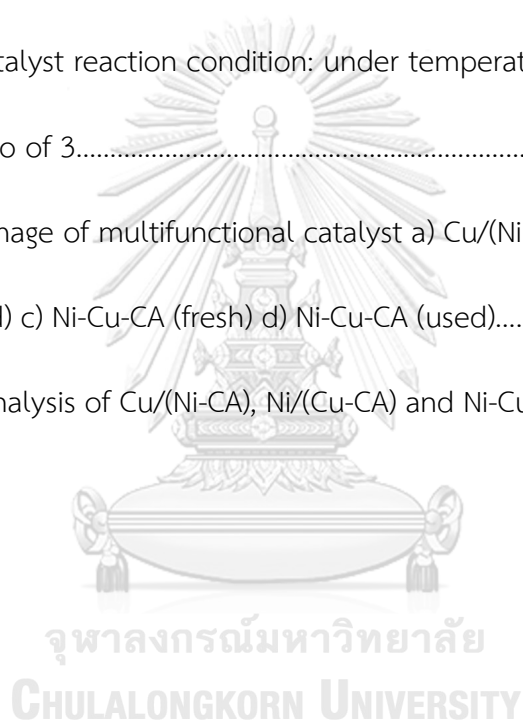
## Figures

<b>Figure 1.1</b> Schematic diagram of research scope.....	4
<b>Figure 2.1</b> The electrochemical process.....	7
<b>Figure 2.2</b> Direct bio-photolysis process.....	8
<b>Figure 2.3</b> Indirect bio-photolysis process.....	8
<b>Figure 2.4</b> The biomass is transformed by yeast into ethanol.....	12
<b>Figure 2.5</b> The CO <sub>2</sub> closed cycle.....	12
<b>Figure 2.6</b> Reaction scheme of ethanol steam reforming.....	13
<b>Figure 2.7</b> Conventional steam reforming process.....	16
<b>Figure 2.8</b> Schematic diagram of sorption enhanced steam reforming process.....	17
<b>Figure 2.9</b> The Sorption enhance chemical looping ethanol steam reforming process.....	18
<b>Figure 2.10</b> The ratio of hydrogen gas used in the industry.....	20
<b>Figure 2.11</b> The mechanism of CaO sorbent.....	23
<b>Figure 2.12</b> Mechanism for calcium aluminate formation.....	24
<b>Figure 3.1</b> The mechanism of transfusion by conventional and multifunctional.....	31
<b>Figure 3.2</b> Process diagram of sol-gel method.....	34
<b>Figure 3.3</b> Sorption enhance chemical looping reforming scheme.....	35
<b>Figure 4.1</b> Schematic of preparation method.....	41
<b>Figure 4.2</b> Diagram of Bragg's law.....	41

<b>Figure 4.3</b> Sample result from TGA-DSC equipment.....	43
<b>Figure 4.4</b> Experimental set up for hydrogen production.....	44
<b>Figure 4.5</b> Single cycle for sorption enhanced steam ethanol reforming chemical looping.....	46
<b>Figure 5.1</b> XRD pattern of multifunctional materials synthesized from different CaO precursors (Cl-Na, Cl-Urea, Ac-Na, Ac-Urea).....	47
<b>Figure 5.2</b> SEM image of multifunctional catalyst a) Cl-Na b) Cl-Urea c) Ac-Na d) Ac-urea.....	48
<b>Figure 5.3</b> Dispersion of Ni metal in multifunctional catalyst from EDX Cl-Na b) Cl-Urea c) Ac-Na d) Ac-urea.....	49
<b>Figure 5.4</b> Adsorption/desorption isotherm of NiO/CaO <sub>Cl-Na</sub> -Ca <sub>12</sub> Al <sub>14</sub> O <sub>33</sub> , NiO/CaO <sub>Cl-Urea</sub> -Ca <sub>12</sub> Al <sub>14</sub> O <sub>33</sub> , NiO/CaO <sub>Ac-Na</sub> -Ca <sub>12</sub> Al <sub>14</sub> O <sub>33</sub> and NiO/CaO <sub>Ac-Urea</sub> -Ca <sub>12</sub> Al <sub>14</sub> O <sub>33</sub> .....	52
<b>Figure 5.5</b> Percent compositions from sorption enhanced ethanol steam reforming using multifunctional materials: a) NiO/CaO <sub>Cl-Na</sub> -Ca <sub>12</sub> Al <sub>14</sub> O <sub>33</sub> (Cl-Na), b) NiO/CaO <sub>Cl-Urea</sub> -Ca <sub>12</sub> Al <sub>14</sub> O <sub>33</sub> (Cl-Urea), c) NiO/CaO <sub>Ac-Na</sub> -Ca <sub>12</sub> Al <sub>14</sub> O <sub>33</sub> (Ac-Na), d) NiO/CaO <sub>Cl-Na</sub> -Ca <sub>12</sub> Al <sub>14</sub> O <sub>33</sub> (Ac-Urea). operating condition under temperature 600 °C, steam/ethanol ratio of 4.....	55
<b>Figure 5.6</b> SEM image of multifunctional catalyst a) Cl-Na b) Cl-Urea c) Ac-Na d) Ac-urea.....	57
<b>Figure 5.7</b> Gas product compositions of 6% Ac-urea: (a) hydrogen concentration, (b) carbon monoxide concentration, (c) methane concentration and (d) carbon dioxide concentration reaction condition: under temperature 600 °C, steam/ethanol ratio of 4 and regeneration CaCO <sub>3</sub> at temperature 850 °C under N <sub>2</sub> flow.....	58

<b>Figure 5.8</b> Dispersion of Al metal in Ac-Urea multifunctional catalyst from EDX.....	59
<b>Figure 5.9</b> XRD pattern of 6%NiO/CaO-Ca <sub>12</sub> Al <sub>14</sub> O <sub>33</sub> multifunctional catalyst for sol-gel and sol-mixing method.....	60
<b>Figure 5.10</b> Image of SEM for multifunctional catalyst a) sol-mixing method b) Sol-gel method.....	61
<b>Figure 5.11</b> Adsorption/desorption isotherm of sol-mixing and sol-gel method.....	62
<b>Figure 5.12</b> Gas product compositions of a) NiO/CaO-Ca <sub>12</sub> Al <sub>14</sub> O <sub>33</sub> (sol-gel) b) NiO/CaO-Ca <sub>12</sub> Al <sub>14</sub> O <sub>33</sub> (sol-mixing), reaction condition at temperature 600 °C, S/E of 4 under atmospheric pressure .....	64
<b>Figure 5.13</b> Thermogravimetric analysis of spent catalyst.....	65
<b>Figure 5.14</b> DTG of spent catalyst.....	65
<b>Figure 5.15</b> XRD pattern of multifunctional catalyst Cu/(Ni-CA), Ni/(Cu-CA) and Ni-Cu-CA.....	67
<b>Figure 5.16</b> SEM image for multifunctional catalyst a) Ni-CA b) Cu/(Ni-CA) c) Ni/(Cu-CA) d) Ni-Cu-CA.....	68
<b>Figure 5.17</b> Dispersion of metal for a) Cu/(Ni-CA) b) Ni/(Cu-CA) c) Ni-Cu-CA multifunctional catalyst from EDX.....	69
<b>Figure 5.18</b> Adsorption/desorption isotherm of Cu/(Ni-CA), Ni/(Cu-CA) and Ni-Cu-CA.....	71
<b>Figure 5.19</b> Gas product compositions of Ni-CA, Cu-CA, Cu-(Ni-CA), Ni-(Cu-CA) and Ni-Cu-CA reaction condition at temperature 500 °C, S/E of 4 under atmospheric pressure.....	76
<b>Figure 5.20</b> Hydrogen purity of Ni-CA, Cu-CA, Cu/(Ni-CA), Ni/(Cu-CA) and Ni-Cu-CA multifunctional catalyst.....	76

<b>Figure 5.21</b> XRD pattern of multifunctional for Cu/(Ni-CA), Ni/(Cu-CA) and Ni-Cu-CA for calcination at the temperature of 800, 825, 850 °C.....	78
<b>Figure 5.22</b> The single cycle of (a) Cu/(Ni-CA) and (b) Ni-Cu-CA.....	80
<b>Figure 5.23</b> The XRD pattern of Cu/(Ni-CA) and Ni-Cu-CA at the reduction step.....	81
<b>Figure 5.24</b> The XRD pattern of Cu/(Ni-CA) and Ni-Cu-CA at the oxidation step.....	81
<b>Figure 5.25</b> The hydrogen concentration of Cu/(Ni-CA) and Ni-Cu-CA multifunctional catalyst reaction condition: under temperature 500 °C, steam/ethanol ratio of 3.....	83
<b>Figure 5.26</b> SEM image of multifunctional catalyst a) Cu/(Ni-CA) (fresh) b) Cu/(Ni-CA) (used) c) Ni-Cu-CA (fresh) d) Ni-Cu-CA (used).....	84
<b>Figure 5.27</b> TGA analysis of Cu/(Ni-CA), Ni/(Cu-CA) and Ni-Cu-CA.....	85



## Tables

<b>Table 2.1</b> Summary of hydrogen production processes.....	5
<b>Table 2.2</b> Efficiency of different hydrogen production techniques.....	10
<b>Table 2.3</b> Properties of ethanol.....	11
<b>Table 2.4</b> Properties of hydrogen.....	19
<b>Table 2.5</b> Properties of carbon dioxide.....	20
<b>Table 2.6</b> Properties of carbon monoxide.....	21
<b>Table 2.7</b> Properties of methane.....	21
<b>Table 2.8</b> Properties of calcium oxide.....	23
<b>Table 2.9</b> Properties of alumina.....	24
<b>Table 3.1</b> Summary of catalysts and supports used for ethanol steam reforming...27	27
<b>Table 3.2</b> Overview of adsorbents for carbon dioxide capture.....	29
<b>Table 3.3</b> Summarize the use of multifunctional material for sorption enhanced steam reforming of ethanol process.....	32
<b>Table 3.4</b> Properties of metal oxide.....	37
<b>Table 4.1</b> Sample name of different precursors.....	39
<b>Table 4.2</b> Condition for single cycle.....	45
<b>Table 5.1</b> Composition of metal at surface of catalyst by EDX.....	49
<b>Table 5.2</b> Textural properties of multifunctional NiO/CaO-Ca <sub>12</sub> Al <sub>14</sub> O <sub>33</sub> catalysts.....	50
<b>Table 5.3</b> Hydrogen purity of all multifunctional catalyst.....	56
<b>Table 5.4</b> Composition of metal at surface of catalyst by EDX.....	61

<b>Table 5.5</b> Textural properties of multifunctional NiO/CaO-Ca <sub>12</sub> Al <sub>14</sub> O <sub>33</sub> catalyst from sol-gel and sol-mixing method.....	62
<b>Table 5.6</b> Composition of metal at surface of catalyst by EDX.....	70
<b>Table 5.7</b> Textural properties of multifunctional catalyst.....	70
<b>Table 5.8</b> XPS analysis results of the multifunctional catalysts.....	84





## CHAPTER I

### INTRODUCTION

#### 1.1 Rationale

Fossil fuels in the form of coal, oil and natural gas are primary energy used in transportation and power plant. However, an increase of human population and industrialization are the main reasons of fast depletion of fossil fuels. Moreover, with the concern of global warming effect, combustion of fossil fuels, which is found to be a cause of greenhouse gas emissions, is a drive of finding alternative renewable energy carriers. Hydrogen has been proposed as a suitable alternative energy carrier because it can burn cleanly with no pollutants emission and possess the highest energy content per unit of weight [1]. In addition, it also be able to use as a feedstock for refinery or petrochemical industries.

Hydrogen can be produced from hydrocarbon or oxygenated compounds such as methane, methanol, ethanol or propane, etc [2]. Bioethanol is one of the most favorable sources for hydrogen production as it is a good source of hydrogen storage. Bioethanol can currently be produced by fermentation of sugar derived from various biomass resources such as corn, sugarcane, lignocellulose, etc [3]. Moreover, it can be produced from various sources, including bio-waste, waste materials from agro-industries, forestry residue materials. The advantages of using bioethanol are non-toxic, high power density and free of sulfur [4].

Hydrogen can be produced from many processes such as thermal decomposition, photocatalytic, plasma reforming, electrolysis, or steam reforming [5]. Among these, steam reforming process is a mature technology used to produce hydrogen. However, the drawback of this technique is high energy consumption due

to endothermic reaction as well as additional CO<sub>2</sub> separation unit to purify the produced hydrogen. Sorption enhanced steam reforming (SESR) is a combination between steam reforming and CO<sub>2</sub> sorption in a single unit. The concept of the process is based on Le Chatelier's principle, in which the reaction equilibrium will be shifted to favor an increase of the reactant conversion by in-situ removal of one of the side products. The advantages of this process are high hydrogen purity, low power consumption, and low cost. However, the SESR is usually required highly energy consumption for sorbent regeneration. Sorption enhanced chemical looping steam reforming (SECR) is therefore invented to decrease energy consumption for sorbent regeneration. In this process, heat supply for sorbent regeneration is provided by oxygen transfer material through oxidation-reduction cycles. In this work, we are interested in study an applying of multifunctional material, which is composed of oxygen carrier, CO<sub>2</sub> sorbent, and support, to sorption enhanced chemical looping steam reforming of ethanol. The effect of CaO precursor, type of oxygen carrier, and synthesis method, were investigated for hydrogen selectivity, CO<sub>2</sub> adsorption, calcination temperature, material stability, and coke formation.

## 1.2 Objective

To develop multifunctional materials for hydrogen production via sorption-enhanced chemical looping ethanol steam reforming.

## 1.3 Scope of work

The scope of this work is divided into three parts

### Part 1

- Investigate the effect of CaO precursor, including calcium precursor (calcium acetate (Ca<sub>2</sub>Ac) and calcium chloride (CaCl<sub>2</sub>)) and carbonate precursor (sodium

carbonate ( $\text{Na}_2\text{CO}_3$ ) and urea ( $\text{CO}(\text{NH}_2)_2$ ) on  $\text{CO}_2$  sorption performances in hydrogen production via sorption enhanced ethanol steam reforming.

### Part 2

- Study the effect of synthesis method of multifunctional material, precipitation and sol-gel method, on hydrogen production and coke formation for sorption enhanced ethanol steam reforming process.

### Part 3

- Develop multi-functional material containing NiO as oxygen transfer material, CuO as oxygen transfer material and heat carrier, CaO as sorbent and  $\text{Al}_2\text{O}_3$  as support for sorption enhanced chemical looping steam ethanol reforming.
- Investigate the effect of preparation method of multi-functional material, including sol-gel and incipience impregnation, on hydrogen production and energy requirement for sorbent regeneration.

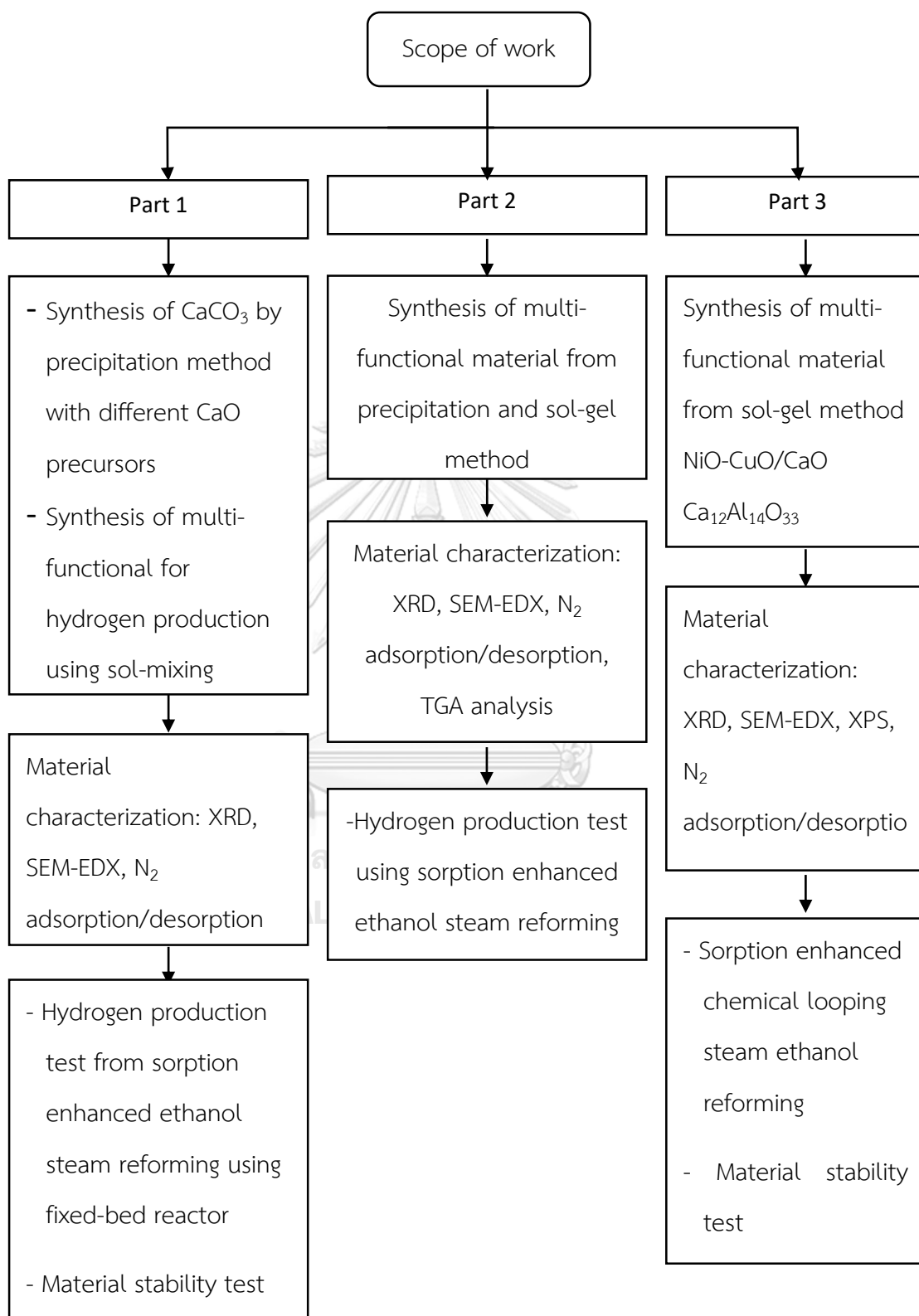


**Figure 1.1** Schematic diagram of research scope.

## CHAPTER 2

## THEORY

This chapter presents theories relating sorption enhanced chemical looping steam reforming, which covers processes for producing hydrogen, advantages and disadvantages of each process, materials used in the processes, such as ethanol, catalyst, CaO, and support  $Al_2O_3$

### 2.1 Hydrogen production process

There are several technologies developed for producing hydrogen, which can be divided into three different routes: thermochemical, electrochemical and biological. Details of each process are summarized in Table 2.1

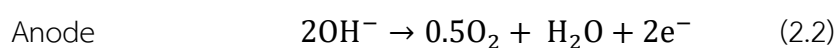
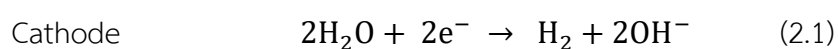
**Table 2.1** Summary of hydrogen production processes [6]

Primary Method	Process	Feedstock	Technique
Thermochemical	Oxidative	Liquid and gaseous hydrocarbon	Steam reforming
			Auto thermal reforming
			Partial oxidation
			Combined dry-steam reforming
			Dry reforming
			Plasma reforming
			Photocatalytic conversion
		Coal	Gasification
		Biomass	Pyrolysis

	Non-oxidative	Liquid and gaseous hydrocarbon	Thermal decomposition
			Catalytic decomposition
		Biomass	Refinery processes
		Water	Plasma
			Pyrolysis
			Thermochemical water splitting
Electrochemical	Electrolysis	Water	Electricity
	Photoelectrochemical	Water	Direct sunlight
Biological	Photobiological	Water and algae	Direct sunlight
	Anaerobic	Biomass	High digestion temperature heat
	Fermentative microorganism	Biomass	High temperature heat

### 2.1.1 Electrochemical process

The production of hydrogen by electrochemical process is a process using direct current through the electrode in the electrolyte solution to decompose water into hydrogen and oxygen. Reactions relating to electrochemical process for hydrogen production are shown in Eqs. (2.1-2.3) and schematic picture of an experiment is shown in Figure 2.1. The electrochemical can produce hydrogen about 56-73 percent. The disadvantage of this process is very endothermic reaction therefore high energy is required.



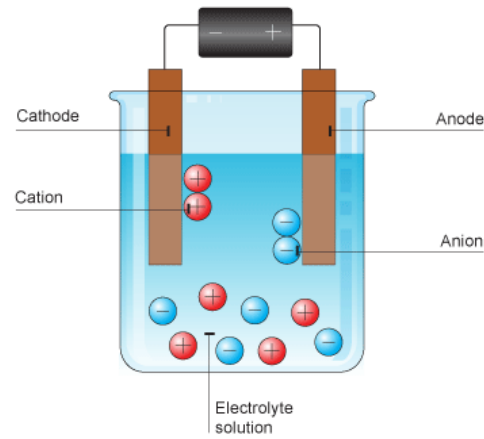
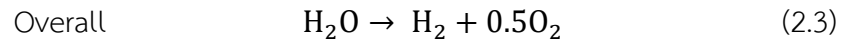


**Figure 2.1** The electrochemical process [7]

### 2.1.2 Biological process

The production of hydrogen by biological process is the use of microalgae in the reaction. The reaction is usually operated at ambient condition: atmospheric pressure and a temperature of 25 °C thus less energy intensive. Biological process can be divided into 2 types: direct bio-photolysis and indirect bio-photolysis. For direct bio-photolysis, water molecules are split into hydrogen and oxygen by green algae via photosynthesis. The hydrogen ions are converted into hydrogen gas by hydrogenase enzyme. The reaction is shown in Eq. 2.4 and Figure 2.2. In indirect bio-photolysis, hydrogen is produced using both hydrogenase and nitrogenase enzymes by cyanobacteria or blue-green algae. The formation of hydrogen from water can be presented in Eq. 2.5-2.6 and Figure 2.3. However, this reaction provides low hydrogen production and the requirement of surface area to collect light, which are main drawbacks of bio-photolysis processes.

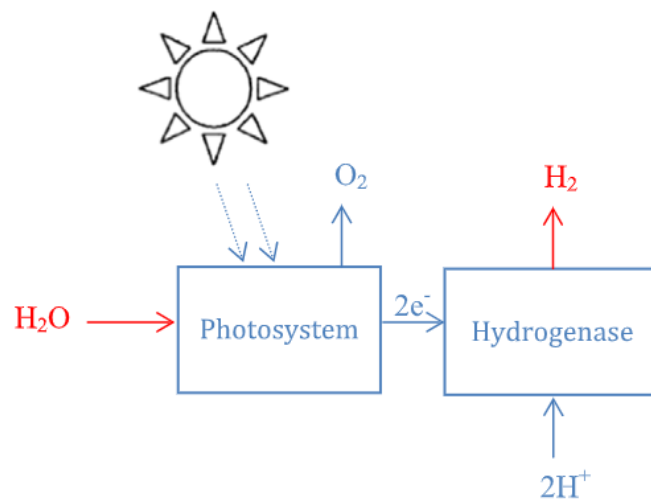
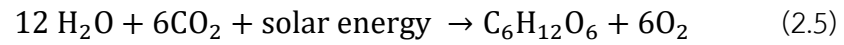
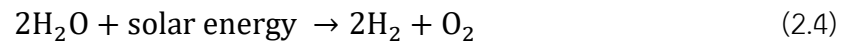


Figure 2.2 Direct bio-photolysis process [6].

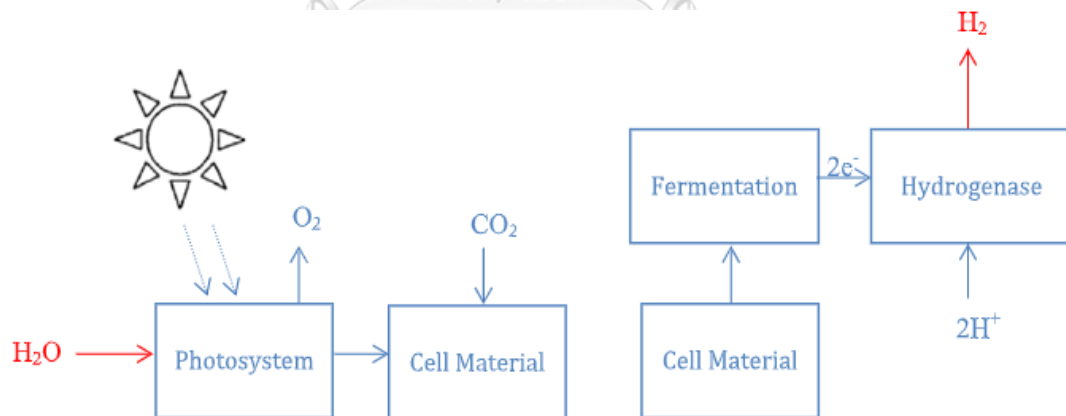


Figure 2.3 Indirect bio-photolysis process [6]

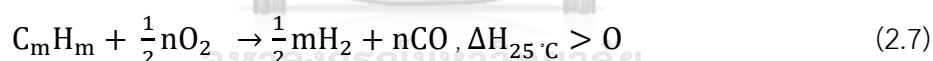


### 2.1.3 Thermochemical process

Thermochemical process is a major technique that used to produce hydrogen. Hydrogen produced from this process is about 96% (48% from natural gas, 30% from heavy oils and naphtha and 18% from coal) of all hydrogen product in the market. The last 4% is produced from electrochemical process. The production of hydrogen from thermochemical process requires heat in the reaction. In this process, reactants can be hydrocarbon, organic compounds, or biomass. Thermochemical process from hydrocarbon such as steam reforming, partial oxidation, and autothermal reforming.

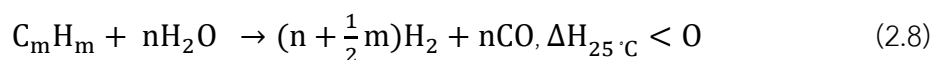
#### 2.1.3.1 Partial oxidation

Partial oxidation method (POX) is the reaction between hydrocarbons and oxygen as shown in Eq. (2.7). The reaction is exothermic, so the energy is released from the process, reducing external energy requirement. However, disadvantage of this process is high operating cost due to it needs a separation process of oxygen from air before entering the system. If the process does not separate oxygen, it will decrease the concentration of hydrogen in the product stream.



#### 2.1.3.2 Steam reforming

Hydrocarbon substrate and steam are converted into hydrogen and carbon monoxide via steam reforming reaction (SR) as shown in Eq. (2.8). Although, the reaction is highly endothermic but reaction is the most common and developed method used for large-scale hydrogen production because the conversion efficiency is in between 74-85%.



### 2.1.3.3 Autothermal reforming

Autothermal reforming (AR) is a new process that combines the advantages of steam reforming and partial oxidation. It combines the two processes by feeding water and oxygen to react with hydrocarbons as shown in Eq. (2.9). The advantages of this process are high hydrogen ratio and less energy intensive.

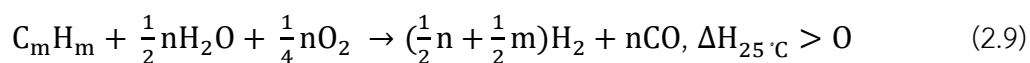


**Table 2.2** Efficiency of different hydrogen production techniques [8].

Process	Efficiency
Partial oxidation (POX)	60-75 %
Steam reforming (SR)	74-85 %
Autothermal reforming (ATR)	60-75 %

## 2.2 Hydrocarbon feedstock

Hydrogen can be produced from hydrocarbon or oxygenated compounds such as methane, methanol, ethanol, or propane, etc [2]. Bioethanol is one of the most favorable sources for hydrogen production as it is a good source of hydrogen storage.

### 2.2.1 Bioethanol

Ethanol or ethyl alcohol is an organic compound that contains carbon, hydrogen, and oxygen. Ethanol is a volatile liquid. It can be dissolved in water and other organic solvents. The properties of ethanol are summarized in Table 2.3.

**Table 2.3** properties of ethanol.

Chemical formula	C <sub>2</sub> H <sub>5</sub> OH
Structure	
Molar mass	46.07 g/mol
Density	0.789 g/cm <sup>3</sup> (at 25 °C)
Viscosity	0.001007 kg/m•s
Boiling point	351.44 K
Octane rating	109
Energy content	26.8 MJ/kg

Ethanol can be produced from different resources of biomass, i.e., starch, sugar, or fiber, etc., by fermentation process. The transformation of ethanol from biomass is shown in Figure 2.4 [9]. Advantages of using ethanol as fuel are renewable and environmentally friendly because the produced CO<sub>2</sub> is consumed in a closed cycle via photosynthesis. Ethanol begins its life as carbon stored in biomass. Then the biomass is converted into ethanol by fermentation process, which is burnt as fuel that emits water and carbon dioxide. Photosynthesis converts the carbon back into biomass, to be used in the next cycle of ethanol production. The CO<sub>2</sub> closed cycle is shown in Figure 2.5. Using ethanol as substrate can reduce the depletion of fossil fuel.

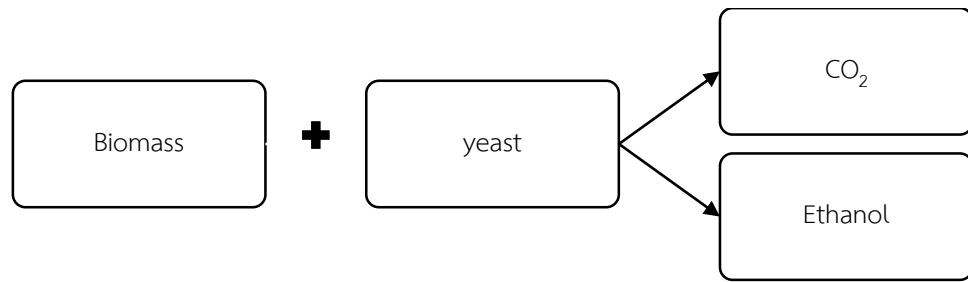


Figure 2.4 The biomass is transformed by yeast into ethanol [10].

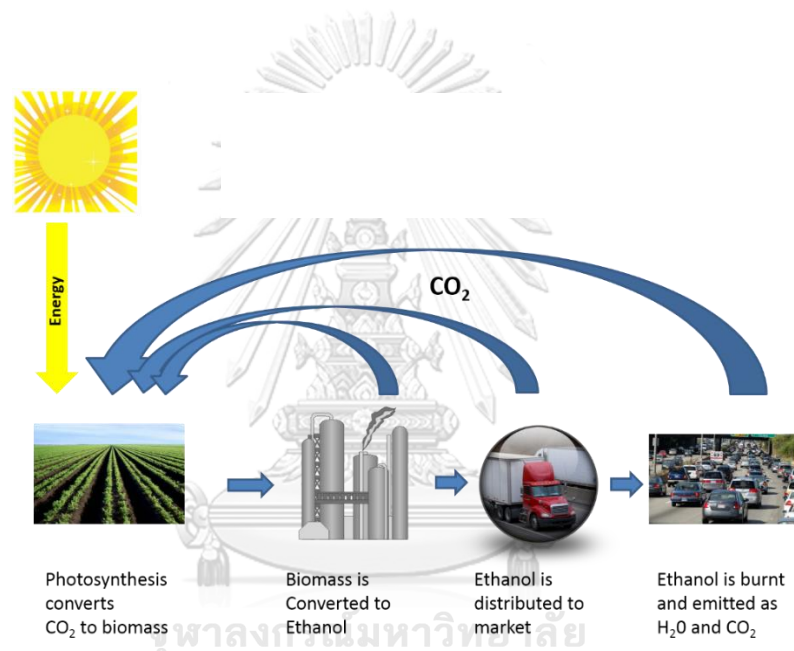


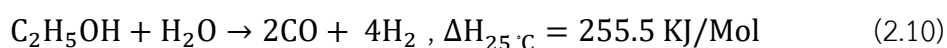
Figure 2.5 The CO<sub>2</sub> closed cycle [20].

### 2.3 Ethanol steam reforming process (ESR)

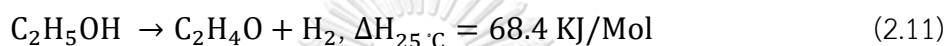
Ethanol steam reforming is a reaction between ethanol and steam to transform ethanol into hydrogen and carbon monoxide (Eq. 2.10). However, ethanol steam reforming has many intermediate products such as carbon monoxide, methane, acetaldehyde and ethylene, which depends on the reaction pathways and operating condition. In commercial process, the main reaction mechanism consists of dehydrogenation or dehydration path, as shown in Figure 2.6. Dehydrogenation

reaction produces acetaldehyde (Eq. 2.11), which can be proceeded by decarbonylation to produce methane and carbon monoxide (Eq. 2.12). Methane can be conducted via steam reforming to produce hydrogen and carbon monoxide (Eq. 2.13).

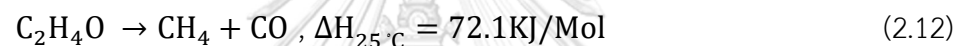
Ethanol steam reforming



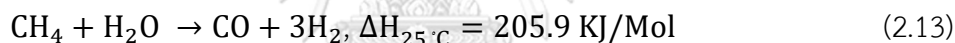
Ethanol dehydrogenation to acetaldehyde



Acetaldehyde decarbonylation to methane and carbon monoxide

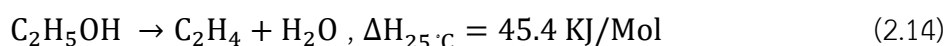


Methane steam reforming

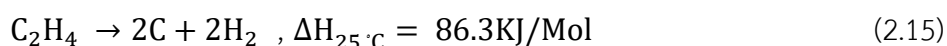


On the other hand, ethanol dehydration reaction produces ethylene as intermediate product (2.14). However, ethylene is easily transformed into carbon, which could deposit on catalyst (Eq. 2.15). Meanwhile, ethylene can be reacted with water by steam reforming reaction to produce hydrogen and carbon monoxide (2.16).

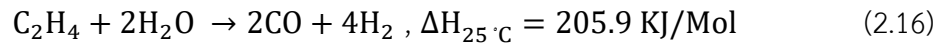
Ethanol dehydration to ethylene



Ethylene transformation to carbon

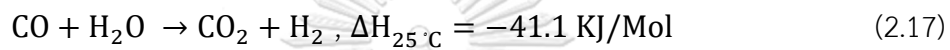


Ethylene steam reforming



As carbon monoxide must be diminished because it is a pollutant; therefore, carbon monoxide is transformed into carbon dioxide and hydrogen through the water-gas shift reaction (Eq. 2.17). Other reactions are shown in Eqs. 2.18-2.22.

Water-gas shift (WGS)



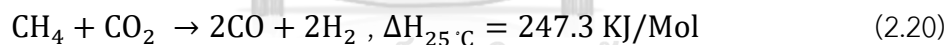
Ethanol decomposition (ED) to  $\text{CH}_4$ ,  $\text{CO}$ , and  $\text{H}_2$



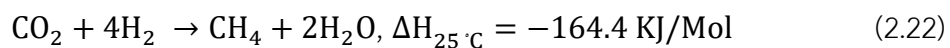
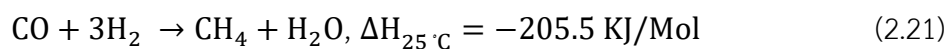
Ethanol hydrogenolysis to  $\text{CH}_4$  and  $\text{H}_2\text{O}$



Dry reforming of methane



Methanation



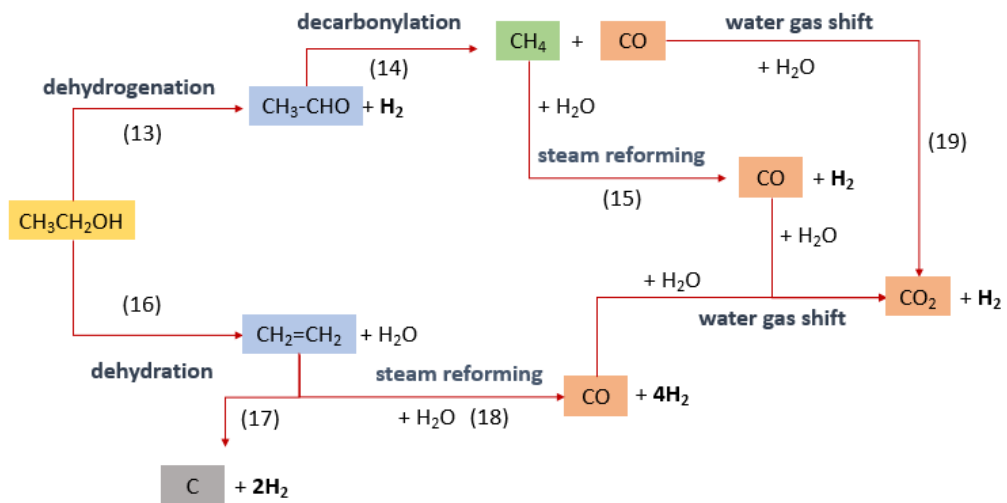


Figure 2.6 Reaction scheme of ethanol steam reforming

Conventional steam reforming process composes mainly of three units, including reforming unit, water-gas shift unit,  $\text{CO}_2$  removal unit. The process is shown in Figure 2.7. The reforming unit is a main reactor that used to change raw materials into hydrogen. This reaction is endothermic. The second unit is the reactor that is used to convert carbon monoxide into carbon dioxide, named water-gas shift reactor. This unit can reduce the amount of carbon monoxide, which pollutes the environment and increases hydrogen product through water-gas shift reaction. This reaction is exothermic, of which the reaction is taken place in between  $400 - 700^\circ \text{C}$ . The last unit is a purification of hydrogen product to separate  $\text{CO}_2$  from hydrogen from the product stream.

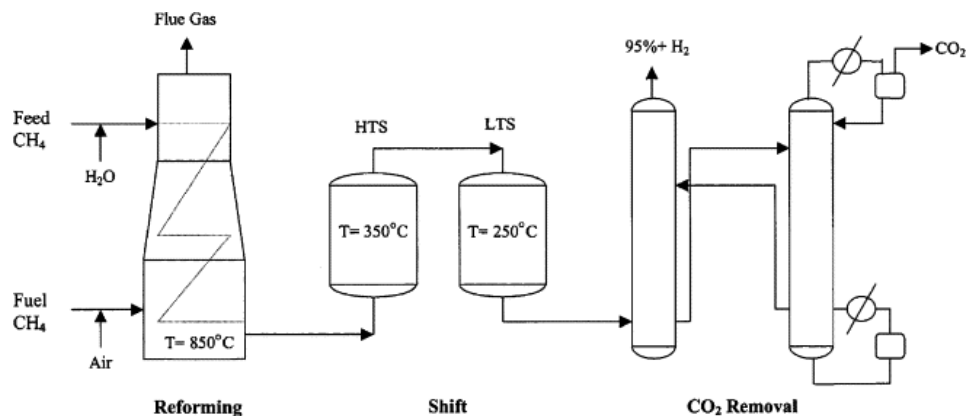
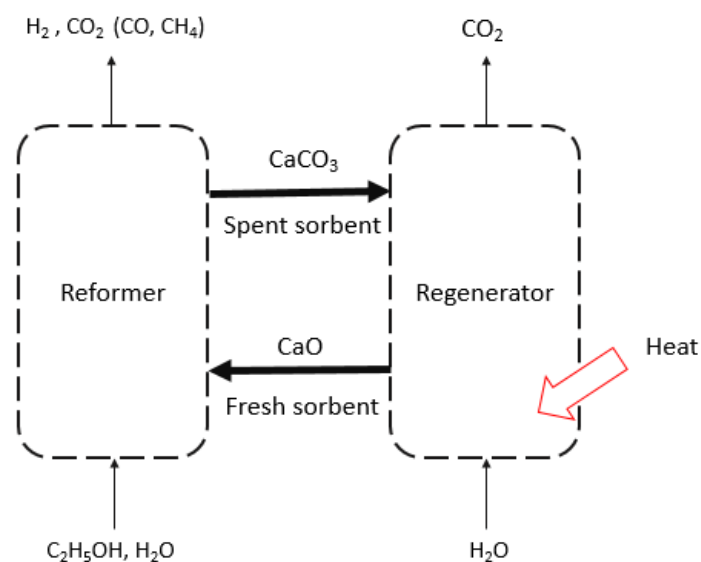


Figure 2.7 Conventional steam reforming process [11].

## 2.4 Sorption enhanced ethanol steam reforming (SER)

Sorption enhanced ethanol steam reforming process is a combination between reaction and sorption in a single unit [4]. The conventional process is shown in Figure 2.8. The concept of sorption enhanced steam reforming is based on Le Chatelier's principle in which the reaction equilibrium will shift to favor an increase of the reactant conversion by in-situ removal of one of the products, which is usually carbon dioxide.

However, the main disadvantage of sorption enhanced ethanol steam reforming is the regeneration of sorbent at high temperature. This drawback can overcome by sorption enhanced chemical looping ethanol steam reforming.



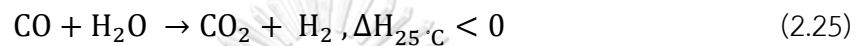
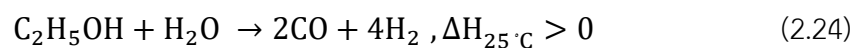
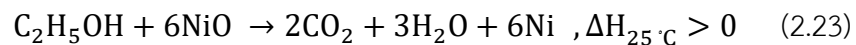
**Figure 2.8** Schematic diagram of sorption enhanced steam reforming process.

## 2.5 Sorption enhanced chemical looping ethanol steam reforming (SECLSR)

Sorption enhanced chemical looping ethanol steam reforming (SECLSR) is a combined process between sorption enhanced ethanol steam reforming and chemical looping reforming. The SECLSR composes of three reactors, including reforming reactor, air reactor, calcination reactor. The process is shown in Figure 2.9.



The reforming reactor (FR) is usually operated at 300 °C - 800 °C. NiO as oxygen carrier was reduced by ethanol according to reaction (Eq. 2.23), then reforming reaction (Eq. 2.24) and water-gas shift reaction (Eq. 2.25) are taken placed, with simultaneous removal of CO<sub>2</sub> (Eq. 2.26)



In the air reactor (AR), which is operated at 400 °C - 800 °C, oxygen carrier is re-oxidized by air (Eq. 2.26). Meanwhile, carbon deposition on catalyst from reforming reactor could also be combusted to carbon dioxide by oxygen (Eq. 2.27). The overall reaction in air reactor is exothermic reaction; the heat from air reactor can be utilized in calcination reactor for sorbent regeneration and reforming reactor, which is possible to reach thermo neutral.



The spent sorbent is fed to a calcination reactor (CR) to regenerate the sorbent for reuse. Mostly, the reaction in calcination reactor is endothermic and is operated at 750-900 °C

As seen, sorption enhanced chemical looping ethanol steam reforming process has advantages, i.e., the process has potential to carry out under self-sufficient condition, WGS reactor and separation units at downstream process can be omitted, and the process is environmentally friendly, where the release of CO<sub>2</sub> into the atmosphere can be diminished.

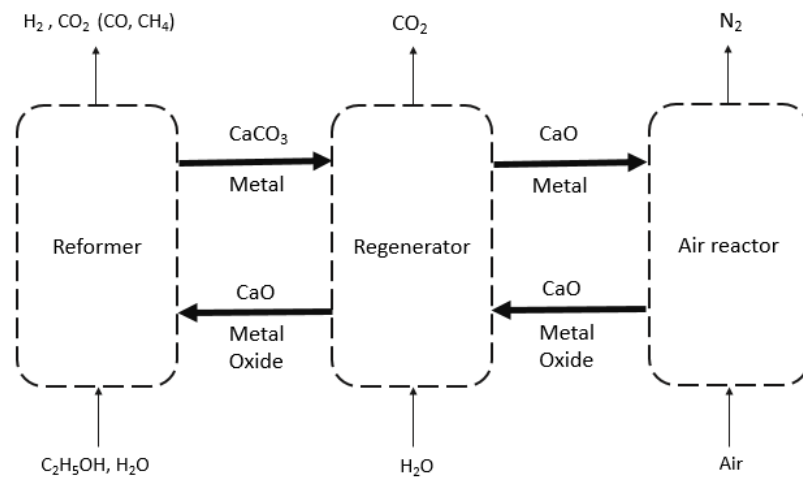


**Figure 2.9** The Sorption enhance chemical looping ethanol steam reforming process.

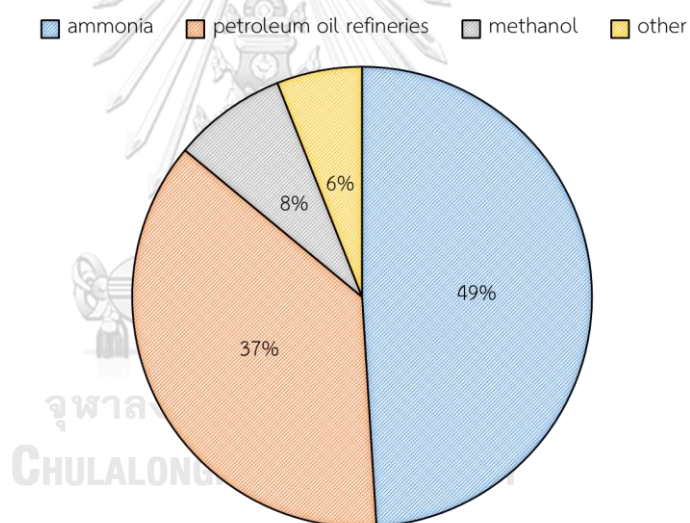
## 2.6 Properties of materials involved hydrogen production process

### 2.6.1 Hydrogen ( $H_2$ )

Hydrogen is the lightest element, and can be produced from various sources. It has the highest energy content per unit of weight when compared to other heat storage materials. Hydrogen is widely used in chemical and petroleum industries [1, 12, 13]; 49% of hydrogen is used in the production of ammonia and 37% of hydrogen is used in petroleum oil refineries [14]. The ratio of hydrogen gas used in industry is shown in Figure 2.10. Hydrogen fuel is a clean energy, or called “clean fuel” because when hydrogen is burnt, it produces only energy and water. The properties of hydrogen are summarized in Table 2.3.

**Table.2.4** Properties of hydrogen

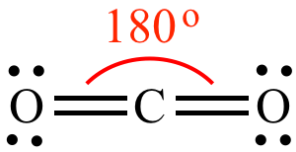
Chemical formula	H <sub>2</sub>
Structure	H-H
Molar mass	2.014 g·mol <sup>-1</sup>
Density	1.312 × 10 <sup>-3</sup> g/cm <sup>3</sup> (gas) 70.973 × 10 <sup>-3</sup> g/cm <sup>3</sup> (liquid)
Viscosity	0.001007 kg/m•s
Boiling point	- 252.78 °C
Octane rating	109
Energy content	119.220 MJ/kg

**Figure 2.10** The ratio of hydrogen gas used in the industry [14]

### 2.6.2 Carbon dioxide (CO<sub>2</sub>)

Carbon dioxide gas is found in the atmosphere; however, it is considered as a greenhouse gas causing global warming effect. CO<sub>2</sub> concentration in atmospheric is increasing due to burning fossils fuels, coal, or hydrocarbons. In addition, CO<sub>2</sub> can dissolve in water to form acidic solutions. The properties of carbon dioxide are summarized in Table 2.5.

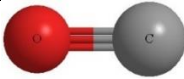
**Table 2.5** Properties of carbon dioxide

Chemical formula	CO <sub>2</sub>
Structure	
Molar mass	44.009 g·mol <sup>-1</sup>
Density	1.562 g/cm <sup>3</sup> (solid at 1 atm and -78.5 °C) 1.101 g/cm <sup>3</sup> (liquid at saturation -37°C) 1.977 × 10 <sup>-3</sup> g/cm <sup>3</sup> (gas at 1 atm and 0 °C)
Solubility in water	1.45 g/L at 25 °C , 100 kPa
Boiling point	-57 °C (at 5.185 bar)

### 2.6.3 Carbon monoxide (CO)

Carbon monoxide consists of one carbon atom and one oxygen atom, connected by a triple bond. The CO is toxic to human beings when its concentration is above 35 ppm as it causes lower metabolism of humans. The properties of carbon monoxide are summarized in Table 2.6.

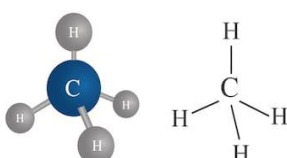
**Table 2.6** Properties of carbon monoxide

Chemical formula	CO
Structure	
Molar mass	28.01 g·mol <sup>-1</sup>
Density	0.789 g/cm <sup>3</sup> , liquid 1.250 × 10 <sup>-3</sup> g/cm <sup>3</sup> at 0 °C, 1 atm 1.145 × 10 <sup>-3</sup> g/cm <sup>3</sup> at 25 °C, 1 atm
Solubility in water	27.6 × 10 <sup>-3</sup> g/L (25 °C)
Boiling point	-191.5 °C

### 2.6.4 Methane (CH<sub>4</sub>)

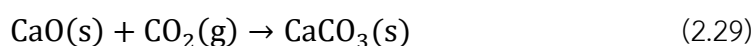
Methane consists of one carbon atom and four hydrogen atoms, connected by a single bond to four hydrogen atoms. Methane can produce by anaerobic digestion (AD) of biomass such as animal waste and industrial waste water [43]. The properties of methane are summarized in Table 2.7.

**Table 2.7** Properties of methane

Chemical formula	CH <sub>4</sub>
Structure	
Molar mass	16.043 g·mol <sup>-1</sup>
Density	0.717×10 <sup>-3</sup> g/cm <sup>3</sup> (gas, 0°C) 0.416 g/cm <sup>3</sup> (liquid)
Solubility in water	Soluble in ethanol, diethyl ether, benzene, toluene, methanol, acetone and insoluble in water
Boiling point	-161.50 °C

### 2.6.5 Calcium oxide (CaO)

Calcium oxide is a white powder, of which molecules are formed from calcium cation Ca<sup>+2</sup> and oxygen anion O<sup>-2</sup>, through an ionic bond. The properties of calcium oxide are summarized in Table 2.8. Calcium oxide can be used as a precursor for production of chemicals such as production of calcium hydroxide via reaction between calcium oxide and water as shown in Eq. 2.28. Calcium oxide can adsorb carbon dioxide at high temperature with the carbonation reaction as shown in Eq. 2.29.



For an application of CaO to CO<sub>2</sub> capture, there are two steps of carbonation reaction on CaO particles; the first step (fast stage) is controlled by chemical reaction between CaO and CaCO<sub>3</sub> interface. The second step (slow stage) is controlled by ion diffusion through the CaCO<sub>3</sub> product layer. The reaction is slow because the product layer inhibited the diffusion of CO<sub>2</sub> molecules to the CaO surface. The mechanism of 2 steps is shown in Figure 2.11.

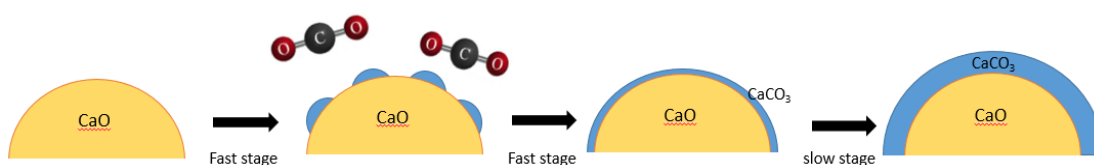
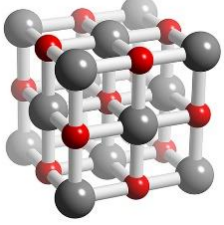


Figure 2.11 The mechanism of CaO sorbent [15]

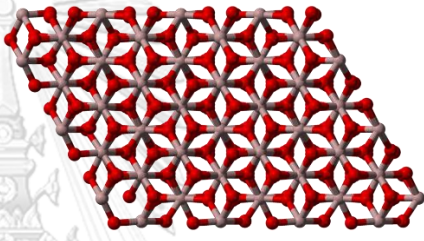
Table 2.8 Properties of calcium oxide

Chemical formula	CaO
Structure	
Molar mass	56.0774 g·mol <sup>-1</sup>
Density	3.35 g/cm <sup>3</sup> (at 25 °C)
Boiling point	3621 °C
Melting point	2899 °C
Solubility in water	Reacts to form calcium hydroxide

### 2.6.6 Aluminum oxide ( $\text{Al}_2\text{O}_3$ )

Alumina is the main component of bauxite. Properties of  $\text{Al}_2\text{O}_3$  are good thermal conductivity, high strength, and high surface area. Using alumina for steam reforming process is easily controlled by surface area and pore size distribution. The properties of alumina are summarized in Table 2.9.

**Table 2.9** Properties of alumina

Chemical formula	$\text{Al}_2\text{O}_3$
Structure	
Molar mass	$101.960 \text{ g}\cdot\text{mol}^{-1}$
Density	$3.987 \text{ g}/\text{cm}^3$
Boiling point	$2,977 \text{ }^\circ\text{C}$
Melting point	$2,072 \text{ }^\circ\text{C}$
Solubility in water	insoluble

### 2.6.7 Calcium aluminate cements ( $\text{Ca}_{12}\text{Al}_{14}\text{O}_{33}$ )

Calcium aluminate cements,  $\text{Ca}_{12}\text{Al}_{14}\text{O}_{33}$ , can be formed from the reaction between  $\text{CaO}$  and  $\text{Al}_2\text{O}_3$ . It is an exothermic reaction, as shown in Eq. 2.30 [16]. The reaction between  $\text{CaO}$  and  $\text{Al}_2\text{O}_3$  can be occurred when the temperature is higher than  $800^\circ\text{C}$ . A proposed mechanism for calcium aluminate formation is proposed in Figure 2.12. In stages 1-2, the calcium and alumina precursors are dehydrated and calcined to  $\text{CaO}$  and  $\text{Al}_2\text{O}_3$ . In stages 3-4, a solid-solid state reaction takes place. The combination between  $\text{Al}_2\text{O}_3$  and  $\text{CaO}$  prevent the structural breakdown of  $\text{CaO}$  at high temperatures. So,  $\text{Ca}_{12}\text{Al}_{14}\text{O}_{33}$  can prevent sintering of  $\text{CaO}$  during calcination reaction.

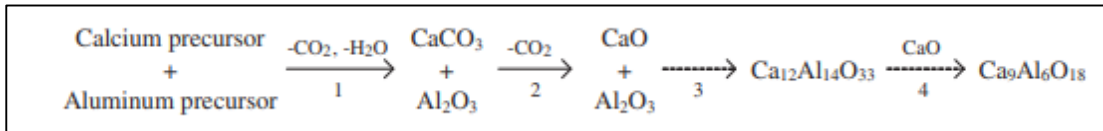
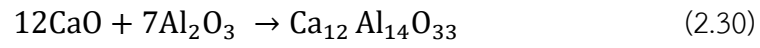


Figure 2.12 Mechanism for calcium aluminate formation [11]





## CHAPTER 3

### LITERATURE REVIEW

In this section, literature review is focused on the development of materials including catalyst, sorbent, oxygen carrier, and support that are used for sorption enhanced chemical looping ethanol steam reforming.

#### 3.1 Catalyst

Catalysts used in ethanol steam reforming can be divided into 2 categories: noble metal and non-noble metal catalysts. The noble metal catalysts, i.e., Rh, Ru, Pd, Pt or Ir, are very active within a wide range of operating temperatures (350 - 800 °C). Excellent catalytic performance obtained from noble metal catalysts is due to excellent capability in C-C and C-O bond cleavage. Rh is found to be the most active noble metal for ethanol conversion and hydrogen production [17]. The Rh on CeO<sub>2</sub>-ZrO<sub>2</sub> support showed the highest yield of hydrogen under the temperature of 450 °C but the Rh / ZrO<sub>2</sub> is founded to facilitate the formation of C<sub>2</sub>H<sub>4</sub>, which could be the cause of rapid catalyst deactivation [18], while Rh/ Al<sub>2</sub>O<sub>3</sub> produced H<sub>2</sub>, CO, and CO<sub>2</sub> selectively with higher CO yield and lower CH<sub>4</sub> yield [19, 20]. Frusteri and Freni [21] compared the performance of catalyst in terms of activity and stability, including Pd, Rh, Ni, and Co on MgO support. The Rh/MgO catalyst was the most active and stable material for steam reforming of ethanol. Ethanol conversion of Rh/MgO was 100 % during 25 h at 650 °C and 40,000 h<sup>-1</sup> of GSHV. While Pd/MgO catalyst had 60 % ethanol conversion and deactivated during the first 5 h of reaction. The Ni/MgO catalyst showed the best performance in term of hydrogen selectivity (95%) because Ni active in steam reforming reaction whereas Rh active in acetaldehyde decomposition and water-gas shift reaction. Moreover, coke formation during reaction at 40,000 h<sup>-1</sup> of GHSV for 20 h was analyzed by CHNS elementary analysis instrument. A very high coke formation was observed with Pd/MgO catalyst (12mg<sub>coke</sub>/g<sub>cat</sub> h). Breen and Burch [22] compared activity of various metals, including Pt, Pd, Rh, and Ni on alumina and ceria-zirconia support for ethanol steam reforming hydrogen production process at 400-750 °C with

a steam/ethanol molar ratio of 3:1. The results showed that support has an effect on the reaction. Alumina support on catalyst offered higher ethanol conversion than ceria/zirconia-supported catalysts because alumina support is active in the dehydration of ethanol to ethylene at low temperature. After that ethylene react with water by steam reforming reaction to produce H<sub>2</sub> and CO. The Pt and Rh catalysts are more active than Pd or Ni when considered in term of product distribution (hydrogen 92%). The Pt and Rh catalysts showed complete ethanol conversion at high space velocity and temperature of 650 °C. Fabien and Yang [10] investigated the effect of different metals (Rh, Pt, Pd, Ru, Ni, Cu, Zn, Fe) and supports (Al<sub>2</sub>O<sub>3</sub>, 12%CeO<sub>2</sub>-Al<sub>2</sub>O<sub>3</sub>, CeO<sub>2</sub>, CeO<sub>2</sub>-ZrO<sub>2</sub>, ZrO<sub>2</sub>) at temperature of 600 and 700 °C with a steam/ethanol molar ratio of 3. The result from this research was divided into 2 parts. The first part was a study of the effect of Al<sub>2</sub>O<sub>3</sub> support on hydrogen selectivity. The Rh and Ni on Al<sub>2</sub>O<sub>3</sub> support catalysts provided high active and selective to hydrogen production for ethanol steam reforming at temperature 700°C under atmospheric pressure, whereas the Rh, Pt, Pd, Cu, Zn, Fe on Al<sub>2</sub>O<sub>3</sub> support catalysts showed low hydrogen selectivity. Ru catalyst was inactive in steam reforming but active in ethanol dehydration reaction, leading to the production of ethylene (38%). In the second part, the role of the oxide support on Rh and Ni catalysts was considered. The 1%Rh/Al<sub>2</sub>O<sub>3</sub> catalyst showed the highest hydrogen selectivity (73.5%) while 1%Rh/CeO<sub>2</sub>-ZrO<sub>2</sub> offered the highest hydrogen yield (5.1 g/h g catalyst) at temperature 600°C under steam/ethanol ratio of 3. He and Yang [23] studied the effect of transition metal oxide support (activated carbon, ZrO<sub>2</sub>, TiO<sub>2</sub> and CeO<sub>2</sub> nanoparticles) for Pt catalyst to produce hydrogen from bioethanol. The catalysts were synthesized with incipient wetness impregnation method. The results showed that Pt on CeO<sub>2</sub> support provided the highest ethanol conversion (85%) while Pt on activated carbon showed the lowest ethanol conversion (40%) (water/ethanol molar ratio equal 3:1 at temperature 300 °C and the atmospheric pressure). The activity of each material is in the order: Pt/CeO<sub>2</sub> < Pt/ZrO<sub>2</sub> < Pt/TiO<sub>2</sub> < Pt/C. After the activity test, amount of coke formation and their species were determined using temperature-programmed oxidation (TPO). The results showed that Pt/CeO<sub>2</sub> catalyst had no coke formation on the surface of catalyst during 5 h after reaction because Pt

and CeO<sub>2</sub> has stronger interaction between each other. On the other hand, Pt/ZrO<sub>2</sub> and Pt/ TiO<sub>2</sub> had high intensity of CO<sub>2</sub> evolution peak. The coke formation was found to be graphite-like carbon species. Goula and Kontou [24] investigated catalytic activity, selectivity, and catalyst stability for different reaction temperatures (220 °C to 700 °C) with the steam/ethanol ratios (3, 4.5, 9, 15). The 5 wt.% Pd/Al<sub>2</sub>O<sub>3</sub> catalyst showed high activity in terms of hydrogen selectivity (98%) and stability (30 h in stream) under steam/ethanol ratio of 9 at the temperature 600 °C.

The second category of catalyst is the non-noble metal catalyst. It was found that using non-noble metal requires greater amount of metal loading than noble metal typically 10 - 25 wt. %. Aupretre and Descorme [25] compared the performance of noble metal (1% Rh) and non-noble metal (10% Ni) on Al<sub>2</sub>O<sub>3</sub> support for hydrogen production from bioethanol steam reforming. The results showed Ni supported on Al<sub>2</sub>O<sub>3</sub> offered the most active and hydrogen selective under the temperature 600°C steam/ethanol ratio of 3 because Ni catalyst has high selectivity for water-gas shift reaction than Rh catalyst. The author also found that Ni is more effective and cheaper than noble metal.

**Table 3.1** Summary of catalysts and supports used for ethanol steam reforming

Catalyst	Condition		Ethanol conversion	Hydrogen concentration	Ref.
	T (°C)	S/E			
Noble metal					
1%Rh/Ce <sub>0.13</sub> Zr <sub>0.87</sub> O <sub>2</sub>	450	4	100	90	[2]
3%Rh/MgO	650	8.5	99	91	[3]
5%Ru/ Al <sub>2</sub> O <sub>3</sub>	800	3	100	96	
0.5Pt/ Al <sub>2</sub> O <sub>3</sub>	340	4	95	40	
Ru/ CeO <sub>2</sub> /YSZ	580	5	100	86.6	
1%Rh/ Al <sub>2</sub> O <sub>3</sub>	600	3	-	73.5	[8]
1%Pt/Al <sub>2</sub> O <sub>3</sub>				46	
0.75%Pd/Al <sub>2</sub> O <sub>3</sub>				55	
0.67%Ru/c-Al <sub>2</sub> O <sub>3</sub>				38	

Non-noble metal					
9.7%Ni/Al <sub>2</sub> O <sub>3</sub>	700	3	-	76	[8]
10%Ni/12%CeO <sub>2</sub> -Al <sub>2</sub> O <sub>3</sub>				65	
10%Ni/CeO <sub>2</sub>				63	
10%Ni/ZrO <sub>2</sub>				68.5	
8.7%Fe/ Al <sub>2</sub> O <sub>3</sub>				44	
9.1%Cu/Al <sub>2</sub> O <sub>3</sub>				40	
10% Ni-W/Al <sub>2</sub> O <sub>3</sub>	500	4	100	66.25	[11]
10% Ni-W/Al <sub>2</sub> O <sub>3</sub>	600			70	
30% Ni-W/Al <sub>2</sub> O <sub>3</sub>	500			67.47	
30% Ni-W/Al <sub>2</sub> O <sub>3</sub>	600			69.94	
6Ni-1.2Au/SBA-15	550	3	100	82	[12]

### 3.2 Sorbent

Sorbent applied for CO<sub>2</sub> capture in sorption enhanced ethanol steam reforming reaction should possess the following properties:

- (1) High selectivity toward carbon dioxide at high temperature.
- (2) High adsorption capacity.
- (3) High adsorption rate for carbon dioxide at operating conditions.
- (4) Recyclability for repeated adsorption.
- (5) Stable adsorption capacity of carbon dioxide after repeated adsorption/regeneration cycles.

From literatures, sorbent such as lithium zirconate [26], sodium zirconate [27, 28], calcium oxide [29-31], or hydrotalcite [32] have been used to adsorb CO<sub>2</sub>. Calcium oxide was widely used because sorption and desorption kinetics are fast. In addition, CaO is high CO<sub>2</sub> sorption capacity and low cost. The calcium carbonate has been widely

used as CaO precursor because it is abundant in nature. Fernandez and Ronning [26] compared CaO with other solid adsorbents such as  $\text{Li}_2\text{ZrO}_3$ , K-doped  $\text{Li}_2\text{ZrO}_3$ ,  $\text{Na}_2\text{ZrO}_3$  and  $\text{Li}_4\text{SiO}_4$  in terms of capacity and stability. CaO showed high sorption capacity and fast  $\text{CO}_2$  sorption greater than  $\text{Na}_2\text{ZrO}_3$  and lithium-based sorbent at the temperature  $575^\circ\text{C}$  under 100%  $\text{CO}_2$ . Summary of different adsorbent types for  $\text{CO}_2$  capture are shown in Table 3.2.

**Table 3.2** Overview of adsorbents for carbon dioxide capture [33]

Material	Temperature ( $^\circ\text{C}$ )	$\gamma_{\text{CO}_2}$ (mol/mol)	Adsorption capacities (mol $\text{CO}_2$ /Kg sorbent)
Calcium oxide	300-700	0.05-1	2.1-17.3
Hydrotalcites	300-500	0.15-1	0.2-1.8
Basic Aluminas	300-500	1	0.4-0.8
Carbons	300	1	0.3
Basic Zirconias	400-600	1	3.0-6.1
Basic Silicas	500-700	0.05-1	0.5-8.2

CaO could be derived from natural sources such as limestone, dolomite or huntite etc., or synthesized from different precursors, for example,  $\text{Ca}(\text{OH})_2$ ,  $\text{Ca}(\text{NO}_3)_2$  and  $\text{Ca}(\text{CH}_3\text{COO})_2$ . CaO obtained from natural mostly contains different mineral impurities, which in some cases have negative effects on  $\text{CO}_2$  sorption applications. For example, the present of  $\text{SiO}_2$  in CaO showed negatively affect to material stability because melting point of  $\text{SiO}_2$  leads to the change of particle morphology. On the other hand, synthetic CaO can control textural and chemical properties of CaO easier than CaO obtained from natural. As a consequence, synthetic CaO is attractive for specific industrial requirements. Lu and Reddy [34] prepared CaO from different precursors, including calcium nitrate tetra hydrate, calcium oxide, calcium hydroxide, calcium carbonate, calcium acetate monohydrate for capture of carbon dioxide at high temperature. The preparation of sorbents was heated to the temperature  $750^\circ\text{C}$  for 30 min. CaO synthesized from calcium acetate monohydrate precursor showed high

surface area 20.2 m<sup>2</sup>/g and pore volume (0.23 cm<sup>3</sup>/g). At 600 °C under 30% v/v CO<sub>2</sub>, CaO derived from calcium acetate displayed ca. 97% conversion during 5 h carbonation process. Santos and Alfonsin [35] compared the performance of CaO synthesized from calcium carbonate with CaO synthesized from calcium nitrate precursor. The CaO from calcium carbonate was prepared by calcination at 800° C for 3 h, whereas CaO from calcium nitrate was synthesized using sol-gel method. The surface area of CaO from calcium nitrate is 45 m<sup>2</sup>/g, which is larger than that of CaO derived from calcium carbonate (8 m<sup>2</sup>/g). The conversion of CaO from sol-gel method is 90% conversion at 700 °C for 15% v/v CO<sub>2</sub>. Meanwhile, the stability of CaO from sol-gel method was tested under calcination-carbonation cycles. The result showed the capacity constant at 0.58 g<sub>CO2</sub>/g<sub>CaO</sub> during the first 14 calcination-carbonation cycles.

Although CaO sorbent can offer high sorption capacity at high temperature but low stability upon multicycles is still faced. The improvement of CaO sorbent stability is therefore required and reviewed in this section. Lu and Khan [36] developed CaO-based sorbents by using various metal types, including Si, Ti, Cr, Co, Zr, and Ce. The addition of cobalt oxide, titania and zirconia on CaO could improve the conversion of CaO at 700 °C under 30 vol% CO<sub>2</sub> (N<sub>2</sub> Balanced) for 300 min. Moreover, the results showed that Zr-doped nanosorbents at ratio Zr:Ca (3:10) by wet impregnation exhibited stability for 100-multicycle carbonation-decarbonation testing because the ratio Zr:Ca (3:10) led to the formation of CaZrO<sub>3</sub> phase, which could prevent the growth of CaO particles as revealed by the results from XRD and TEM images. Radfarnia and Iliuta [37] studied the use of Al, Zr, Mg and Y to stabilize CaO. The optimum composition of Zr and Al stabilized CaO in term of the metal/Ca molar ratio was found to be 0.1, providing maximum activities of 0.29 g<sub>CO2</sub>/g<sub>sorbent</sub> and 0.33 g<sub>CO2</sub>/g<sub>sorbent</sub> for sorption temperature at 650 °C under 15vol% CO<sub>2</sub> (N<sub>2</sub> balanced) and desorption at 750 °C under 100 vol% argon. Luo and Zheng [38] improved the stability of CaO adsorption capacity for CO<sub>2</sub> capture during carbonation/calcination using La<sub>2</sub>O<sub>3</sub> and Al<sub>2</sub>O<sub>3</sub> in a fixed-bed reactor. The material was prepared by sol-gel method with the weight ratio of CaO : La<sub>2</sub>O<sub>3</sub> or Al<sub>2</sub>O<sub>3</sub> = 80:20. The addition of Al<sub>2</sub>O<sub>3</sub> to CaO formed inert Ca<sub>12</sub>Al<sub>14</sub>O<sub>33</sub> phase and it showed an enhancement of sorption capacity (73% conversion) during 11

cyclic reactions under 100% CO<sub>2</sub>. The main reason is the inert material Ca<sub>12</sub>Al<sub>14</sub>O<sub>33</sub> can prevent sintering and aggregation of CaCO<sub>3</sub> grain. Xu and Xie [39] compared percent of CaO mixing with Al<sub>2</sub>O<sub>3</sub> (CaO:70%,80%,90%) for CO<sub>2</sub> capture performance and stability. The reaction between CaO and Al<sub>2</sub>O<sub>3</sub> synthesized by sol-gel method showed the formation of Ca<sub>9</sub>Al<sub>6</sub>O<sub>18</sub> as an inert phase. The ratio 70:30 of CaO/Al<sub>2</sub>O<sub>3</sub> sorbent showed good performance for CO<sub>2</sub> capture as 96.4% conversion was observed in the 1<sup>st</sup> cycle and 90.9% conversion was observed in the 35<sup>th</sup> cycle under 15% CO<sub>2</sub> (N<sub>2</sub> balanced) at 650 °C and calcination at 800 °C under pure N<sub>2</sub>. Phromprasit and Powell [15] modified CaO sorbent by Mg, Sr and Al metals by wet mixing method. The sorbent CaO/Al<sub>2</sub>O<sub>3</sub> provided sorption capacity of 0.257 g<sub>CO2</sub>/g<sub>sorbent</sub> in the 1<sup>st</sup> cycle and 0.243 g<sub>CO2</sub>/g<sub>sorbent</sub> in the 10<sup>th</sup> cycle at sorption temperature of 600 °C. The addition of Al formed inert phase material, Ca<sub>12</sub>Al<sub>14</sub>O<sub>33</sub>, in the structure of CaO due to the formation of inert phase Ca<sub>12</sub>Al<sub>14</sub>O<sub>33</sub> prevented sintering of CaO while doping Mg metal covered only the surface of sorbent. Therefore, modification of CaO using Al metal showed good performance for stability at high temperature.

### 3.3 Multifunctional material

Modified CO<sub>2</sub> sorbent used in various high temperature cycles have been applied to sorption enhanced ethanol steam reforming process. The combination of catalyst and sorbent for multifunctional reactor is an important for mass transfusion of CO<sub>2</sub> molecule. The mass transfusion of multifunctional material was greater than convectional particles. Because, it can decrease distance between catalyst and sorbent. The mechanism of transfusion by conventional particle and multifunctional particle is shown in Figure 3.1. In a multifunctional particle the CO<sub>2</sub> molecule(C) can be adsorbed directly in the particle, while in a convectional CO<sub>2</sub> molecule (C) has to be transferred from catalyst particle via bulk phase into the adsorbent particle [40].

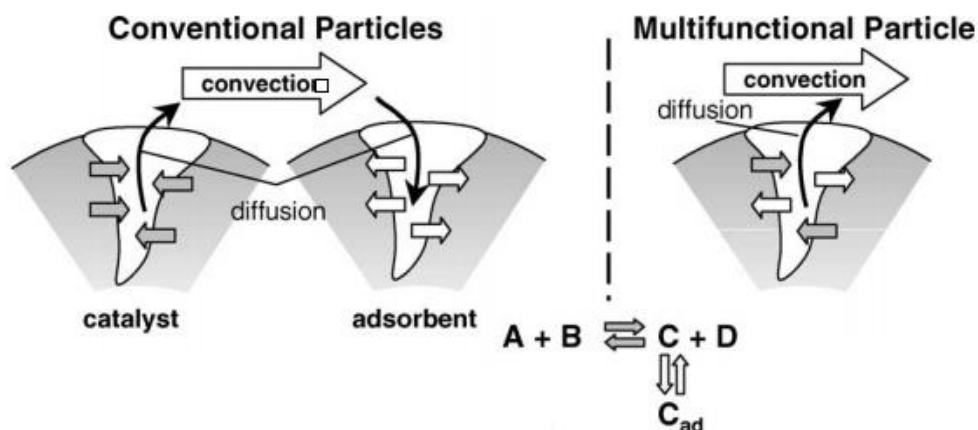


**Figure 3.1** The mechanism of transfusion by conventional and multifunctional [40].

Dewoolkar and Vaidya [32] investigated hydrotalcite-based (HTlc) materials in combination with reforming catalyst as hybrid system for sorption enhanced hydrogen production. The four different metals modified ( $Mg^{2+}$ ,  $Ca^{2+}$ ,  $Cu^{2+}$  and  $Zn^{2+}$ ) HTlc based-sorbents were investigated for sorption enhanced steam reforming of ethanol. The results showed copper-based hybrid material reported the highest adsorption capacity of 1.2 mol  $CO_2$ /kg sorbent at 300 °C producing almost 99 mol % hydrogen. The stability of hybrid materials was assessed over 25 cyclic tests under steam/ethanol ratio of 5. Gunduz and Dogu [1] studied the addition of Ni and Co metals on MCM-41 mesoporous support for steam reforming of ethanol (SRE) and sorption enhanced steam reforming of ethanol (SESRE) reactions. The Ni on MCM-41 catalyst showed high activity toward sorption enhanced ethanol reforming in term of hydrogen yield (5.6) in the pre-breakthrough stage during 40 min at reaction temperature 550° C. While the hydrogen yield of ethanol reforming reaction is 4.0 under the same condition. Wu and Zhang [13] used Ni–CaO– $Al_2O_3$  multifunctional material derived from hydrotalcite-like compounds (HTlcs) for sorption enhanced steam reforming of ethanol to produce hydrogen. The maximum adsorption of  $CO_2$  reached 24.8% at 500 °C over the ratio Ca/Al of 3.5 catalyst while the ratio Ca/Al of 3.0 catalyst performed the best considering balanced adsorption ability and catalytic activity in the SESRE process. The multifunctional material for sorption enhanced steam reforming of ethanol process summarized in Table 3.3



**Table 3.3** Summarize the use of multifunctional material for sorption enhanced steam reforming of ethanol process.

Catalyst	Condition		Ethanol conversion	Hydrogen concentration	Ref.
	T (°C)	S/E			
NiMgHTlc	400	9	100	80	[32]
NiCaHTlc				70	
NiCuHTlc				90	
NiZnHTlc				75	
Ni/MCM-41	500	3.2	100	90	[3]
Co/MCM-41				80	
Co-Ni/HTlc with CaO	500	10	100	N/A	[5]
Ni/Al <sub>2</sub> O <sub>3</sub> with Li <sub>4</sub> SiO <sub>4</sub>	627	6		87	
Ni/Al <sub>2</sub> O <sub>3</sub> with HTlc	400	10		21.8	
Cu-HTl	400	10		24.4	
Ni-HTlc	500	10		95.7	
K-Ni- HTlc	500	10		96.5	

Preparation method for multifunctional material is also found to affect properties of catalyst, such as, textural properties and morphology, etc. sol-mixing method is the mixing of soluble precursor with solid precursor. Pecharaumporn and Wongsakulphasatch [41] prepared one-body catalyst/sorbent material by sol-mixing method and wet-mixing method for sorption enhanced steam methane reforming process at temperature of 600 °C under atmospheric pressure and steam/methane ratio of 3. The SEM images of sol-mixing method showed the larger aggregated particles than wet-mixing method. In term of one-body catalyst/sorbent materials performance

found that the sol-mixing method showed the pre-breakthrough period about 30 min and 94% of hydrogen purity. The wet-mixing method had longer breakthrough period about 60 min with hydrogen purity of 88 %. The sol-gel method was developed in the 1960s because of the need of new synthesis methods in the nuclear industry. The sol-gel synthesis divided into three steps [42]. The first step is calling gelation(sol). In this step, the powder was dissolved in solution. Second step is hydrolysis and poly-condensation process of alkoxide or nitrate precursors that formed the gel. A gel is a interconnected, rigid network of particle. Lastly, gel was dry under ambient atmospheres. After drying process, we obtained the xerogel or aerogel. The different between xerogel and aerogel are the separation solvent. the xerogel is evaporation while aerogel is extraction of solvent. The process diagram of sol-gel method showed in Figure 3.2.

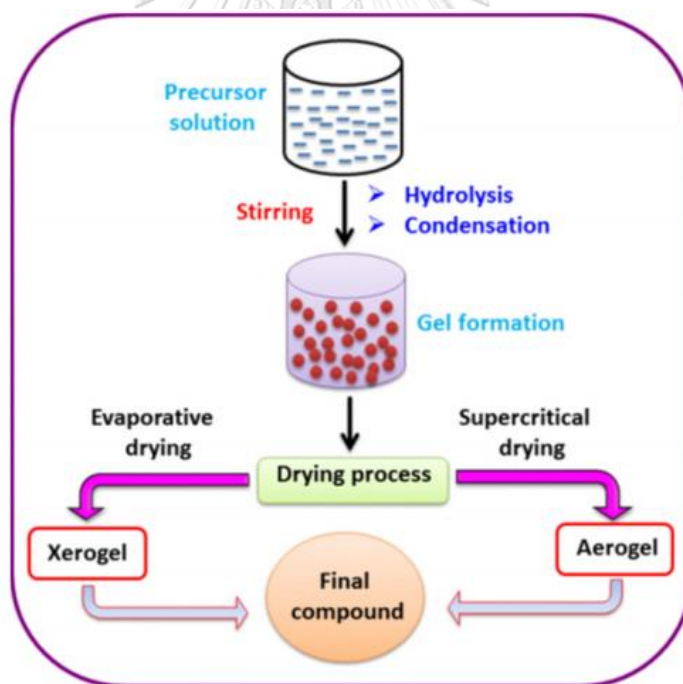


**Figure 3.2** Process diagram of sol-gel method. [43]

Yao and Yang [44] investigated the three different preparation method of Ni/Al<sub>2</sub>O<sub>3</sub> catalysts by co-precipitation, impregnation and sol-gel method for the pyrolysis-steam reforming of waste plastic. The catalyst activity was studied in term of the hydrogen

and carbon monoxide production at the temperature of 500°C at 40°C min<sup>-1</sup>. The result found that the Ni catalyst via sol-gel method showed a surface area of 305.21 m<sup>2</sup>/g higher than impregnation and co-precipitation. The sol-gel method showed the highest hydrogen yield of 98.36 mmol g<sup>1</sup><sub>plastic</sub> for polystyrene steam reforming. In addition, from the TPO results, the type of coke is filamentous form while co-precipitation method inhibited amorphous type. Zhao and Zhou [45] prepared the Ni/CaO-CaZrO<sub>3</sub> bi-functional catalyst by sol-gel method from sorption enhanced steam methane reforming. The hydrogen concentration of 15Ni/CaO-CaZrO<sub>3</sub> was 96 % dry basis during 40 min under temperature 600°C, steam/methane ratio of 3 at and pressure 1 bar. In addition, in this work studied the stability of catalyst. As the result, the present of CaZrO<sub>3</sub> can prevent the sintering of CaO particles.

### 3.4 Oxygen carrier (metal oxide)

The hydrogen production from sorption enhanced reforming process requires high temperature for the regeneration of sorbent; therefore, the reduction of external energy requirements for calcination reactor is required. The addition of oxygen carrier for energy supply in sorption enhance chemical looping ethanol steam reforming process has potential to carry out under self-sufficient condition. The benefits of the process are the elimination of WGS reactor and separation units in the process. Schematic sorption enhanced chemical looping reforming scheme is shown in Figure 3.3.

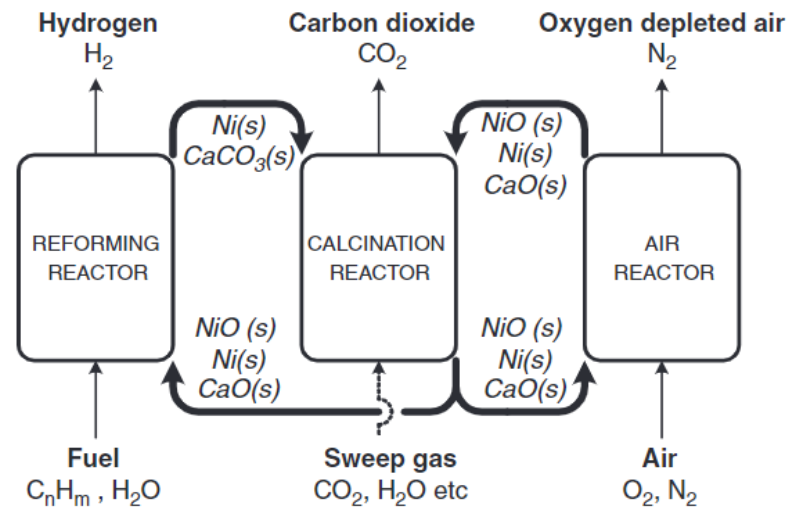


**Figure 3.3** Sorption enhance chemical looping reforming scheme. [46]

Oxygen carriers for sorption enhanced chemical looping reforming should provide good oxygen carrying capacity, high reaction rate, great mechanism strength and long-term stability. The common catalyst used as oxygen carrier are non-noble metal (Ni, Fe, Cu, Co, Mn). Wang and dou [47] studied the CeNi/SBA-15 oxygen carrier via chemical looping steam reforming of ethanol at 650 °C under atmospheric pressure with a steam to carbon ratio of 3 in a fixed-bed reactor. The oxygen carrier was prepared by impregnation method. NiO in the 12CeNi/SBA-15 was found to be ease for reducibility (30 s). In addition, the 12CeNi/SBA-15 showed high activity and stability in chemical looping ethanol steam reforming reaction. Hydrogen selectivity is 84.7% after 14 cycles stability test. Dou and Zhang [48] studied the effect of Ca/Ni molar ratio on hydrogen production via sorption enhanced chemical looping ethanol steam reforming process. The Ca/Ni molar ratio of 2 and 3 showed high hydrogen selectivity of 97% and 96%, respectively, at temperature of 600 °C, steam/carbon ratio of 3. Dou and Zhang [49] investigated the effect of NiO support for chemical looping steam reforming of ethanol, including NiO/SBA-15, NiO/MCM-41, NiO/MMT and NiO/Al<sub>2</sub>O<sub>3</sub>. The results showed that the rate of reduction for NiO/MCM-41 and NiO/SBA-15 were higher than NiO/MMT and NiO/Al<sub>2</sub>O<sub>3</sub> due to the difference in physicochemical and reduction kinetic of support material. The NiO/SBA-15 showed the highest hydrogen selectivity (88%) at

temperature 650 °C under atmospheric pressure, a mixture of steam and ethanol = 3. Chiu and Ku [50] compared properties of metal oxide, including Ni, Fe, Cu, Mn and Co for chemical looping steam reforming of ethanol as shown in Table 3.4. The Fe oxygen carrier showed the highest melting point, good mechanical strength, low cost and environmentally friendly. However, the reactivity of Fe catalyst is lower than those of Ni, Mn and Cu. Ni and Mn catalysts presented high oxygen capacity and reactivity. The main drawbacks of Ni and Mn are high cost, toxicity and carbon formation. On the other hand, Cu demonstrates similar oxygen capacity and reactivity to Ni and Mn but Cu both oxidation and reduction reactions are exothermic. As a consequence, heat requirement for the process can be supplied from the exothermic oxidation/reduction of CuO/Cu. Fernandez [56] explained the concept of calcium-copper chemical looping, involves (1) the production of hydrogen by reforming of ethanol reaction and carbonation reaction of sorbent, followed by (2) Oxidation of Cu by O<sub>2</sub> to form CuO under conditions of minimum calcination temperature, and (3) regeneration of CaCO<sub>3</sub> by mean of the reduction of CuO using natural gas, CO or H<sub>2</sub> [51]. Chen and Lin [52] studied the effect of Cu-Ni bi-metallic catalyst for ethanol steam reforming. The solely Cu catalyst offered almost 100 % conversion at 390 °C while the solely Ni catalyst needed 500 °C to reach 100 % conversion. This result show that Cu catalyst is more active than Ni at low temperature. However, bi-metallic Cu-Ni/SiO<sub>2</sub> with Cu/Ni ratio greater than or equal to 1 provided higher ethanol conversion than the solely Cu and Ni catalyst at temperature below 360 °C and steam/ethanol ratio of 6. Zheng and Sun [53] studied the effect of Fe-Cu-Ni catalyst for ethanol steam reforming. The 1.5%Fe-1.5%Cu-10Ni catalyst showed 70 % of hydrogen selectivity while the 10Ni catalyst demonstrated low hydrogen selectivity of 60 % at operating temperature of 450 °C. This result is due to the addition of Cu and Fe on Ni catalyst can decrease the byproduct, leading to high hydrogen selectivity; Cu is selective to water-gas shift reaction and ethanol dehydrogenation reaction, whereas, Fe is selective to methane steam reforming. Moreover, the stability of 1.5%Fe-1.5%Cu-10Ni catalyst was found to be stable during 24 h. Westbye and Aranda [54] combined CuO as O<sub>2</sub> carrier and CO<sub>2</sub> sorbent for calcium copper looping technology. The materials observed by TGA testing showed that 40 wt% of copper loading (Cu(OH)<sub>2</sub>) offered high sorption capacity and

maintained its properties for 40 cycles, while, the 50 wt% of copper loading lost sorption capacity during 40 cycles due to the formation of copper sheet.

**Table 3.4** Properties of metal oxide. [49]

Properties	Fe <sub>2</sub> O <sub>3</sub>	NiO	CuO	Mn <sub>3</sub> O <sub>4</sub>	CoO
Oxygen capacity (wt%)	30	21	20	20	21
Cost	Low	High	Medium	Medium	Medium
Reactivity	Medium	High	High	Medium	Low
Mechanical Strength	High	Low	Low	Medium	Medium
Impacts on Environment and Health	Medium	High	Medium	High	High
Reduction	endothermic	endothermic	exothermic	endothermic	endothermic

## CHAPTER 4

### EXPERIMENTAL

#### 4.1 Material

Calcium acetate monohydrate ( $C_4H_8CaO_5$ , POCH) and calcium chloride ( $CaCl_2$ , AJAX) were used as calcium precursors. Carbonate anhydrous ( $Na_2CO_3$ , AJAX) and urea ( $CO(NH_2)_2$ , AJAX) as carbonate precursor Aluminum nitrate aneahydrate ( $Al(NO_3)_3 \cdot 9H_2O$ , Ajax Finechem) and Nickel nitrate hexahydrate ( $Ni(NO_3)_2 \cdot 6H_2O$ , Sigma Aldrich) and copper nitrate ( $Cu(NO_3)_2 \cdot H_2O$ , KemAus) were used as nickle, copper and aluminum precursors. Citric acid ( $C_6H_8O_7$ ), AJAX as a metal-complex agent.

#### 4.2 Multifunctional material preparation

##### Preparation of sorbent (CaO)

CaO were prepared via precipitation method. In case of using sodium carbonate precursor ( $Na_2CO_3$ ) with calcium acetate ( $Ca(CH_3COO)_2$ ) or calcium chloride precursor ( $CaCl_2$ ), 250 ml of 2.5 M sodium carbonate anhydrous was mixed with 250 ml of 2.5 M of acetate hydrate or calcium chloride and stirred for 3 h at room temperature and standed it for 5 h. After that, the precipitate thus obtained was filtered and washed several times with de-ionized water. The resulting material was dried at 30 °C overnight, followed by calcined under air at 850 °C for 30 min. The resulting products named  $CaO_{Ac-Na}$  or  $CaO_{Cl-Na}$  were obtained. For the use of urea ( $CO(NH_2)_2$ ) as carbonate precursor with calcium acetate ( $Ca(CH_3COO)_2$ ) or calcium chloride precursor ( $CaCl_2$ ), 250 ml of 2.5 M urea was mixed with 250 ml of 2.5 M acetate hydrate or calcium chloride precursor and stirred at 90 °C for 24 h. The obtained precipitate was filtered and washed 3 times with de-ionized water. The resulting material was dried at 30 °C overnight, then calcined under air at 850 °C for 30 min. we obtain  $CaO_{Ac-Urea}$  or  $CaO_{Cl-Urea}$  was obtained.

### Preparation of multifunctional material

Multifunctional material (catalyst/sorbent) were synthesized by sol-mixing method. To prepare the material, nickel nitrate hexahydrate ( $\text{Ni}(\text{NO}_3)_2 \cdot 6\text{H}_2\text{O}$ ), aluminum nitrate nanohydrate ( $\text{Al}(\text{NO}_3)_3 \cdot 9\text{H}_2\text{O}$ ) and calcium oxide (CaO) from precipitation method were mixed in de-ionized water. The suspension stir for 3 h at room temperature and dried at 110 °C, and followed by calcination at 500 °C for 3 h in air. The precipitate was washed, dried at 110 °C overnight and calcined at 700 °C for 3 h and 900 °C for 1 h in air. Multifunctional catalyst 7%NiO/CaO- $\text{Ca}_{12}\text{Al}_{14}\text{O}_{33}$  was obtained.

**Table 4.1** Sample name of different precursors

Multifunctional material	Sample name
NiO/CaO (Cl-Na) - $\text{Ca}_{12}\text{Al}_{14}\text{O}_{33}$	Cl-Na
NiO/CaO (Cl-Urea) - $\text{Ca}_{12}\text{Al}_{14}\text{O}_{33}$	Cl-Urea
NiO/CaO (Ac-Na) - $\text{Ca}_{12}\text{Al}_{14}\text{O}_{33}$	Ac-Na
NiO/CaO (Ac-Urea) - $\text{Ca}_{12}\text{Al}_{14}\text{O}_{33}$	Ac-Urea

The preparation of catalyst from sol-gel method using citric acid as a metal-complex agent. The first step, a certain amount of calcium acetate monohydrate, nickel nitrate hexahydrate, aluminum nitrate aneahydrate and citric acid monohydrate (the ratio of citric acid to cation was 1.2) were dissolved in DI water. After that the solution was heated to 80°C for 2 h under reflux. Next, the ethylene glycol (the mass ratio of ethylene glycol to citric acid was 0.5) was added, and the mixed solution was continuously stirred under reflux for 6 h at 105 °C. Later, the gel was dried at temperature 110 °C 24 h. Finally, the powder was calcined at 850 °C with a heating rate of 10 °C/min.

The developed multi-functional material, containing NiO and CuO as oxygen carrier, CaO as sorbent and  $\text{Al}_2\text{O}_3$  as support, was used to produce hydrogen via



sorption-enhanced steam ethanol reforming chemical looping. Three different synthesis steps were studied in this work.

Pattern I: CuO/NiO-CaO-Ca<sub>12</sub>Al<sub>14</sub>O<sub>33</sub> (Cu/(Ni-CA))

NiO-CaO-Ca<sub>12</sub>Al<sub>14</sub>O<sub>33</sub> samples were prepared via sol-gel method. Nickel nitrate hexahydrate (Ni(NO<sub>3</sub>)<sub>2</sub>·6H<sub>2</sub>O, Sigma Aldrich), calcium acetate monohydrate (C<sub>4</sub>H<sub>8</sub>CaO<sub>5</sub>, POCH), aluminum nitrate annehhydrate (Al(NO<sub>3</sub>)<sub>3</sub>·9H<sub>2</sub>O, Ajax Finechem), and copper nitrate trihydrate (Cu(NO<sub>3</sub>)<sub>2</sub>·3H<sub>2</sub>O, Ajax Finechem) were used as precursors. The first Ni Ca and Al precursor was dissolved and stirred under 20 min. After that citric acid was employed to adjust the pH value of the solution. After hydrolysis at 105 °C for 6 h, the obtained gel was dried at 110 °C for 12 h, followed by calcination at 850 °C for 2 h. The obtained NiO/CaO-Ca<sub>12</sub>Al<sub>14</sub>O<sub>33</sub>. The last step, multifunctional material CuO/(NiO-CaO-Ca<sub>12</sub>Al<sub>14</sub>O<sub>33</sub>) was prepared by incipience impregnation. Copper nitrate trihydrate was used as copper precursor and solution was dried at 120 °C for 24 h followed by calcination at 850 °C for 2 h.

Pattern II: NiO /CuO-CaO-Ca<sub>12</sub>Al<sub>14</sub>O<sub>33</sub> (Ni/(Cu-CA))

CuO-CaO-Ca<sub>12</sub>Al<sub>14</sub>O<sub>33</sub> catalyst was prepared same the pattern I but the sequence of CuO was mix CaO and Al<sub>2</sub>O<sub>3</sub> in sol-gel method. after that Ni precursor was dissolved in solution and dropped in to CuO-CaO-Ca<sub>12</sub>Al<sub>14</sub>O<sub>33</sub>. The last step aqueous was dried at 110 °C for 24 h followed by calcination at 850 °C for 2 h.

Pattern III: NiO-CuO-CaO-Ca<sub>12</sub>Al<sub>14</sub>O<sub>33</sub> (Ni-Cu-CA)

Multifunctional material preparation by sol-gel method. Nitrate annehhydrate, copper nitrate trihydrate, calcium acetate monohydrate and aluminum nitrate annehhydrate were used as nickle, copper, calcium, aluminum precursors, respectively and critric acid was employed to adjust the pH value of the solution. After hydrolysis at 105 °C for 6 h, the obtained gel was dried at 110 °C for 12 h, followed by calcination at 850 °C for 2 h. the obtained NiO-CuO-CaO-Ca<sub>12</sub>Al<sub>14</sub>O<sub>33</sub>.

The sample composed by adding Cu after sol-gel method is denoted Cu/(Ni-CA) and sample composed by addition Ni after sol-gel method is named as Ni/(Cu-CA). For the single step method of Cu and Ni is donated as Ni-Cu-CA. The pattern of preparation method showed in Figure 4.1.

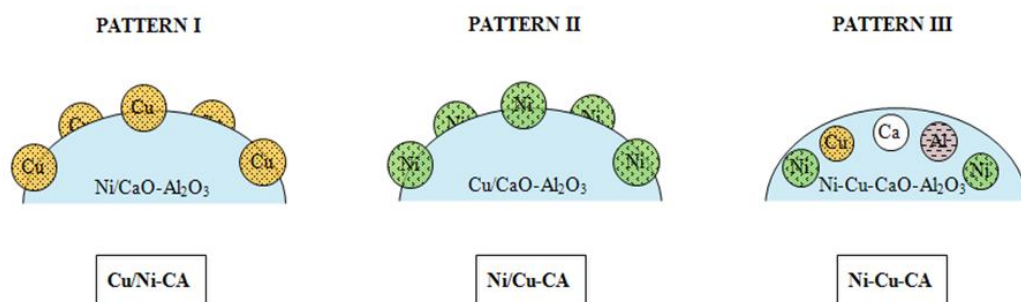


**Figure 4.1** Schematic of preparation method.

### 4.3 Characterization of material

#### 4.3.1 X-ray diffraction technique

X-ray diffraction (XRD) technique was used to specify the type of compounds and determine the crystalline structure of catalyst. The XRD was examined qualitative and quantitative. The specific lattice planes produce peaks at their corresponding angular positions  $2\theta$ , determined by Bragg's law (Eq.4.1) [55].

$$2d\sin\theta = n\lambda \quad (4.1)$$

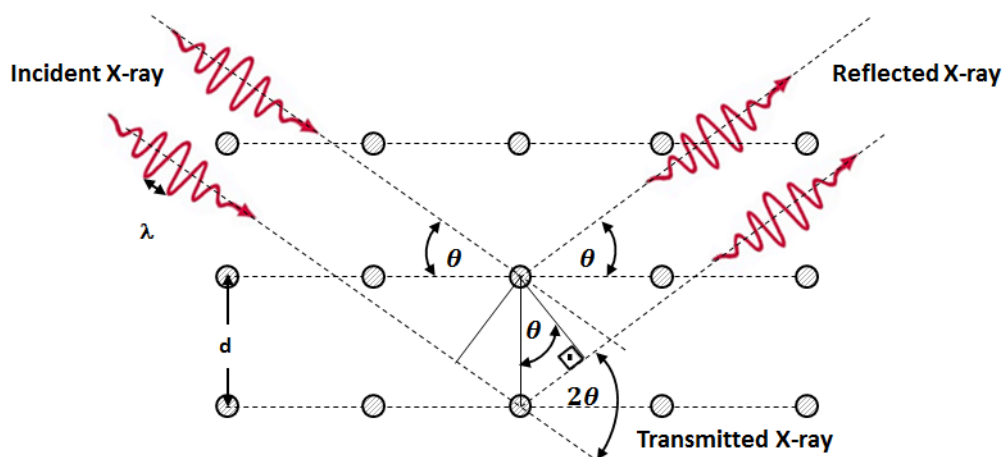


Figure 4.2 Diagram of Bragg's law [56]

Phases and crystallite sizes of multifunctional materials were determined by X-ray diffraction technique (XRD) using a D8 Advance, Bruker equipped with a long fine focus Cu  $K\alpha$  X ray source. The XRD patterns were recorded at  $10^\circ < 2\theta < 80^\circ$  with a step of  $0.04^\circ$ , wavelength of 1.54056 nm and scan speed of 0.5 s/step

#### 4.3.2 N<sub>2</sub> adsorption/desorption isotherm

The surface area of each samples was determined by the Brunauer-EmmettTeller (BET) method using N<sub>2</sub> adsorption/desorption at  $-196^\circ\text{C}$  (Micromeritics Chemisorp 2750). Pore sizes and pore volumes of the samples were determined by desorption isotherm using BarretJoyner-Halender (BJH) method.

#### 4.3.3 Scanning electron microscope

Morphologies of the modified sorbents and multifunctional material (both fresh and used) were analyzed using a scanning electron microscope, SEM, (Hitachi S-71326122255 3400N) coupled with X-ray energy dispersive spectroscopy, X-ray EDS, (AMETEK EDAX, APOLLO X) for analyzing the local dispersion of elements in the material.

#### 4.3.4 Thermogravimetric Analysis (TGA)

Thermogravimetric analysis is used for measuring the physical or chemical properties as functions of temperature. The thermal analysis can measure the properties such as

□ Structural changes (glass transition melting/crystallization, crosslinking, volatilization,

phase transitions in the solid and liquid state)

□ Mechanical properties (elastic behavior, damping)

□ Thermal properties (expansion/shrinkage, specific heat capacity, melting/crystallization temperature, coefficient of expansion)

□ Chemical reactions (decomposition and thermal stability in different gaseous environments chemical reactions in solutions or liquid phase, reactions with the purge gas, dehydration).

In this chapter the coke deposited on the surface catalyst was characterized by thermogravimetric analysis. For each thermal analysis, around 5 mg of spent catalyst was heat from 25 °C to 900 °C in air at a heating rate of 10 °C /min. The sample result from TGA-DTG equipment showed in Figure 4.3 [46].

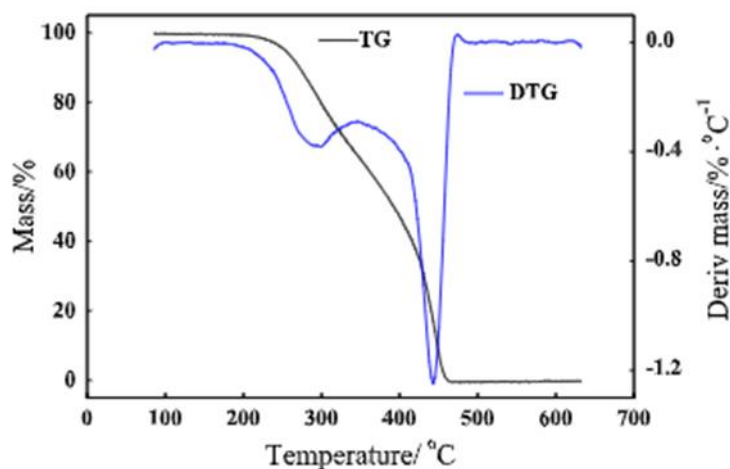
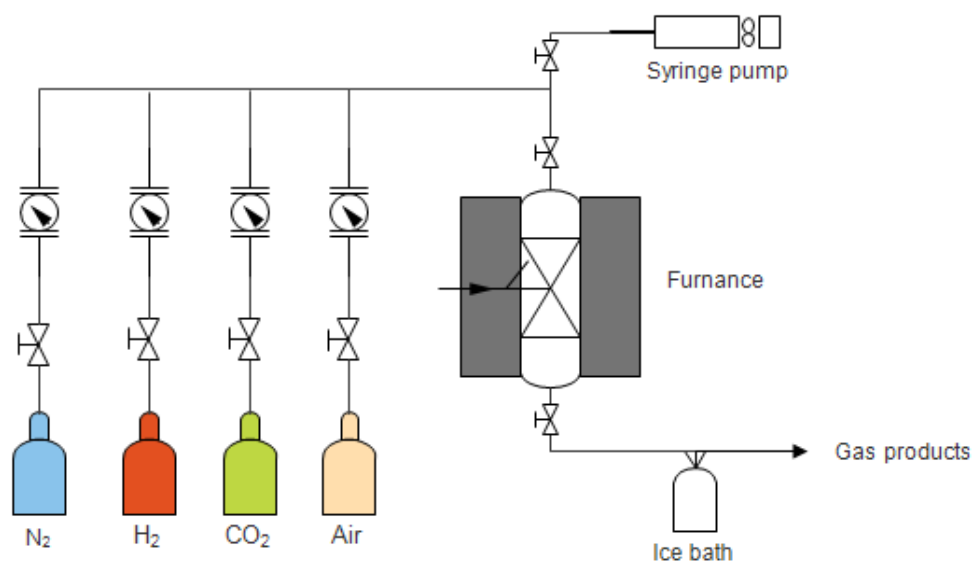


Figure 4.3 Sample result from TGA-DSC equipment [57]

#### 4.4 Hydrogen production

For each experiment, Three gram of catalyst was placed in the fixed bed reactor supported by quartz wool. The catalyst was pretreated at 850 °C for 30 min under 100% N<sub>2</sub> flow and then reduced by 10% hydrogen (balanced N<sub>2</sub>) at 850 °C for 1 h for elimination of moisture content from the catalyst. The temperature was thereafter decreased to the reaction temperature of 600 °C. The operating conditions were: a steam to ethanol molar ratio (S/E) of 4:1, balanced with N<sub>2</sub> at a total flow rate of 50 mL/min, temperature of 600 °C and pressure of 1 atm. The product gas compositions were measured by gas chromatography (GC-8A, SHIMADZU) equipped with two columns - Molecular Sieve 5A and PoraPLOT Q. Ethanol compositions was measured by flame ionization detector (FID). The conversion of feed and product selectivity were calculated using the following Equations (4.2), (4.3) respectively. Figure 4.4 shows the experimental set up for hydrogen production.



**Figure 4.4** Experimental set up for hydrogen production

Ethanol conversion:

$$\text{Conversion (C}_2\text{H}_5\text{OH): (X) (\%)} = \frac{F_{\text{Ethanol,in}} - F_{\text{Ethanol,Out}}}{F_{\text{Ethanol,in}}} \times 100 \quad (4.2)$$

where  $F_{\text{Ethanol,in}}$  is molar flow rate of ethanol at the inlet steam and  $F_{\text{Ethanol,out}}$  is molar flow rate of ethanol at the outlet steam

Selectivity of products:

$$\text{Selectivity: S (\%)} = \frac{n_i}{\sum_n n_i} \times 100 \quad (4.3)$$

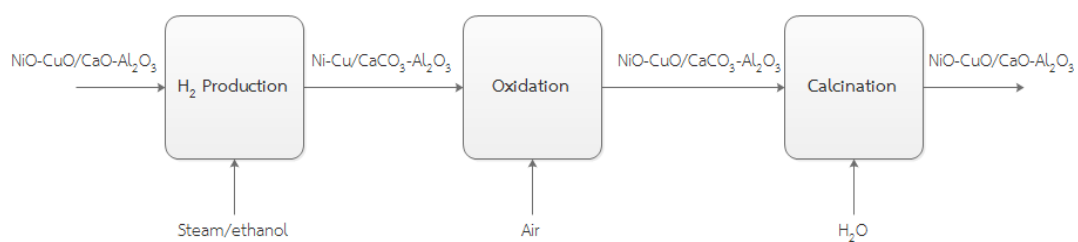
where  $n_i$  is the number of moles of each product, and  $\sum_n n_i$  is the sum of the number of moles of all gaseous products. In the case of sorption enhanced steam ethanol reforming chemical looping process for hydrogen production, it is the same method of sorption enhanced steam ethanol reforming without the reduction of catalyst with hydrogen. Operating conditions were a steam to ethanol molar ratio (S/E) of 3:1, balanced with  $\text{N}_2$  at a total flow rate of 50 mL/min, temperature of 500 °C and pressure of 1 atm.

#### 4.5 The single cycle for sorption enhanced steam ethanol reforming chemical looping

Single cycle divided into 5 step as showed in Table. 4.2. First step is hydrogen production. The ethanol and steam was fed to reactor with total flow rate of 50 mL/min at the temperature of 500 °C. After that,  $\text{N}_2$  was fed for gas sweeping to prepare for next step. In the oxidation step,  $\text{O}_2$  carrier was oxidized at 500 °C with air flow rate of 30 mL/min. The next step is heating. The reactor was heated from 500 °C to 800° C with a rate of 10°C/min. The last step is regeneration of sorbent at the temperature of 800 °C with steam flow rate of 10 mL/min.

**Table 4.2** Condition for single cycle.

	Temperature (°C)	N <sub>2</sub> (ml/min)	Air (ml/min)	Steam/ethanol (ml/min)	H <sub>2</sub> O (ml/min)
Hydrogen production	500	30	0	20	0
N <sub>2</sub> sweeping	500	30	0	0	0
Oxidation	500	0	30	0	0
Heating	500-800	30	0	0	0
Calcination	800	30	0	0	10

**Figure 4.5** Single cycle for sorption enhanced steam ethanol reforming

CHULALONGKORN UNIVERSITY  
chemical looping

## CHAPTER 5

## RESULTS AND DISCUSSION

### 5.1 Influence of calcium oxide precursor on hydrogen production from sorption enhanced ethanol steam reforming

#### 5.1.1 Characteristic of multifunctional material

Composition and crystallinity of synthetic multifunctional materials were characterized by X-ray diffraction technique (XRD) as shown in Figure 4.1. Diffraction peaks of CaO are observed at  $2\theta = 32.2, 37.4$  and  $53.9$  [58], and the peaks assigned to NiO at  $2\theta = 43.1, 62.65$  [59] is detected in all samples. The formation of calcium aluminate cement ( $\text{Ca}_{12}\text{Al}_{14}\text{O}_{33}$ ) is observed at  $2\theta = 18, 29.8, 36.4, 40.9, 54.9$ . [58]

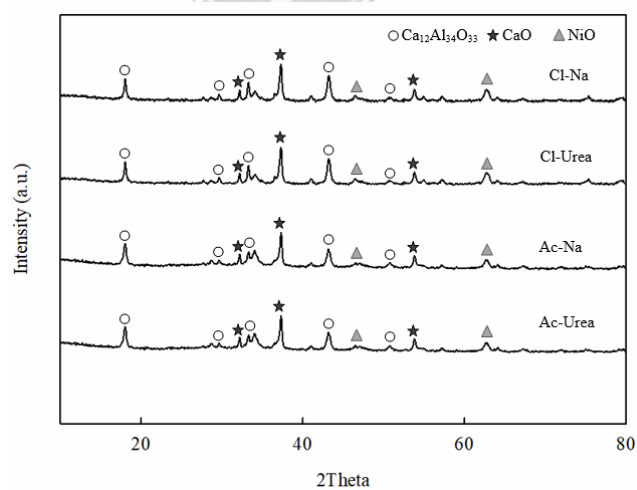


**Figure 5.1** XRD pattern of multifunctional materials synthesized from different CaO precursors (Cl-Na, Cl-Urea, Ac-Na, Ac-Urea).



Surface morphology of multifunctional catalysts detected by scanning electron microscopy (SEM) is demonstrated in Figure 5.2. The morphology of all catalysts showed connection of small particles with void space among the particles. Distribution of Ni metal and percent weight of loading on the catalyst surface were determined by energy dispersive x-ray spectroscopy (EDX) technique as shown in Figure 5.3. The result of NiO/CaO<sub>Cl-Na</sub>-Ca<sub>12</sub>Al<sub>14</sub>O<sub>33</sub>, NiO/CaO<sub>Ac-Na</sub>-Ca<sub>12</sub>Al<sub>14</sub>O<sub>33</sub> and NiO/CaO<sub>Ac-Urea</sub>-Ca<sub>12</sub>Al<sub>14</sub>O<sub>33</sub> shows a good dispersion of Ni metal. While, NiO/CaO<sub>Ac-Na</sub>-Ca<sub>12</sub>Al<sub>14</sub>O<sub>33</sub> presents low Ni metal dispersion. The percent weight of metal loading at surface of sorbent was showed in Table 5.1. The percent weight of NiO/CaO<sub>Ac-Urea</sub>-Ca<sub>12</sub>Al<sub>14</sub>O<sub>33</sub> shows the highest metal loading at surface of 5.86 %.

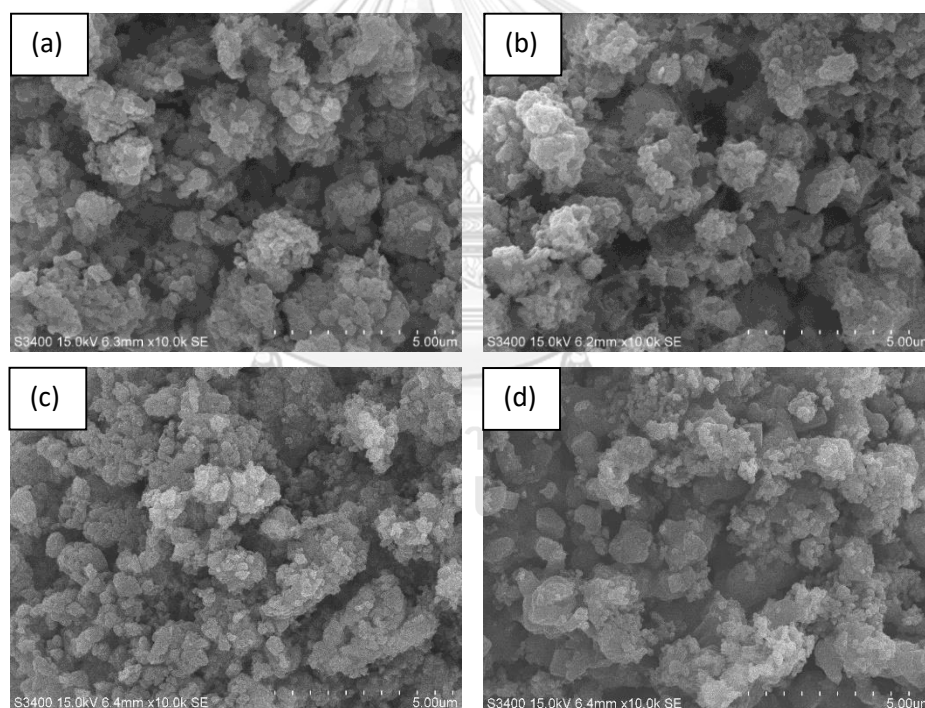


**Figure 5.2** SEM image of multifunctional catalyst

a) Cl-Na b) Cl-Urea c) Ac-Na d) Ac-urea

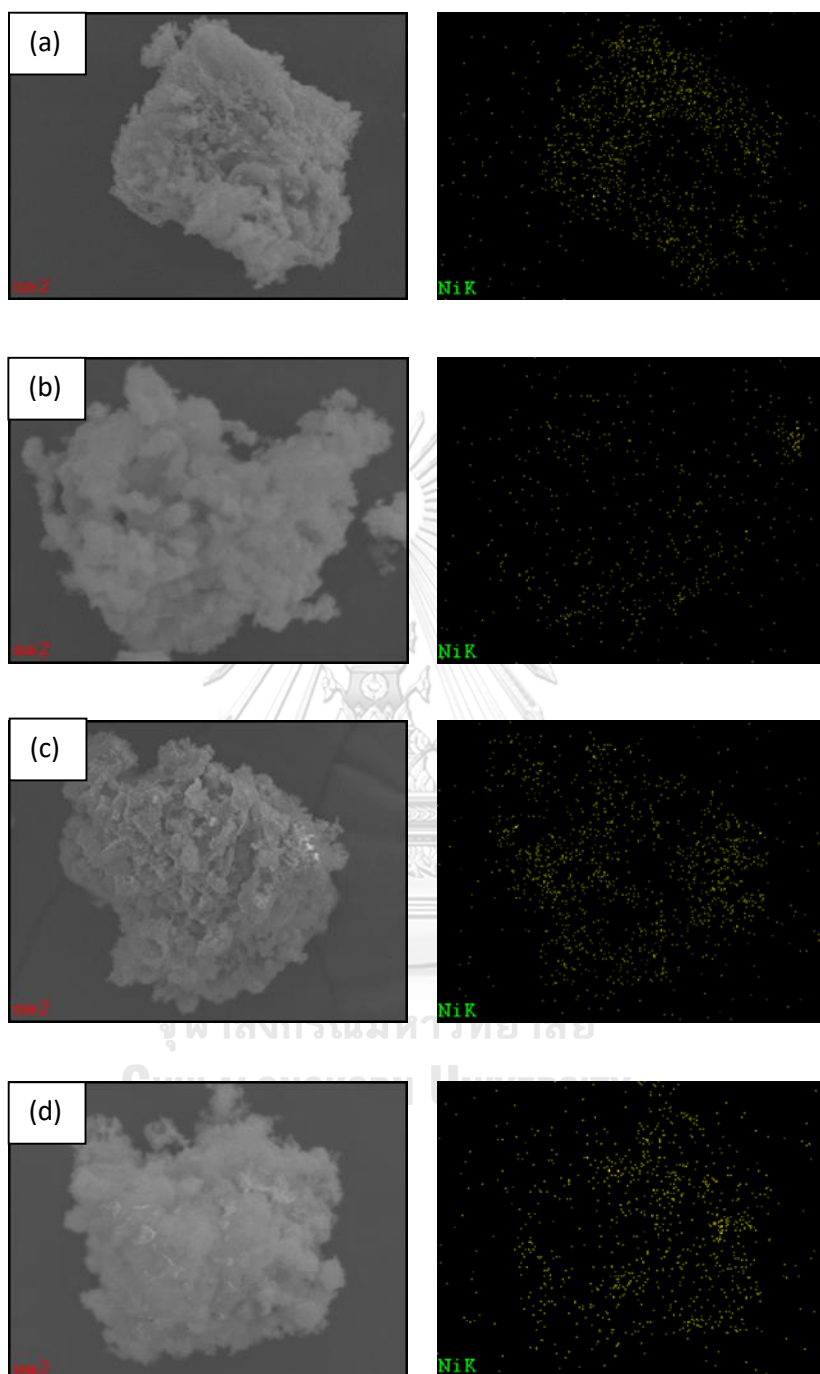


**Figure 5.3** Dispersion of Ni metal in multifunctional catalyst from EDX

a) Cl-Na b) Cl-Urea c) Ac-Na d) Ac-urea

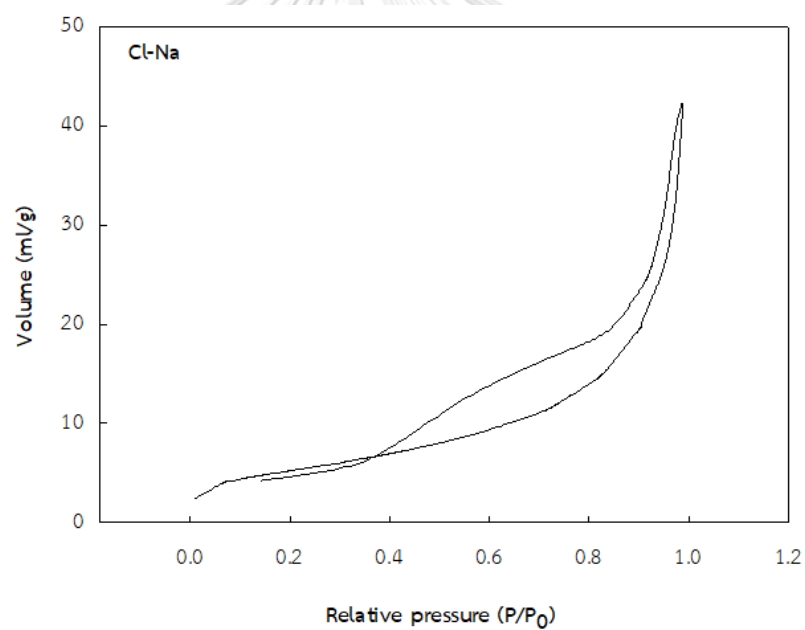
**Table 5.1** Composition of metal at surface of catalyst by EDX

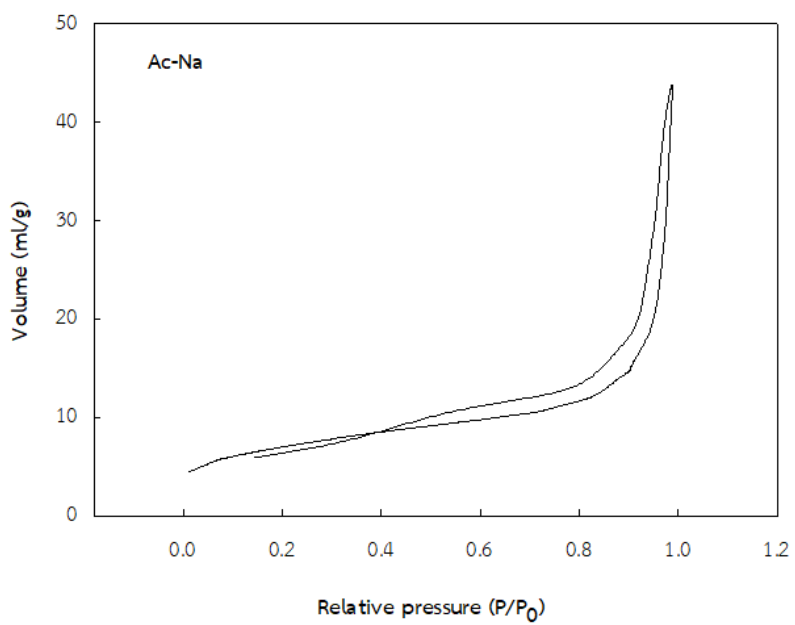
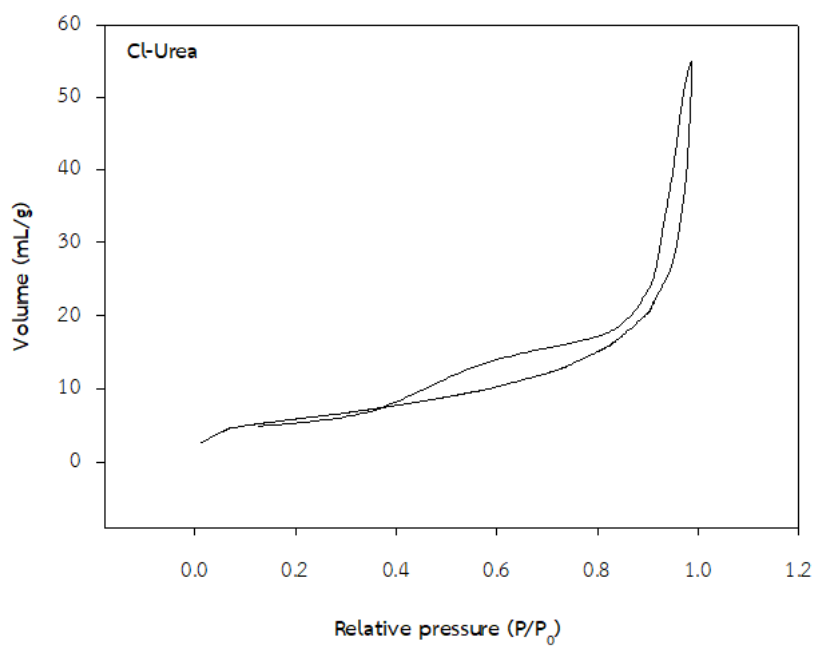
Sample	% Ni
NiO/CaO <sub>Cl-Na</sub> -Ca <sub>12</sub> Al <sub>14</sub> O <sub>33</sub>	5.68
NiO/CaO <sub>Cl-Urea</sub> -Ca <sub>12</sub> Al <sub>14</sub> O <sub>33</sub>	5.55
NiO/CaO <sub>Ac-Na</sub> -Ca <sub>12</sub> Al <sub>14</sub> O <sub>33</sub>	5.23
NiO/CaO <sub>Ac-Urea</sub> -Ca <sub>12</sub> Al <sub>14</sub> O <sub>33</sub>	5.86

Textural properties of multifunctional material including surface area, pore volume and pore size were measured by N<sub>2</sub> adsorption-desorption isotherm as shown in Figure 5.4 and Table 5.2. The isotherm type of all catalysts show type IV according to the IUPAC classification [60] as shown in Figure 5.4, indicating mesoporous (2-50 nm) structure of catalyst. The NiO/CaO<sub>Cl-Na</sub>-Ca<sub>12</sub>Al<sub>14</sub>O<sub>33</sub> catalyst shows surface area of 21.02 m<sup>2</sup>/g with the lowest pore volume of 0.05 cm<sup>3</sup>/g and pore size diameter of 6 nm, respectively. The NiO/CaO<sub>Cl-Urea</sub>-Ca<sub>12</sub>Al<sub>14</sub>O<sub>33</sub> shows the lowest surface area of 20.09 m<sup>2</sup>/g, pore volume of 0.07 cm<sup>3</sup>/g and pore size diameter of 9 nm. The NiO/CaO<sub>Ac-Na</sub>-Ca<sub>12</sub>Al<sub>14</sub>O<sub>33</sub> shows surface area of 23.08 m<sup>2</sup>/g, the highest pore volume of 0.07 cm<sup>3</sup>/g and pore size diameter of 9 nm. The NiO/CaO<sub>Ac-Urea</sub>-Ca<sub>12</sub>Al<sub>14</sub>O<sub>33</sub> catalyst possesses the highest surface area of 28.07 m<sup>2</sup>/g, pore volume of 0.07 cm<sup>3</sup>/g and the highest pore size diameter of 10 nm.

**Table 5.2** Textural properties of multifunctional NiO/CaO-Ca<sub>12</sub>Al<sub>14</sub>O<sub>33</sub> catalysts

Sample	Surface area (m <sup>2</sup> /g)	Pore volume (cm <sup>3</sup> /g)	Pore size diameter (nm)
NiO/CaO <sub>Cl-Na</sub> -Ca <sub>12</sub> Al <sub>14</sub> O <sub>33</sub>	21.02	0.05	6
NiO/CaO <sub>Cl-Urea</sub> -Ca <sub>12</sub> Al <sub>14</sub> O <sub>33</sub>	20.09	0.07	9
NiO/CaO <sub>Ac-Na</sub> -Ca <sub>12</sub> Al <sub>14</sub> O <sub>33</sub>	23.08	0.09	9
NiO/CaO <sub>Ac-Urea</sub> -Ca <sub>12</sub> Al <sub>14</sub> O <sub>33</sub>	28.07	0.07	10





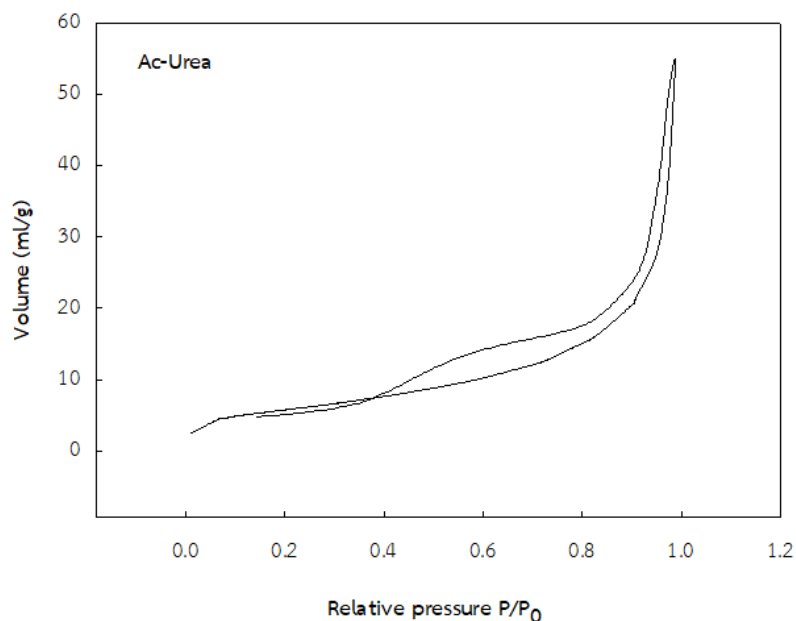
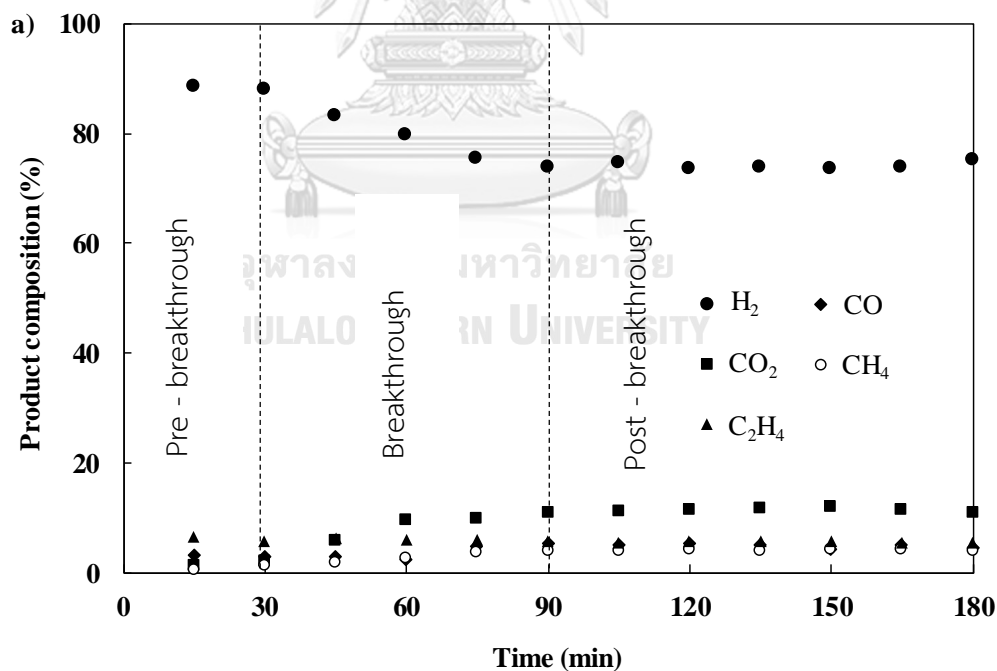


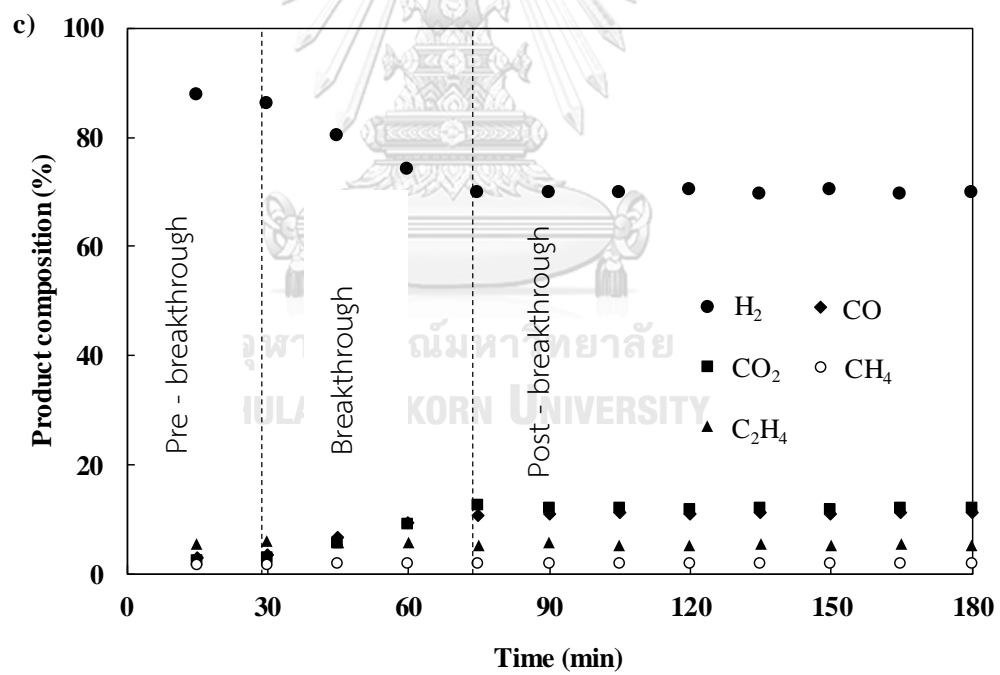
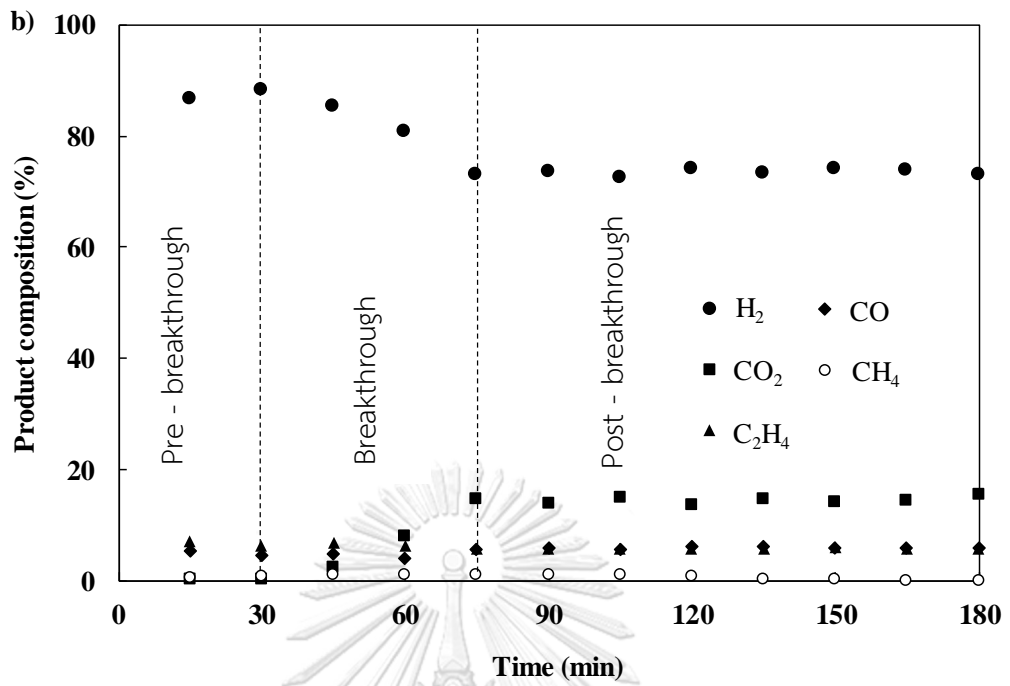
**Figure 5.4** Adsorption/desorption isotherm of NiO/CaO<sub>Cl-Na</sub>-Ca<sub>12</sub>Al<sub>14</sub>O<sub>33</sub>, NiO/CaO<sub>Cl-Urea</sub>-Ca<sub>12</sub>Al<sub>14</sub>O<sub>33</sub>, NiO/CaO<sub>Ac-Na</sub>-Ca<sub>12</sub>Al<sub>14</sub>O<sub>33</sub> and NiO/CaO<sub>Ac-Urea</sub>-Ca<sub>12</sub>Al<sub>14</sub>O<sub>33</sub>

#### 5.1.2 Effect of CaO precursors on hydrogen production via sorption enhanced ethanol steam reforming.

The effect of CaO precursor was studied in terms of hydrogen composition and CO<sub>2</sub> sorption capacity (pre-breakthrough period). The multifunctional catalysts were tested at temperature of 600 °C under ethanol/steam ratio about 4. The results of NiO/CaO<sub>Ac-Urea</sub>-Ca<sub>12</sub>Al<sub>14</sub>O<sub>33</sub> catalyst shows the longest pre-breakthrough period about 60 min with 88% of hydrogen purity. This result is due to particle of NiO/CaO<sub>Ac-Urea</sub>-Ca<sub>12</sub>Al<sub>14</sub>O<sub>33</sub> possesses high surface area and small particle size, which enhance the sorption performance of CaO for CO<sub>2</sub> adsorption. After 60 min the CaO sorbent is saturated with CO<sub>2</sub> leading to an increase of CO<sub>2</sub> concentration and a decrease of hydrogen concentration in the post-breakthrough period. Hydrogen concentration in post-breakthrough period is 70% as shown in Figure 5.5, which is a result of steam reforming reaction. The main products are H<sub>2</sub>, CO<sub>2</sub>, CO, CH<sub>4</sub> and C<sub>2</sub>H<sub>4</sub>. This observation could imply the reaction path way as ethanol dehydration reaction produces ethylene

(Eq.5.2) and ethanol dehydrogenation process produces  $C_2H_4O$  and  $H_2$  (Eq.5.3).  $C_2H_4O$  can be proceeded by decarbonylation to produce  $CH_4$  and  $CO$  (Eq.5.4). After that, the carbon monoxide was transformed into carbon dioxide and hydrogen through water gas shift reaction (Eq.5.5). Methane reacted with water via methane steam reforming to produce hydrogen and carbon monoxide (Eq.5.6). The  $NiO/CaO_{Cl-Na}-Ca_{12}Al_{14}O_{33}$  shows hydrogen purity of 88% in the pre-breakthrough period for 30 min. The  $NiO/CaO_{Cl-Urea}-Ca_{12}Al_{14}O_{33}$  presented the hydrogen purity with 86% in the pre-breakthrough period about 30 min.  $NiO/CaO_{Ac-Na}-Ca_{12}Al_{14}O_{33}$  demonstrated the hydrogen purity with 87% in the pre-breakthrough period at 30 min of the pre-breakthrough period. The result of  $NiO/CaO_{Cl-Na}-Ca_{12}Al_{14}O_{33}$ ,  $NiO/CaO_{Cl-Urea}-Ca_{12}Al_{14}O_{33}$  and  $NiO/CaO_{Ac-Na}-Ca_{12}Al_{14}O_{33}$  represented less  $CO_2$  sorption capacity at 30 min of the pre-breakthrough period due to the catalysts possesses low surface area and small pore size diameter, leading to adsorb  $CO_2$  molecules performance.







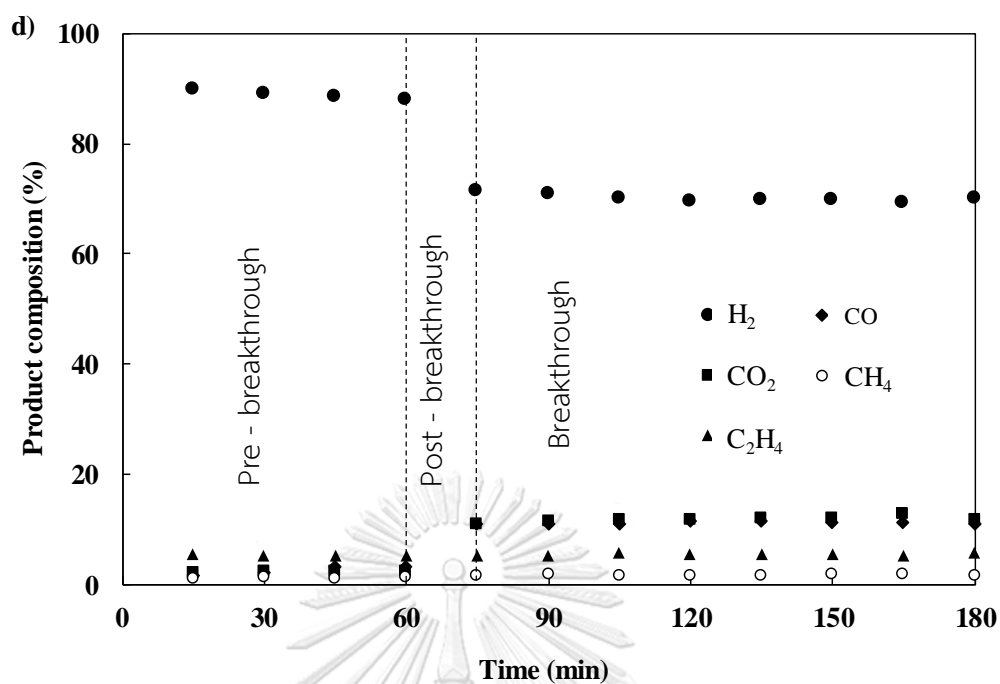
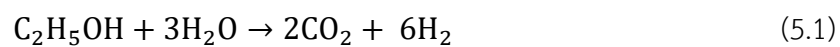


**Figure 5.5** Percent compositions from sorption enhanced ethanol steam reforming using multifunctional materials: a) NiO/CaO<sub>Cl-Na</sub>-Ca<sub>12</sub>Al<sub>14</sub>O<sub>33</sub>(Cl-Na), b) NiO/CaO<sub>Cl-Urea</sub>-Ca<sub>12</sub>Al<sub>14</sub>O<sub>33</sub>(Cl-Urea), c) NiO/CaO<sub>Ac-Na</sub>-Ca<sub>12</sub>Al<sub>14</sub>O<sub>33</sub>(Ac-Na), d) NiO/CaO<sub>Cl-Na</sub>-Ca<sub>12</sub>Al<sub>14</sub>O<sub>33</sub>(Ac-Urea). operating condition under temperature 600° C, steam/ethanol ratio of 4.

**Table 5.3** Hydrogen purity of all multifunctional catalyst

Sample	Pre-breakthrough time (min)	Hydrogen purity (%)
NiO/CaO <sub>Cl-Na</sub> -Ca <sub>12</sub> Al <sub>14</sub> O <sub>33</sub>	30	88
NiO/CaO <sub>Cl-Urea</sub> -Ca <sub>12</sub> Al <sub>14</sub> O <sub>33</sub>	30	86
NiO/CaO <sub>Ac-Na</sub> -Ca <sub>12</sub> Al <sub>14</sub> O <sub>33</sub>	30	87
NiO/CaO <sub>Ac-Urea</sub> -Ca <sub>12</sub> Al <sub>14</sub> O <sub>33</sub>	60	88

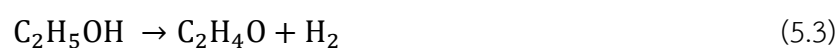
Ethanol steam reforming overall



Ethanol dehydration to ethylene



Ethanol dehydrogenation to acetaldehyde



Acetaldehyde decarbonylation to methane and carbon monoxide



Water gas shift (WGS)



Methane steam reforming



In addition, all multifunctional catalysts inhibit resistance the sintering effect this result is confirmed by image of SEM of spent catalyst as shown in Figure 5.5.

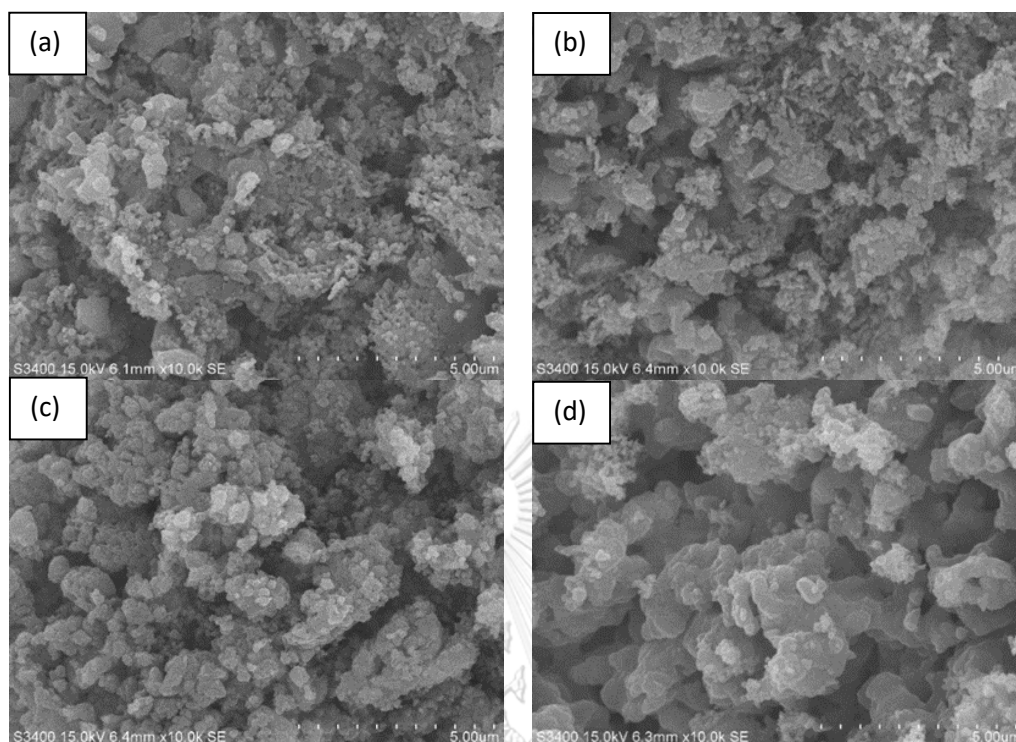


**Figure 5.6** SEM image of multifunctional catalyst

a) Cl-Na b) Cl-Urea c) Ac-Na d) Ac-urea

### 5.1.3 Stability test of multifunctional catalysts.

As seen in the previous section,  $\text{NiO}/\text{CaO}_{\text{Ac-Urea}}-\text{Ca}_{12}\text{Al}_{14}\text{O}_{33}$  provides the longest pre-breakthrough period, in this section, stability of  $\text{NiO}/\text{CaO}_{\text{Ac-Urea}}-\text{Ca}_{12}\text{Al}_{14}\text{O}_{33}$  was tested over 10 cycles of repeated sorption enhanced ethanol steam reforming as shown in Figure 5.7. The result shows that hydrogen purity can be maintained at 88% in the pre-breakthrough period over 10 cycles at the temperature of  $600^\circ\text{C}$  and regeneration  $\text{CaCO}_3$  at temperature of  $850^\circ\text{C}$ . The  $\text{NiO}/\text{CaO}_{\text{Ac-Urea}}-\text{Ca}_{12}\text{Al}_{14}\text{O}_{33}$  multifunctional catalyst demonstrated the good performance in term of catalytic/sorption and stability for sorption enhanced ethanol steam reforming. This observation is due to well dispersed of Al ( $\text{Ca}_{12}\text{Al}_{14}\text{O}_{33}$ ) in catalyst as shown in Figure 5.8, leading to the prevent of CaO sintering [15].

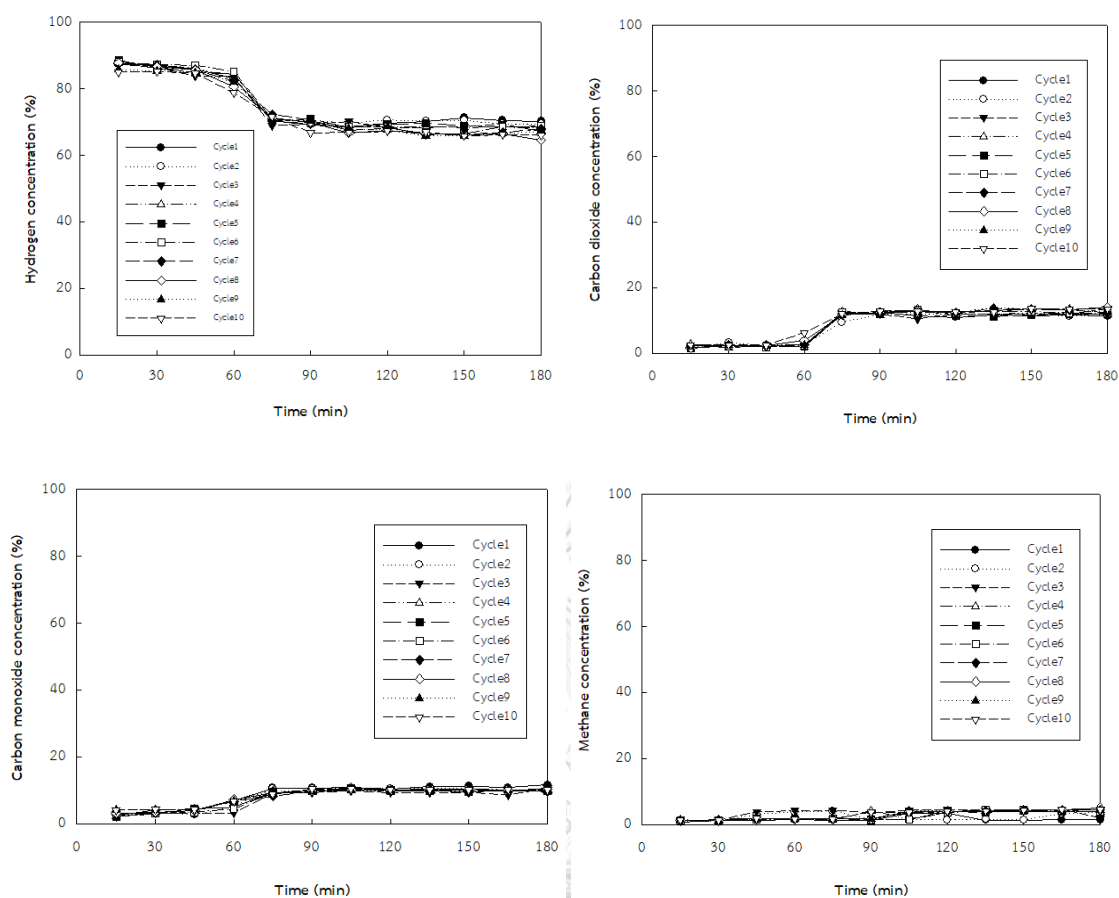


**Figure 5.7** Gas product compositions of 6% Ac-urea: (a) hydrogen concentration, (b) carbon monoxide concentration, (c) methane concentration and (d) carbon dioxide concentration reaction condition: under temperature 600 °C, steam/ethanol ratio of 4 and regeneration  $\text{CaCO}_3$  at temperature 850 °C under  $\text{N}_2$  flow.

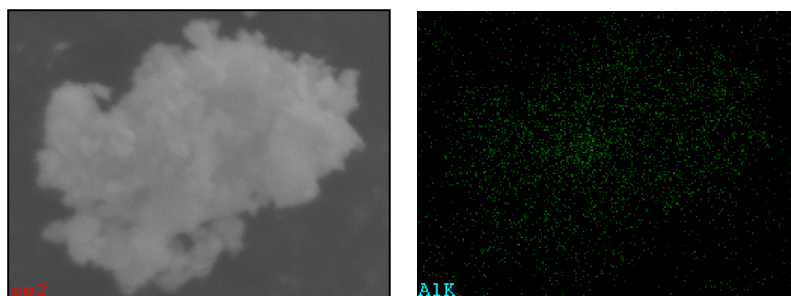


**Figure 5.8** Dispersion of Al metal in Ac-Urea multifunctional catalyst from EDX

## 5.2 Effect of multifunctional material preparation method on sorption enhanced ethanol steam reforming.

The results from section 5.1 showed that calcium acetate precursor and urea provided good performances for hydrogen production from sorption enhanced ethanol steam reforming. However, preparation method is another important factor that affect properties of catalyst such as, textural properties, morphology, and selective. In this section we investigated the effect of preparation technique: sol-mixing and sol-gel method, on hydrogen production performances in terms of hydrogen yield, hydrogen purity, and CO<sub>2</sub> sorption capacity.

### 5.2.1 Characterization

The crystalline structures of catalysts were examined by X-ray diffraction technique (XRD) and the results are shown in Figure 5.3. The XRD pattern found the phase of NiO, CaO and Ca<sub>12</sub>Al<sub>14</sub>O<sub>33</sub> in both preparation methods. The diffraction of CaO at  $2\theta = 32.2, 37.4, 53.9,$  and  $64.2$  [58] and the peaks assigned to NiO at  $2\theta = 43.1, 62.65$  [59] are detected in all samples. The formation of calcium aluminate cement (Ca<sub>12</sub>Al<sub>14</sub>O<sub>33</sub>) is observed at  $2\theta = 18, 29.8, 36.4, 40.9, 54.9.$  [57]

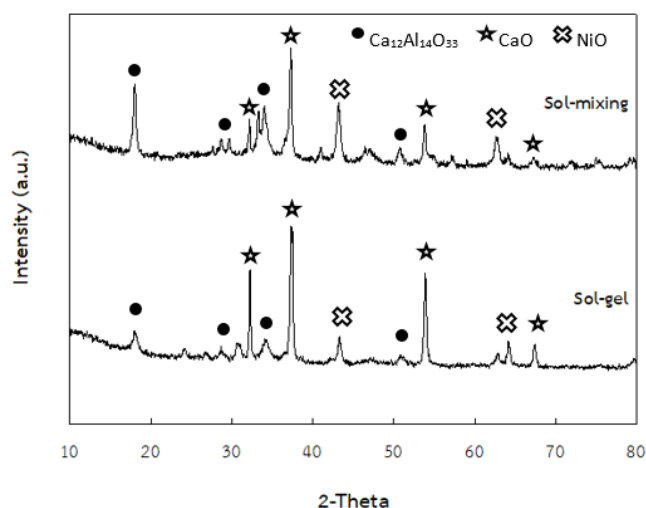


**Figure 5.9** XRD pattern of 6%NiO/CaO-Ca<sub>12</sub>Al<sub>14</sub>O<sub>33</sub> multifunctional catalyst for sol-gel and sol-mixing method

The morphology of catalyst was investigated by using scanning electron microscopy (SEM) as shown in Figure 5.10. The results show that the catalyst prepared by sol-mixing densed packing of small particles connecting to each other, whereas, the catalyst prepared by sol-gel method offers network of particles during wet-gel step. The percent weight of metal loading on surface of catalyst is shown in Table 5.4. The NiO/CaO-Ca<sub>12</sub>Al<sub>14</sub>O<sub>33</sub> (sol-mixing) and NiO/CaO-Ca<sub>12</sub>Al<sub>14</sub>O<sub>33</sub> (sol-gel) have metal loading on surface of 5.68 % and 5.86% respectively. Furthermore, the textural properties of all catalysts were determined by N<sub>2</sub> adsorption-desorption isotherm. The isotherm type of all catalysts shows type IV according to the IUPAC classification [59] as shown in Figure 5.11, indicating mesoporous structure. The highest specific surface area is observed with in NiO/CaO-Ca<sub>12</sub>Al<sub>14</sub>O<sub>33</sub> (sol-gel) catalyst with small pore volume (0.06 cm<sup>3</sup>/g) and pore size diameter (5.3 nm). On the other hand, the NiO/CaO-Ca<sub>12</sub>Al<sub>14</sub>O<sub>33</sub> (sol-mixing) shows higher pore volume (0.07 cm<sup>3</sup>/g) and pore size diameter (10 nm) (Table 5.5). Different preparation technique: sol-mixing and sol-gel method, show difference in morphology and textural properties of catalyst. The material prepared from sol-gel method demonstrates the network of particles while the material prepared from sol-mixing shows packing particles. The network connected particle observed with sol-gel method would lead to higher surface area and pore volume, and hence higher CO<sub>2</sub> sorption capacity.

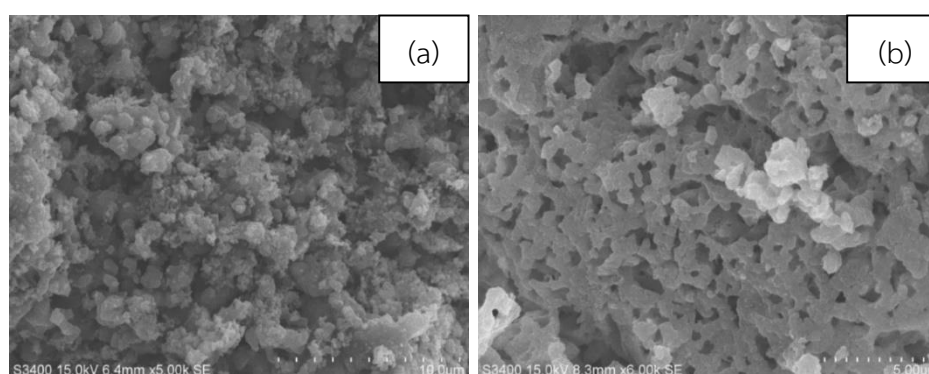


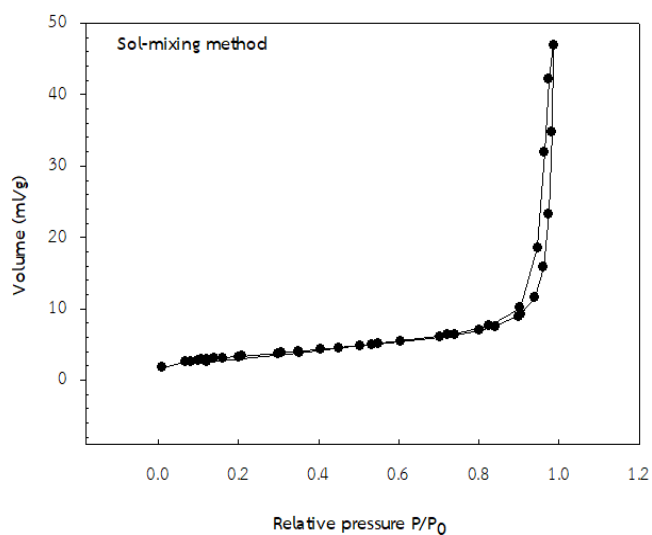
**Figure 5.10** Image of SEM for multifunctional catalyst a) sol-mixing method b) Sol-gel method

**Table 5.4** Composition of metal at surface of catalyst by EDX

Sample	% Ni
NiO/CaO-Ca <sub>12</sub> Al <sub>14</sub> O <sub>33</sub> (sol-gel)	5.68
NiO/CaO-Ca <sub>12</sub> Al <sub>14</sub> O <sub>33</sub> (sol-mixing)	5.86

**Table 5.5** Textural properties of multifunctional NiO/CaO-Ca<sub>12</sub>Al<sub>14</sub>O<sub>33</sub> catalyst from sol-gel and sol-mixing method

Sample	Surface area (m <sup>2</sup> /g)	Pore volume (cm <sup>3</sup> /g)	Pore size diameter (nm)
NiO/CaO-Ca <sub>12</sub> Al <sub>14</sub> O <sub>33</sub> (sol-gel)	29.16	0.06	5.3
NiO/CaO-Ca <sub>12</sub> Al <sub>14</sub> O <sub>33</sub> (sol-mixing)	28.07	0.07	10



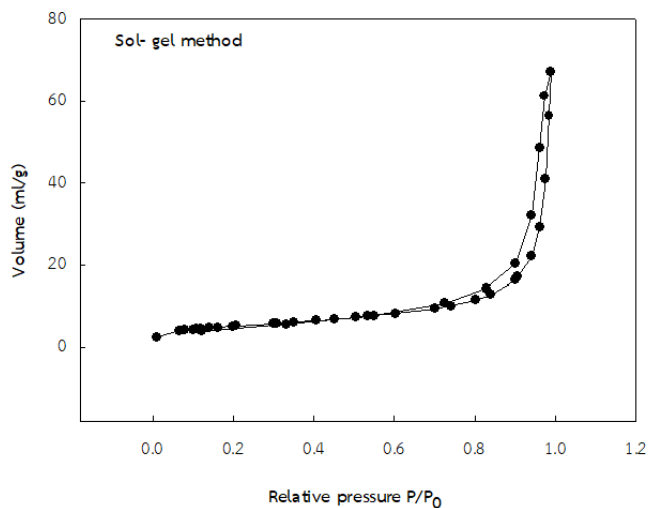


**Figure 5.11** Adsorption/desorption isotherm of sol-mixing and sol-gel method

### 5.2.2 Hydrogen production

Effect of catalyst synthesis method, sol-gel and sol-mixing method, were investigated in terms of gaseous products, hydrogen purity, and coke formation, for sorption enhanced ethanol steam reforming at total flow rate of 50 ml/min, temperature of 600 °, steam/ethanol ratio of 4 as shown in Figure 5.12. The NiO/CaO- $\text{Ca}_{12}\text{Al}_{14}\text{O}_{33}$  (sol-gel) exhibits high sorption capacity approximately 91% hydrogen purity during 45 min in pre-breakthrough period. After that, the hydrogen purity dropped to equilibrium in the post-breakthrough period (approx. 72% hydrogen purity), whereas, NiO/CaO- $\text{Ca}_{12}\text{Al}_{14}\text{O}_{33}$  (sol-mixing) has long pre-breakthrough period of 60 min and 87% for hydrogen purity. This result demonstrates that  $\text{CO}_2$  sorption capacity of the catalyst prepared from sol-gel method is higher than that prepared from sol-mixing method because NiO/CaO- $\text{Ca}_{12}\text{Al}_{14}\text{O}_{33}$  (sol-gel) had higher intensity of CaO and low intensity of  $\text{Ca}_{12}\text{Al}_{14}\text{O}_{33}$  complex phase but NiO/CaO- $\text{Ca}_{12}\text{Al}_{14}\text{O}_{33}$  (sol-mixing) shows high intensity of  $\text{Ca}_{12}\text{Al}_{14}\text{O}_{33}$  complex phases as confirmed by XRD results appeared in Figure 5.9.



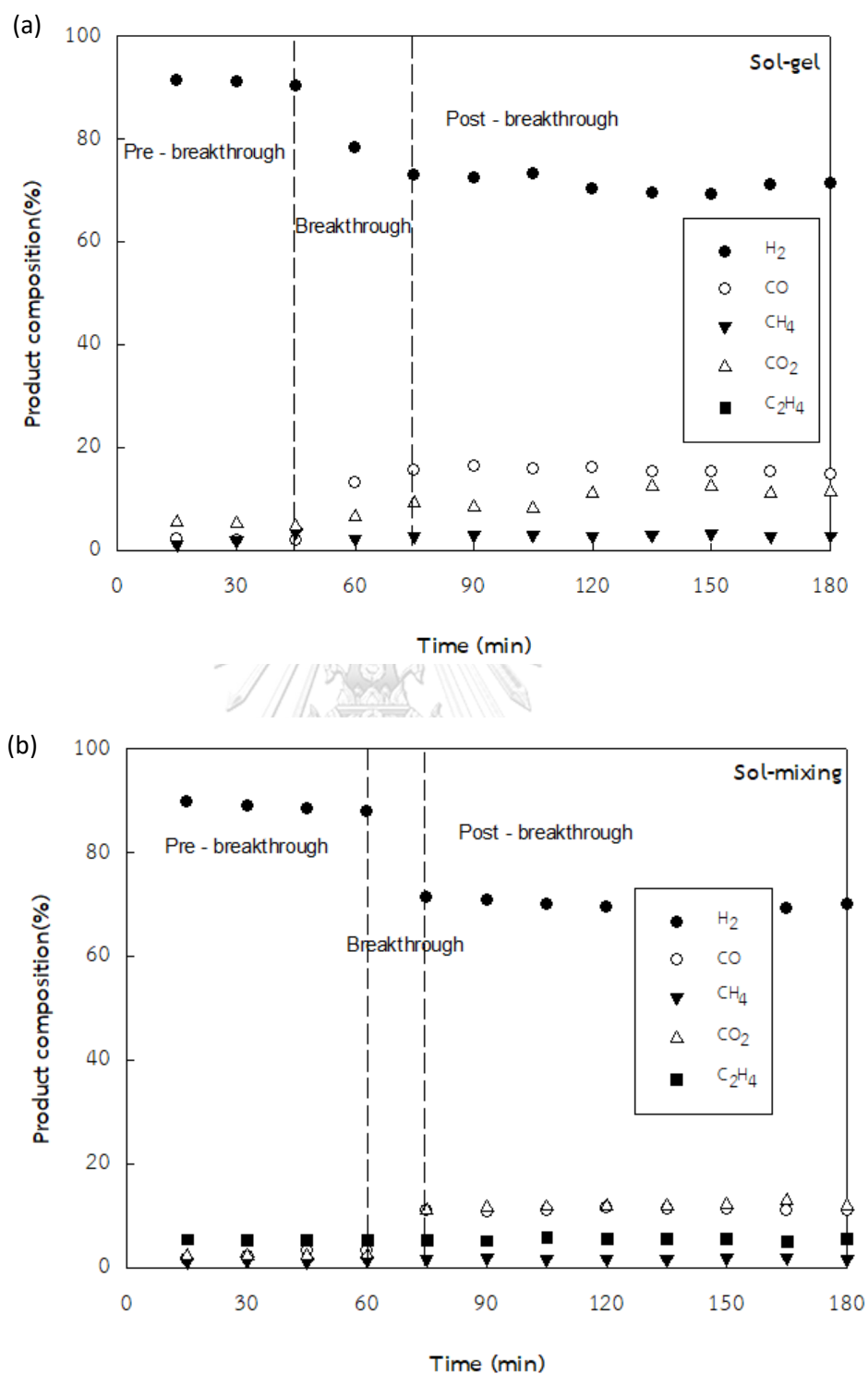


**Figure 5.12** Gas product compositions of a) NiO/CaO-Ca<sub>12</sub>Al<sub>14</sub>O<sub>33</sub> (sol-gel) b) NiO/CaO-Ca<sub>12</sub>Al<sub>14</sub>O<sub>33</sub> (sol-mixing), reaction condition at temperature 600° C, S/E of 4 under atmospheric pressure.

### 5.2.3 Coke deposition in catalyst

TGA-DSC was used to investigate coke deposition on the used catalyst. As shown in Figure 5.13 and 5.14, The sol-mixing method showed the removal of hydroxyl group in the range of 200-300 °C [45]. Normally, coke loss was found in the range of 400-450°C but the sol-mixing and sol-gel method in this study did not show in this range. The loss weight at 790°C is the decomposition of  $\text{CaCO}_3$  to  $\text{CaO}$  [57].

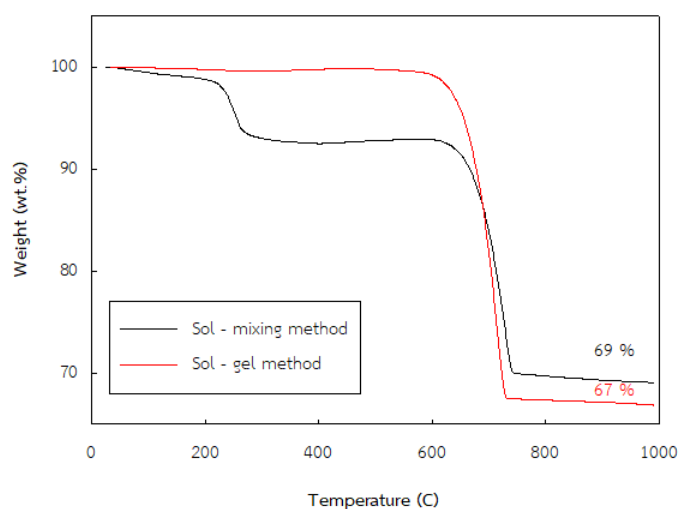


Figure 5.13 Thermogravimetric analysis of spent catalyst

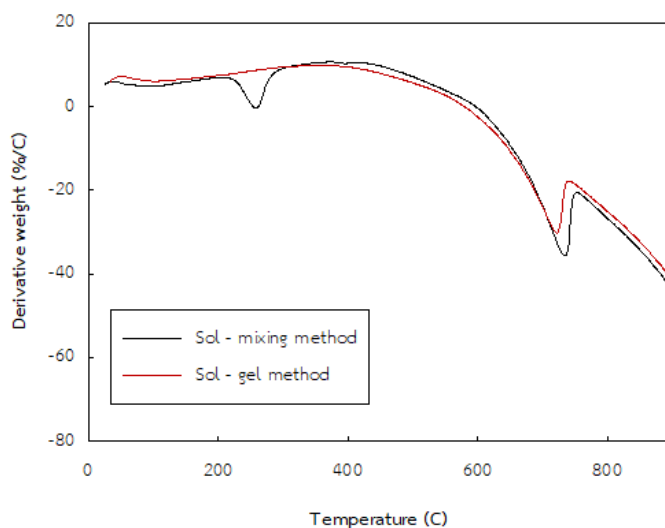


Figure 5.14 DTG of spent catalyst

### 5.3 The effect of copper addition and preparation method of multifunctional material on hydrogen production from sorption enhanced steam reforming chemical looping process

we are interested in using bi-metallic oxygen carrier for hydrogen production from sorption enhanced steam ethanol reforming chemical looping. The work is focused on investigating the effect of multifunctional material synthesis method, CuO/NiO-CaO-Ca<sub>12</sub>Al<sub>14</sub>O<sub>33</sub>, on hydrogen selectivity, CO<sub>2</sub> adsorption, calcination temperature, material stability, and coke formation.

#### 5.3.1 Characterization

Crystalline structure of Cu/(Ni-CA), Ni/(Cu-CA) and Ni-Cu-CA multi-functional materials were investigated by XRD technique. The result in Figure 4.15 shows four main peaks corresponding to CuO at  $2\theta = 35.50, 38.69, 51$  [59], NiO at  $2\theta = 37.23, 43.2, 62.8, 75$  [58] CaO at  $2\theta = 32.2, 53.9, 64.2, 67.4$  [58], and Ca<sub>12</sub>Al<sub>14</sub>O<sub>33</sub> inert support at  $2\theta = 18, 29.8, 33.2, 40.9, 46.4, 49, 54.9, 57.2$  [57] The morphology of catalyst was examined by using scanning electron microscopy (SEM) as shown in Figure 4.16. The result from image of SEM shows the Ni-CA having small particle network. While after impregnation of Ni on Cu/(Ni-CA) exhibited small particle connecting. Addition characteristic of Ni-(Cu-CA) displays merging of particle. The mixture of Ni-Cu-CA by sol-gel method combined between small particle connecting and merging of particles as shown in Figure 5.16(d) Distribution of Ni and Cu Bi-metallic catalyst were examined by energy dispersive x-ray spectroscopy (EDX) technique as shown in Figure 5.17. The result of Cu/(Ni-CA) shows a good dispersion of Ni and Cu metal. While, the Ni/(Cu-CA) and Ni-Cu-CA presented low Ni and Cu metal dispersion. The impregnation synthesis of Cu into Ni-CA shows metal loading of Cu on the surface about 31.07 % and metal loading Ni on surface about 1.33 %. While the impregnation of Ni into Cu-CA presents Ni and Cu on the surface of 9.73% and 5.08, respectively. The mixture of Ni and Cu in one-pot synthesis demonstrates Ni metal on the surface about 1.97% and Cu metal about

7.41%. So, the difference of multifunctional material synthesis method led to different amount of metal at the surface. The incipient wetness impregnation of Ni or Cu after the combination of CaO and Al<sub>2</sub>O<sub>3</sub> by sol-gel method shows higher amount of Ni or Cu at the surface than the mixture of Ni and Cu in one-pot synthesis. Figure 5.18 shows the adsorption isotherm of catalysts of which type IV according to the IUPAC classification is obtained, indicating mesopore (2-50 nm) structure [59].

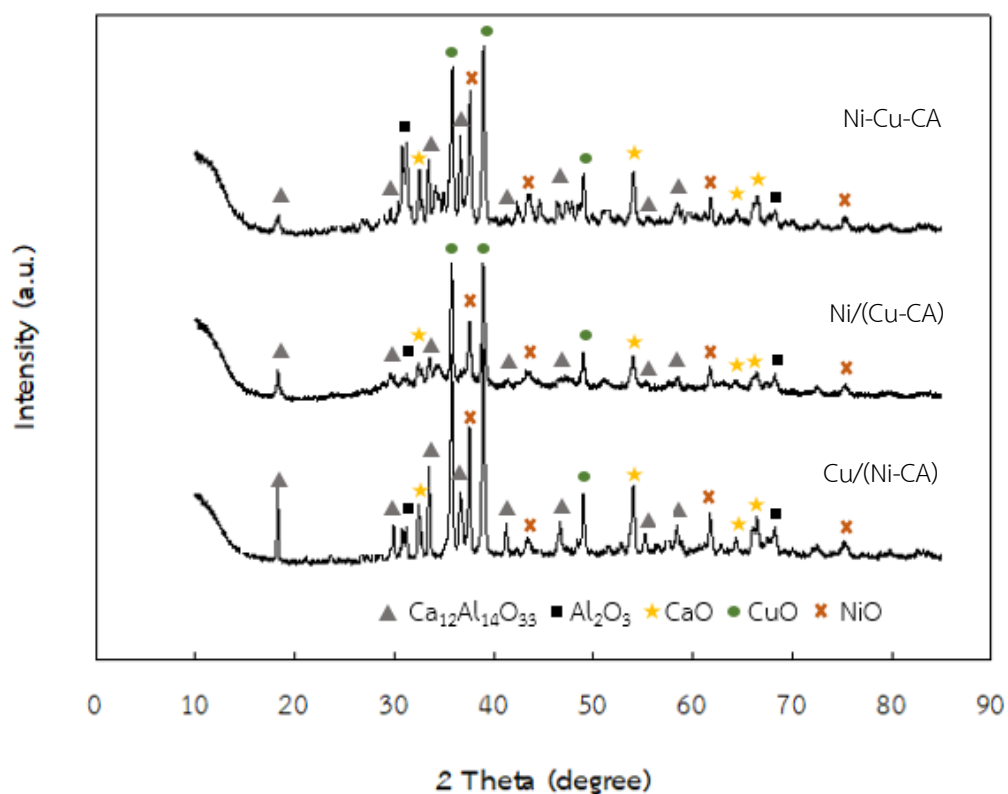


**Figure 5.15** XRD pattern of multifunctional catalyst Cu/(Ni-CA), Ni/(Cu-CA) and Ni-Cu-CA

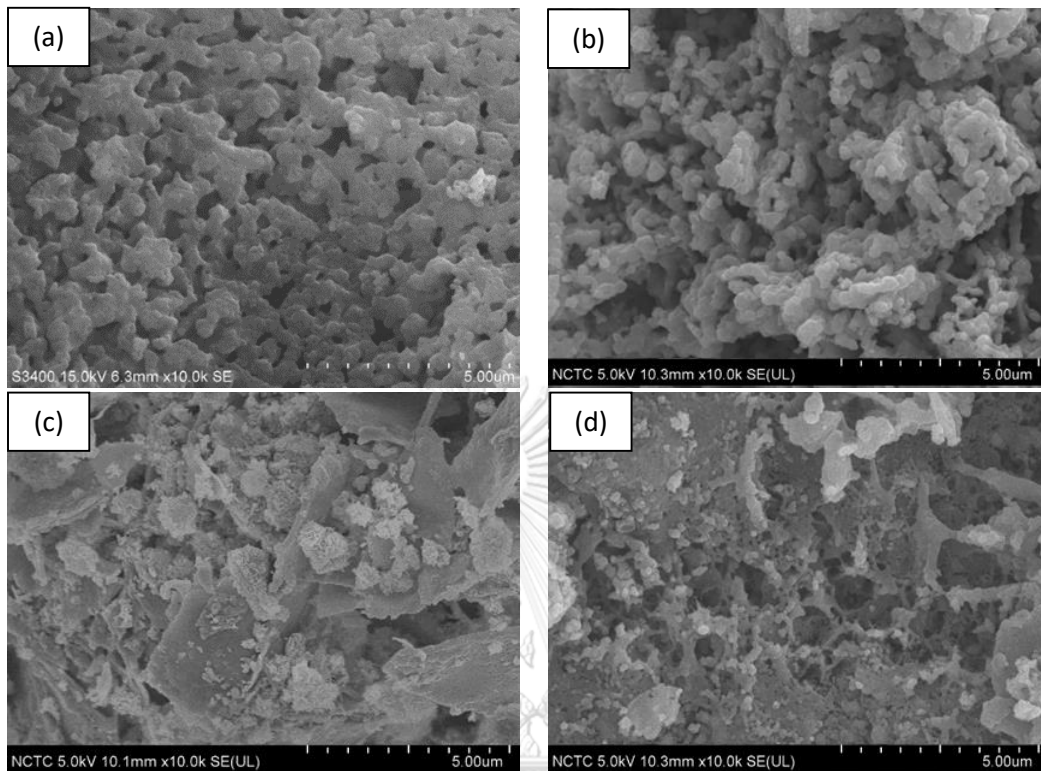
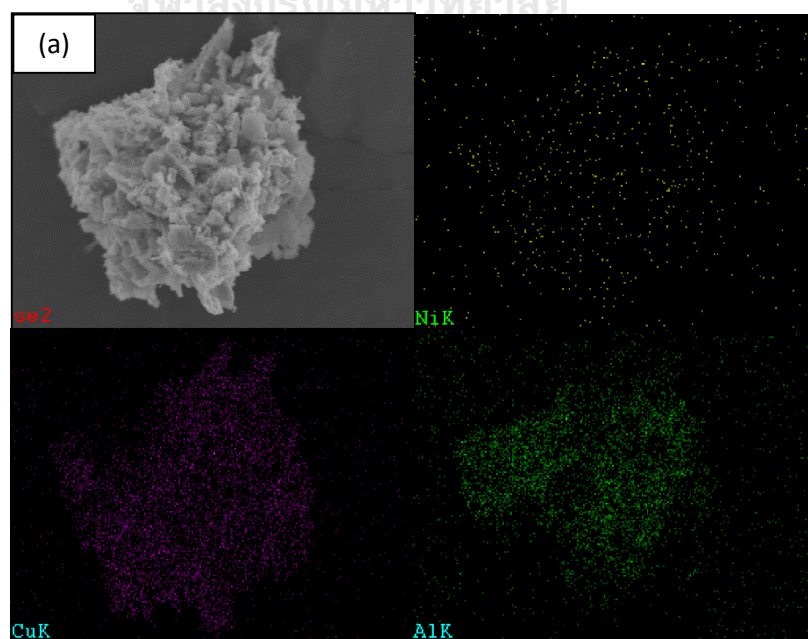


Figure 5.16 SEM image for multifunctional catalyst a) Ni-CA b) Cu/(Ni-CA)

a) Ni/(Cu-CA) d) Ni-Cu-CA



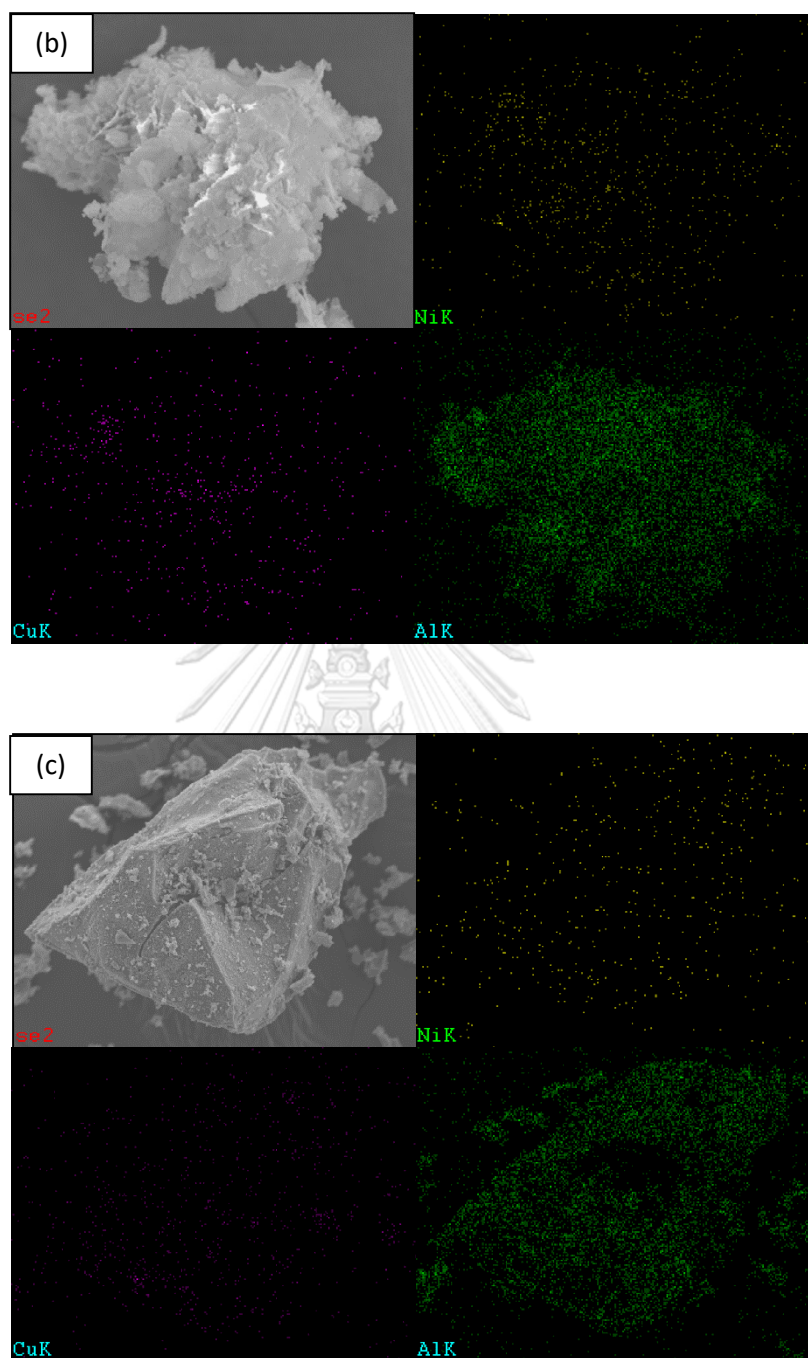


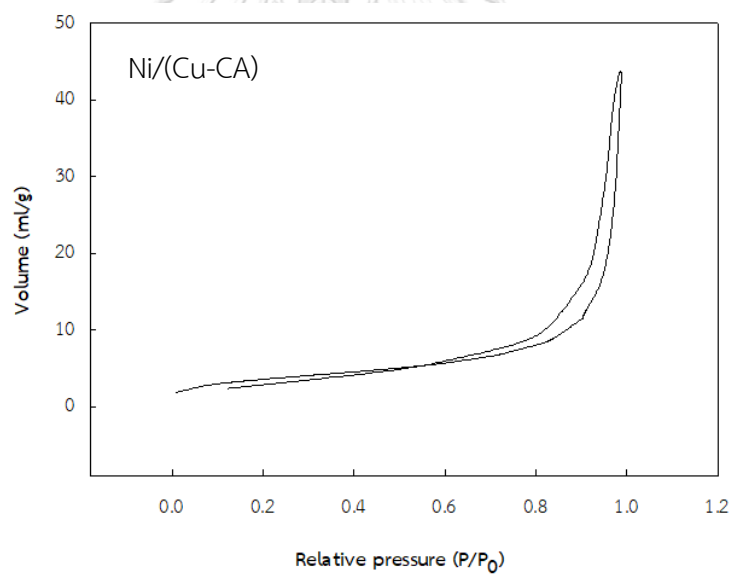
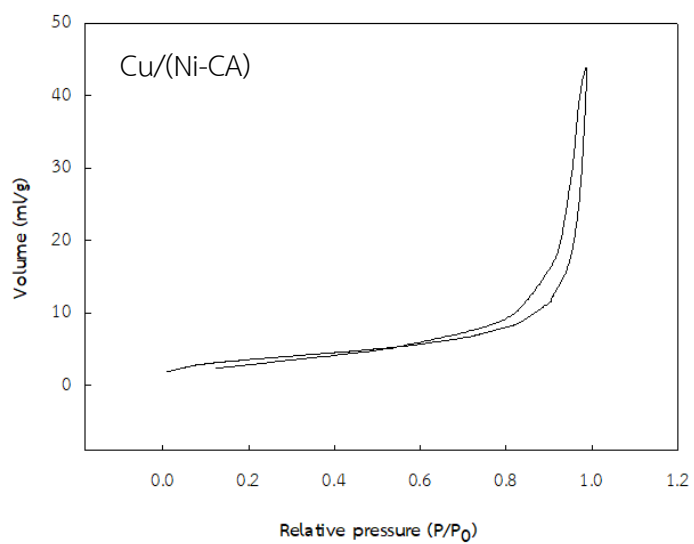
Figure 5.17 Dispersion of metal for a) Cu/(Ni-CA) b) Ni/(Cu-CA) c) Ni-Cu-CA multifunctional catalyst from EDX

**Table 5.6** Composition of metal at surface of catalyst by EDX

Sample	% Ni	% Cu
Cu/(Ni-CA)	1.33	31.07
Ni/(Cu-CA)	9.73	5.08
Ni-Cu-CA	1.97	7.41

**Table 5.7** Textural properties of multifunctional catalyst

Sample	Surface area (m <sup>2</sup> /g)	Pore volume (cm <sup>3</sup> /g)	Pore size diameter (nm)
Ni-CA	24.23	0.08	7
Cu/(Ni-CA)	13.35	0.04	5
Ni/(Cu-CA)	6.50	0.03	4
Ni-Cu-CA	18.48	0.06	6





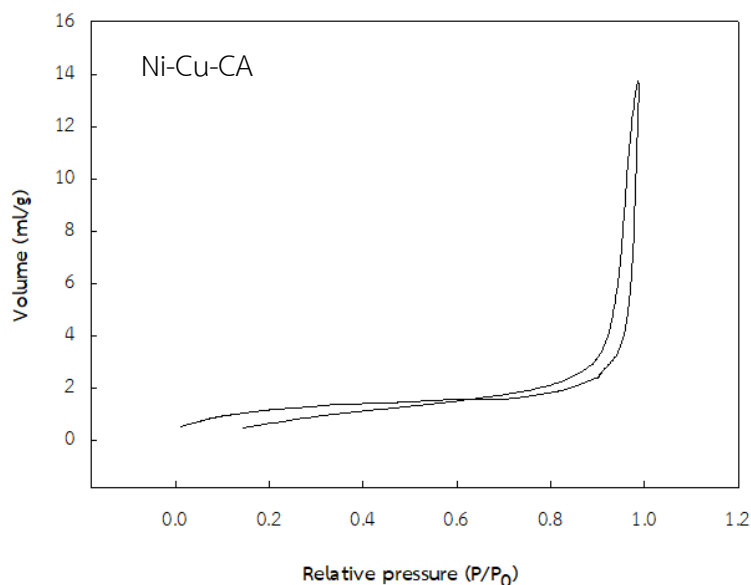


**Figure 5.18** Adsorption/desorption isotherm of Cu/(Ni-CA), Ni/(Cu-CA) and Ni-Cu-CA

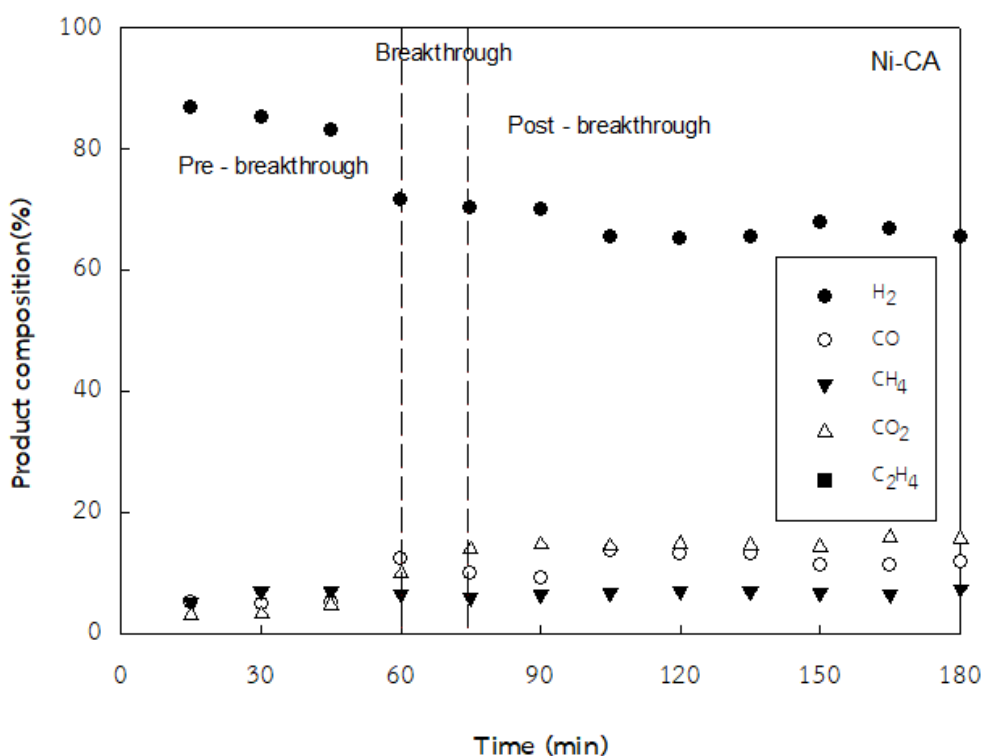
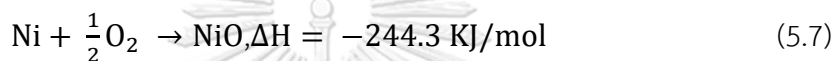
### 5.3.2 Hydrogen production

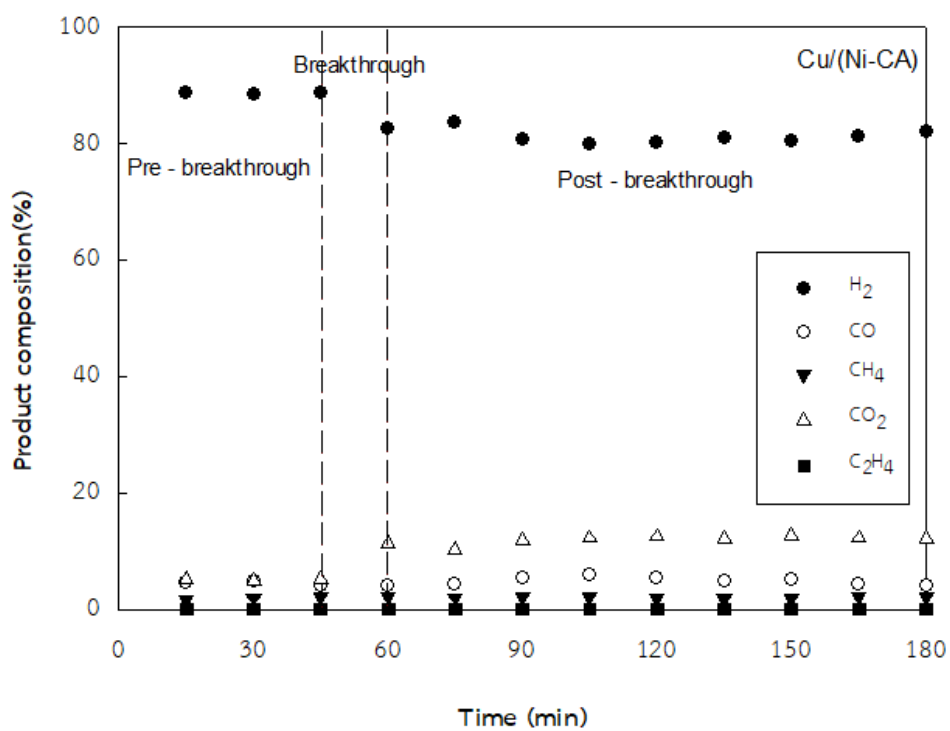
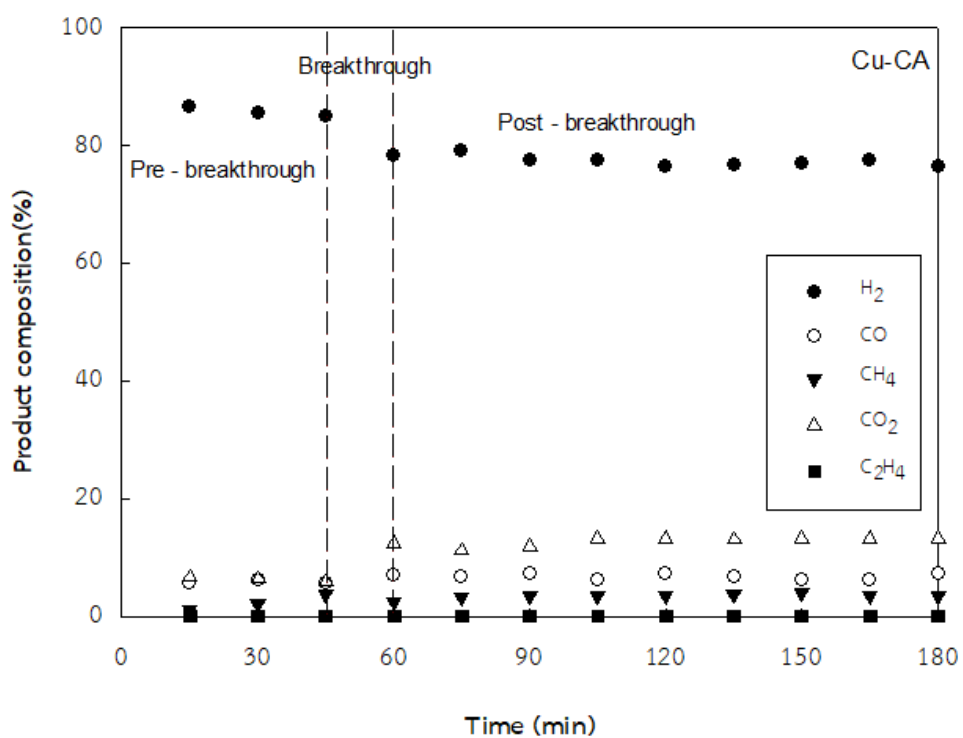
The performance of the multifunctional material Ni-CA, Cu-CA, Cu/(Ni-CA), Ni/(Cu-CA) and Ni-Cu-CA were studied for hydrogen production from sorption enhanced steam ethanol reforming chemical looping process under temperature of 500 °C, steam/ethanol ratio equals to 3 at atmospheric pressure. The preparation method in one-pot synthesis Ni-Cu-CA material by sol-gel method (Figure.5) provides the highest hydrogen purity approximately 94% for 60 min. This result is because of the effect of carbon dioxide absorption. Which, makes the reaction can be carried forward and an increase hydrogen purity. As the reaction time progressed, CaO sorbent converted into CaCO<sub>3</sub> due to the reaction with CO<sub>2</sub>, leading to an increase of CO<sub>2</sub> concentration and a decrease of hydrogen concentration. The hydrogen purity in the post-breakthrough period shows 77 % and CO<sub>2</sub> concentration about 13% due to ethanol steam reforming reaction. In the case of Cu/(Ni-CA), 88 % hydrogen purity was achieved in pre-breakthrough period about 45 min. The pre-breakthrough time of Cu/(Ni-CA) (45 min) was shorter than Ni-Cu-CA (60 min), indicating Cu/(Ni-CA) offers lower CO<sub>2</sub> sorption

performance than Ni-Cu-CA. The impregnation synthesis of Cu into Ni-CA shows hydrogen purity in post-breakthrough period ca. 79 % since the reduction reaction of CuO by ethanol is exothermic reaction, leading to an increase of temperature and progress ethanol steam reforming reaction. The exothermic reaction of CuO with ethanol was confirmed by the result of Ni-CA catalyst. The Ni-CA catalyst showed the hydrogen selectivity at the post-breakthrough of 67.6%. Therefore, the hydrogen selectivity of solely Ni was low than the hydrogen selectivity of Ni-Cu bi-metallic catalyst. The hydrogen purity of Ni/(Cu-CA) was achieved at the pre-breakthrough period about 30 min of 83% hydrogen purity and hydrogen purity in the post-breakthrough period is 65%. This could be due to the accumulation of particles (Figure.5.16).

From Figure 5.20 the best sequence for loading Cu in the multifunctional material is the single step synthesis method as Ni-Cu-CA when considered in terms of hydrogen production and CO<sub>2</sub> sorption performance for sorption enhanced chemical looping ethanol steam reforming. As the use of multifunctional material is required for multicycle operation, regeneration of sorbent via calcination reaction is necessary. However, the calcination reaction is highly endothermic, which results in high cost of operation. Oxidation of Ni and Cu by oxygen in air reactor is exothermic, therefore, heat of reaction occurred in the air reactor is collected in solid multifunctional material. As a consequence, in regeneration step, heat from solid catalyst can be utilized in calcination reactor. Hence, we extended the investigation to the effect of adding CuO on calcination temperature by examining temperature at which CaCO<sub>3</sub> can be completely recovered using H<sub>2</sub>O/N<sub>2</sub> (1.5V/V H<sub>2</sub>O) as gas carrier in fixed bed reactor. The phase of CaO after calcination reaction was confirmed by X-ray diffraction technique (XRD) (Figure 5.21). From Figure 5.21 the CaCO<sub>3</sub> of Cu-(Ni-CA) multifunctional material can be converted into CaO at the temperature 800 °C and 825°C while CaCO<sub>3</sub> is still observed in the Ni-(Cu-CA) and Ni-Cu-CA at the same temperature. So, Ni-(Cu-CA) and Ni-Cu-CA multifunctional material cannot regeneration at temperature of 800

°C and 825 °C. The reason is that the oxidation of Ni (Eq. 5.7) is higher exothermic reaction than the oxidation of Cu (Eq. 5.8); thus, the combination of Ni and CaO in directly (Cu-(Ni-CA)) shows the best performance for heat transfer in regeneration step. The synthesis method from different patterns affect regeneration temperature of CaCO<sub>3</sub>. The Cu-(Ni-CA) can be regenerated at the temperature of 800 °C due to the oxidation of Ni while the CaO Ni-(Cu-CA) and Ni-Cu-CA multifunctional material cannot be regenerated at temperature of 800 °C. This result is because lower heat transfers between oxygen carrier and sorbent.





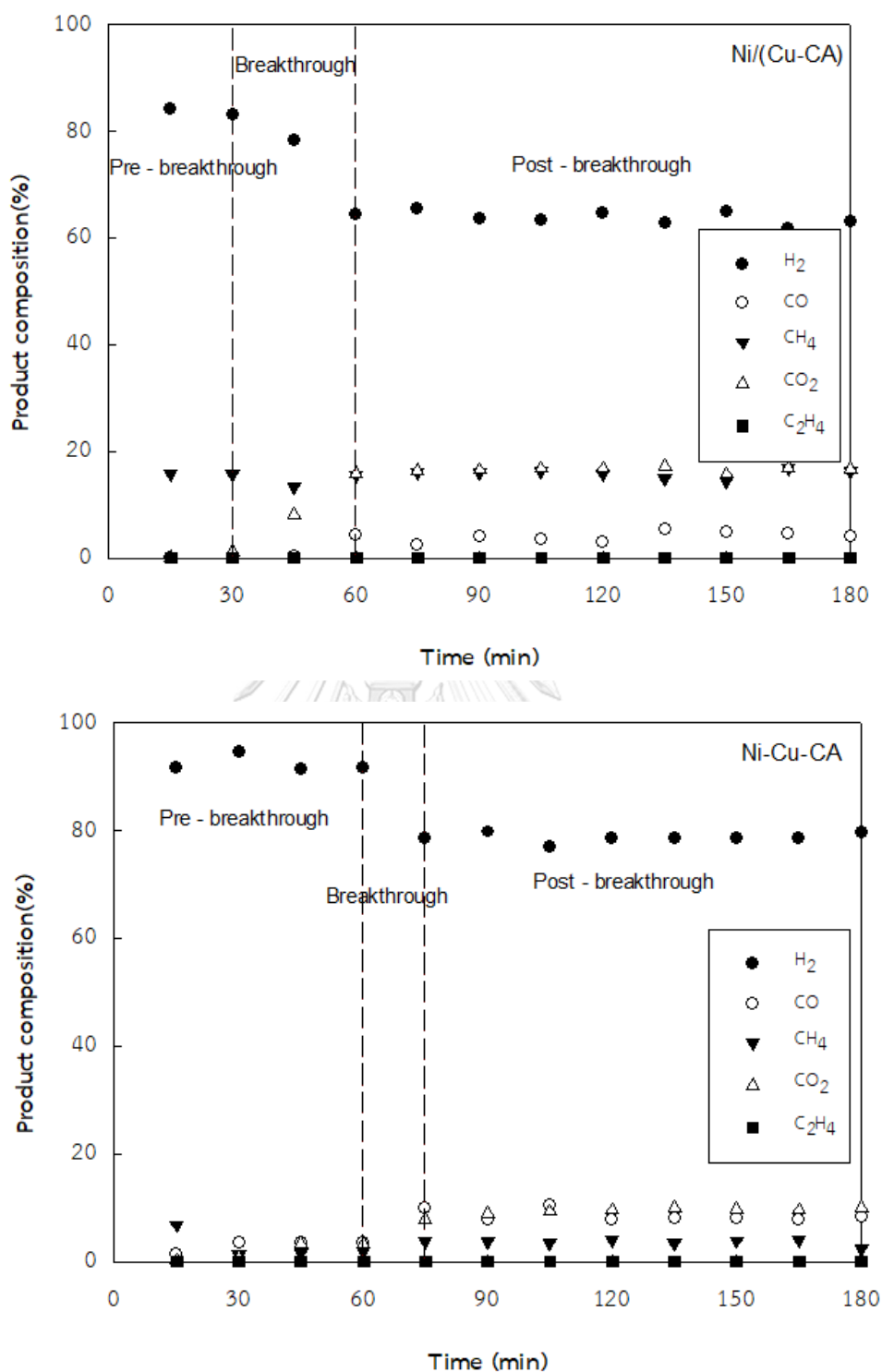


**Figure 5.19** Gas product compositions of Ni-CA, Cu-CA, Cu-(Ni-CA), Ni-(Cu-CA) and Ni-Cu-CA reaction condition at temperature 500 °C, S/E of 4 under atmospheric pressure

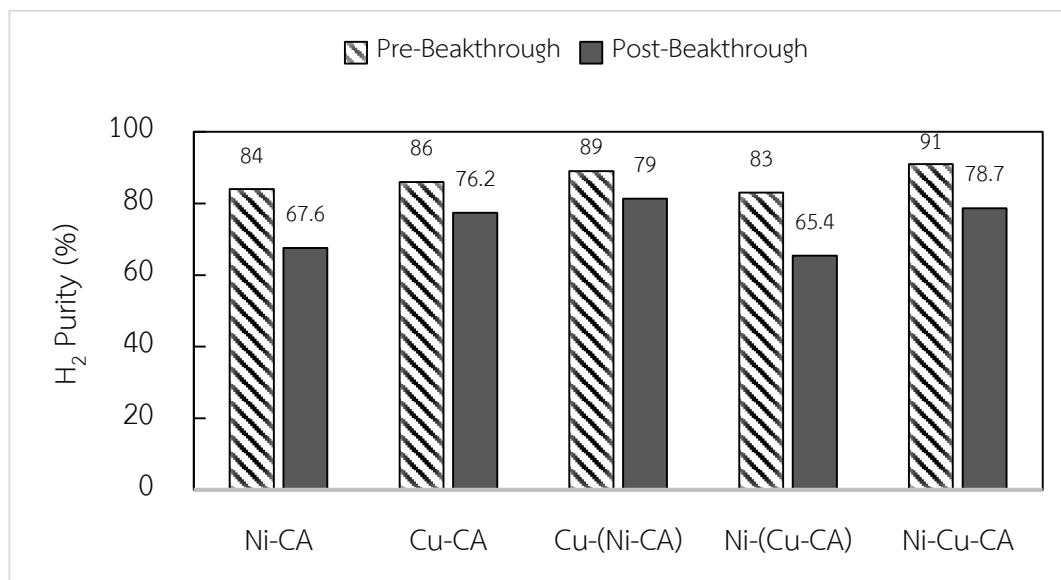
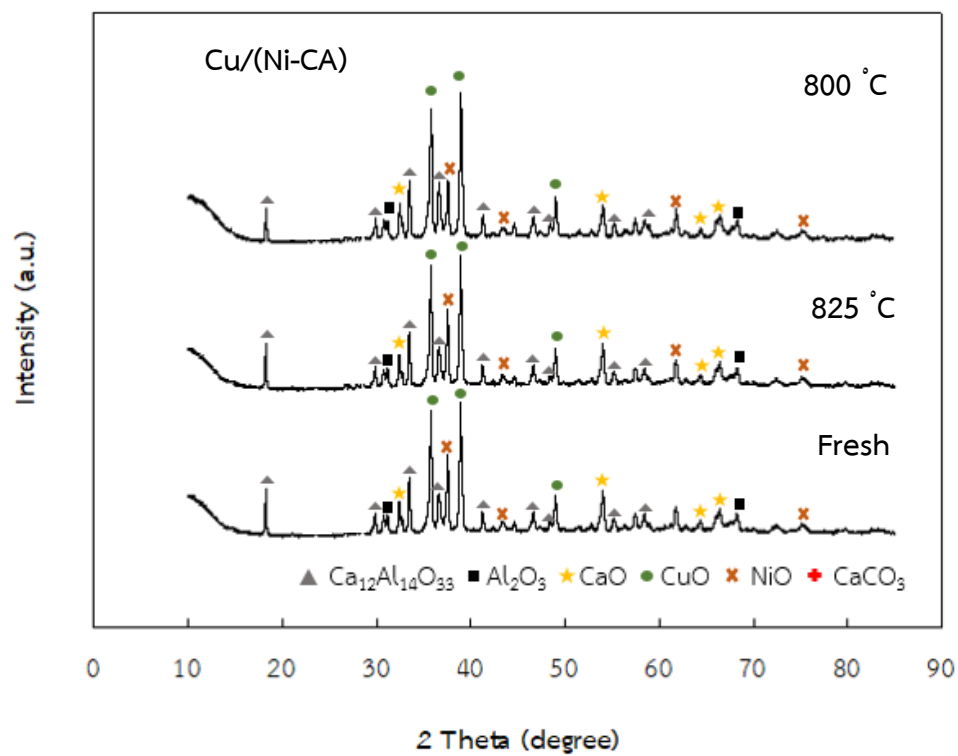


Figure 5.20 Hydrogen purity of Ni-CA, Cu-CA, Cu/(Ni-CA), Ni/(Cu-CA) and Ni-Cu-CA multifunctional catalyst



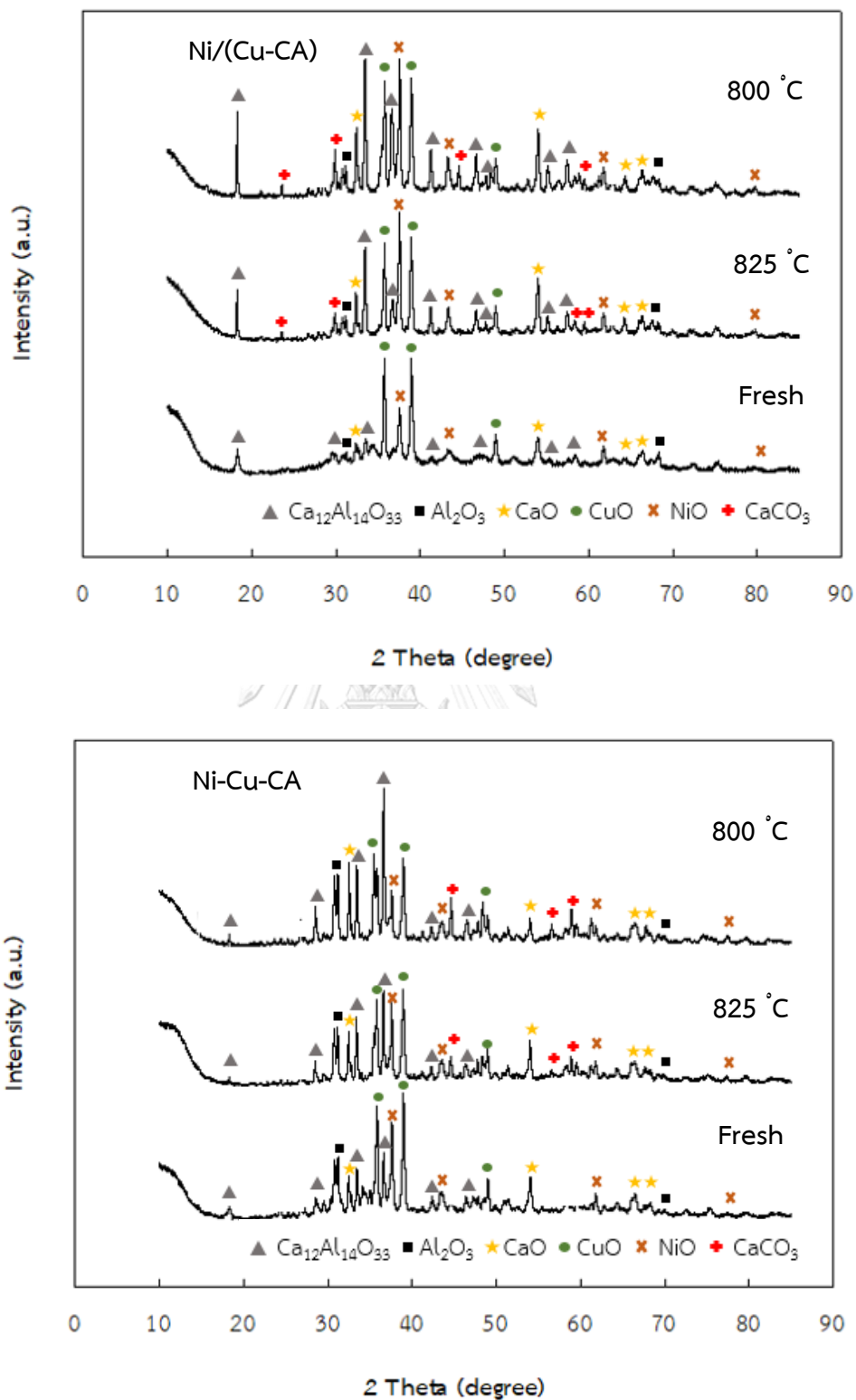


Figure 5.21 XRD pattern of multifunctional for Cu/(Ni-CA), Ni/(Cu-CA) and Ni-Cu-CA for Calcination at the temperature of 800, 825, 850 °C.

### 5.3.3 Single cycle for sorption enhanced chemical looping ethanol steam reforming process

The ethanol steam forming requires high amount of water and energy for hydrogen production. The sorption enhance chemical looping ethanol steam reforming process has potential to carry out under self-sufficient condition and low energy consumption. The multifunctional material as Cu/(Ni-CA) and Ni-Cu-CA were investigated in single step to clarify performances of each multifunctional material in each step of reaction as shown in Figure 5.22. The process contains reduction step, sorption enhanced ethanol steam reforming step, oxidation step, and calcination step. First step, NiO and CuO were reduced to Ni and Cu, to produce hydrogen and CO<sub>2</sub>. The reduction of NiO and CuO was confirmed by XRD pattern shown in Figure. 5.23. The XRD peak of Ni shows at  $2\theta = 51.8, 76.5$  [59] and The XRD peak of Cu shows at  $2\theta = 43.2$  [59], indicating that NiO and CuO can be reduced to Ni and Cu by ethanol during this step of about 15 min. In step two, sorption enhanced ethanol steam reforming takes place where hydrogen and CO<sub>2</sub> are produced. Step three, Ni and Cu are oxidized in this step by air at the temperature of 500 °C as confirmed by XRD shown in Figure 5.24; the XRD peak of NiO shows at  $2\theta = 43.3, 62.9$  [59] and CuO shows at  $2\theta = 35.5, 38.69, 51$  [59]. Last step, the spent sorbent is calcined to CaO and CO<sub>2</sub>. The difference between the Cu/(Ni-CA) and Ni-Cu-CA is the sorption time, oxidation time and calcination temperature. The Cu/(Ni-CA) multifunctional catalyst shows sorption time of 45 min while the Ni-Cu-CA demonstrates sorption time of 60 min. In the oxidation step, the time to complete oxidation of Ni and Cu for Cu/(Ni-CA) is shorter than the Ni-Cu-CA. So, different synthesis methods lead to the difference in contacting between reactant and oxygen carrier particles. Therefore, Cu metal at the surface (Cu/(Ni-CA)) can be oxidized by air easier than the Cu metal inside the catalyst (Ni-Cu-CA). In the last step, the temperature for calcination of Cu/(Ni-CA) is lower than the Ni-Cu-CA due to the oxidation of Ni is higher exothermic reaction than the oxidation of Cu. In addition,



the sorbent and oxygen carrier particles of Cu/(Ni-CA) were contact closer than Ni-Cu-CA.

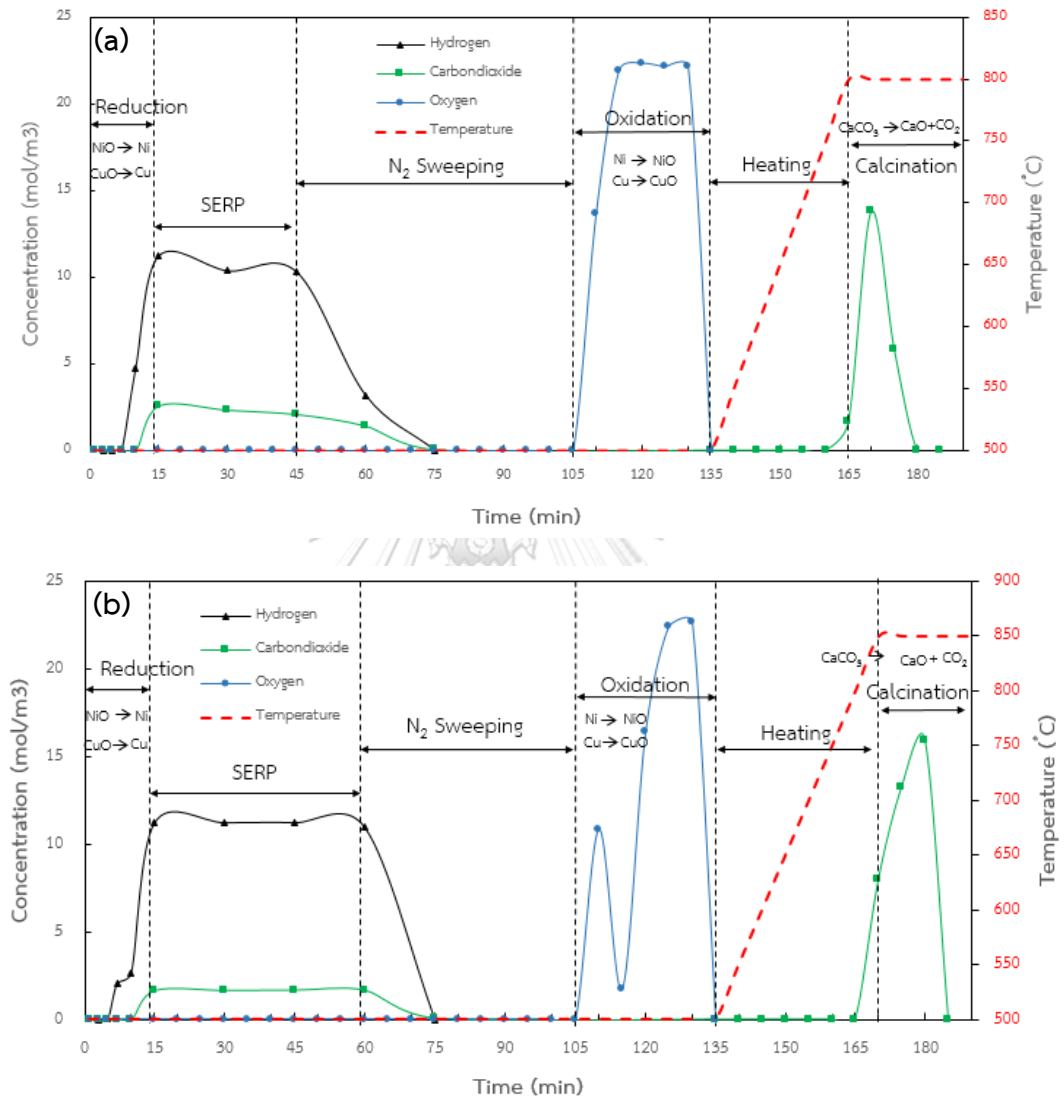


Figure 5.22 The single cycle of (a) Cu/(Ni-CA) and (b) Ni-Cu-CA

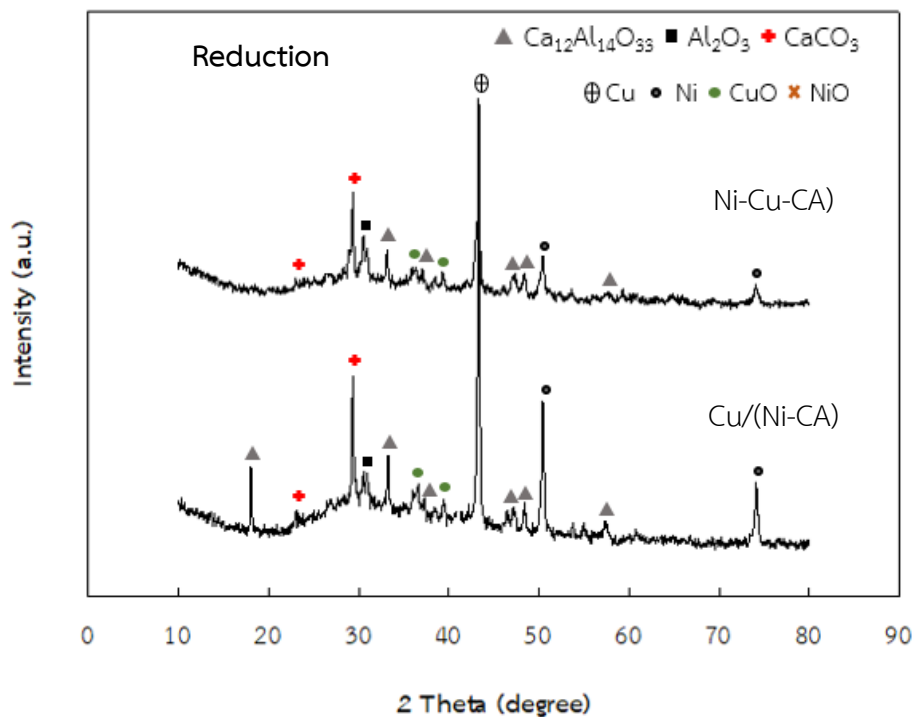


Figure 5.23 The XRD pattern of Cu/(Ni-CA) and Ni-Cu-CA at the reduction step.

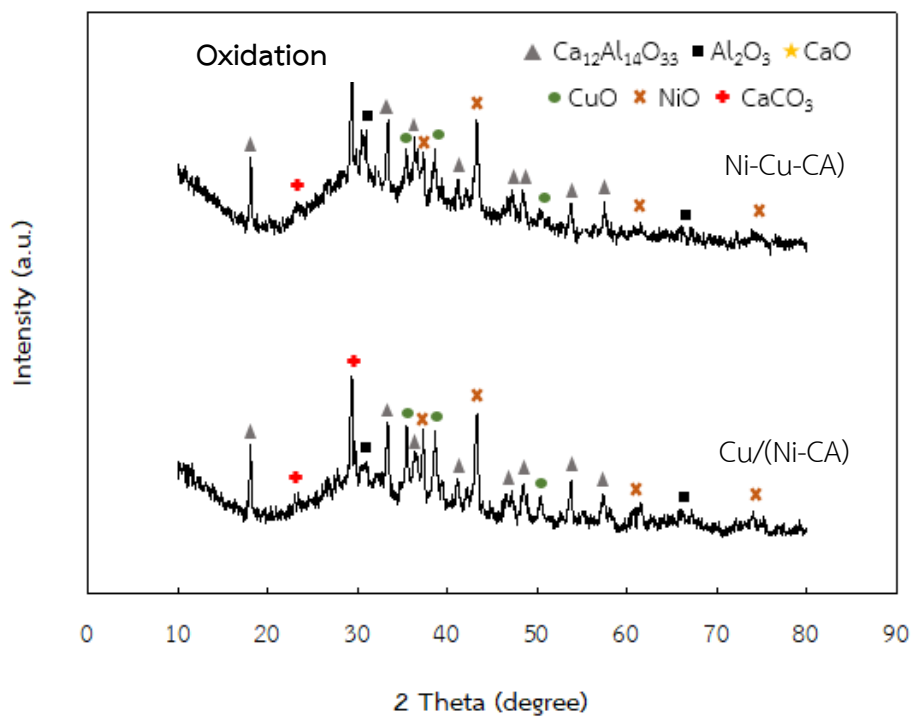
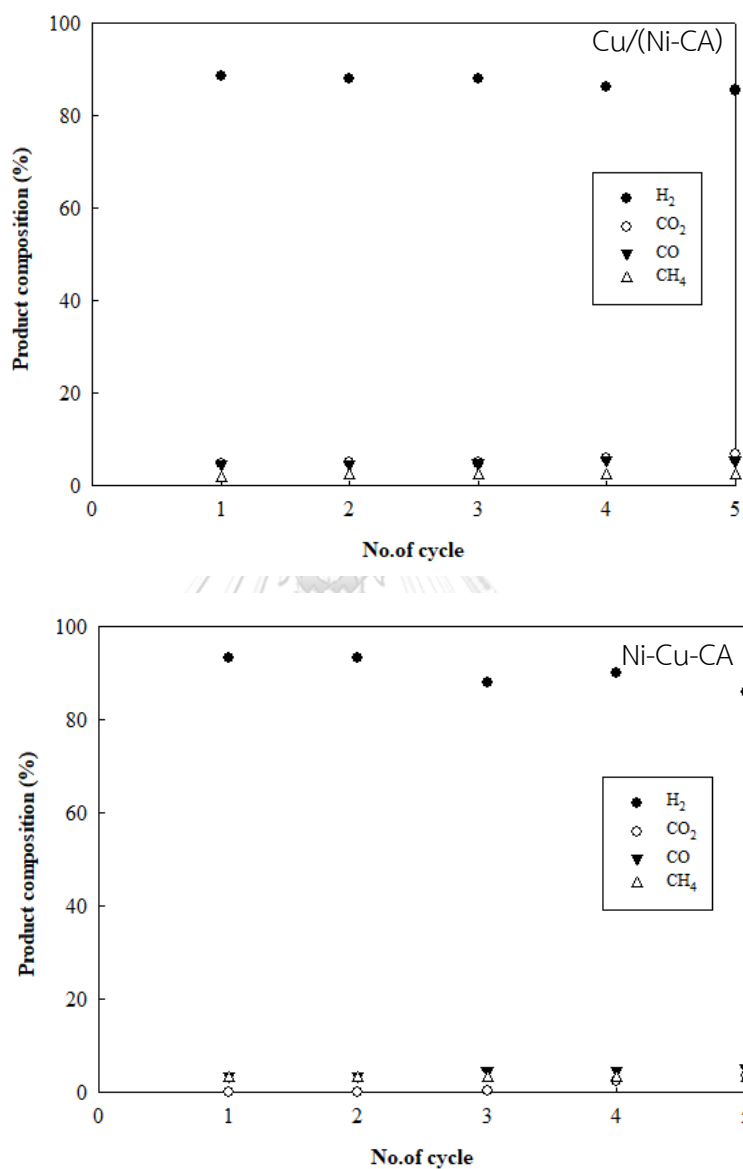


Figure 5.24 The XRD pattern of Cu/(Ni-CA) and Ni-Cu-CA at the oxidation step

### 5.3.5 Stability of multifunctional catalyst

The stability of the multifunctional material Cu/(Ni-CA) and Ni-Cu-CA over 5 cycles of hydrogen production by sorption enhanced chemical looping ethanol steam reforming is shown in Figure 4.25. The Cu/(Ni-CA) material shows that hydrogen purity can be maintained at ca. 88% in pre-breakthrough period while the Ni-Cu-CA exhibit 93% hydrogen purity and slightly decrease of hydrogen purity to 87% after 5 cycles. The multifunctional material Cu/(Ni-CA) and Ni-Cu-CA were loss active sites as confirmed by XPS results shown in Table 4.7. The Ni atomic concentration at the surface of Cu-Ni-CA decreases from 8.06% to 7.49%. The atomic concentration at the surface of Cu metal decrease from 2.70% to 1.47% on the used catalyst because a densification resulting in the loss of active sites as confirmed by SEM images (Figure 4.26 (d)). The Ni atomic concentration at the surface of Cu/(Ni-CA) decreases from 3.40% to 2.22% and Cu metal decreases from 7.48% to 4.47% on the used catalyst and the SEM image of Cu/(Ni-CA) used catalyst is the same as fresh catalyst. The good stability of catalyst was obtained is because the multifunction catalyst produced small amount of coke. The amount of coke formation was determined by TGA analysis and the result is shown in Figure 5.27. The mass change under air condition included the coke combustion and oxidation of Ni and Cu. The mass loss is the coke combustion and the added mass is the oxidation due to  $\text{Ni} \rightarrow \text{NiO}$  and  $\text{Cu} \rightarrow \text{CuO}$ . The mass loss of Cu-(Ni-CA) shows 87% and the mass loss of Cu-(Cu-CA) and Ni-Cu-CA present 90%. The weight loss is found for sorption enhanced chemical looping ethanol steam

reforming with Ni-(Cu-CA), Ni-(Cu-CA) and Ni-Cu-CA, indicating small amount of coke deposited on multifunctional catalyst lead to stable under stability test.



**Figure 5.25** The hydrogen concentration of Cu/(Ni-CA) and Ni-Cu-CA multifunctional catalyst reaction condition: under temperature 500 °C, steam/ethanol ratio of 3

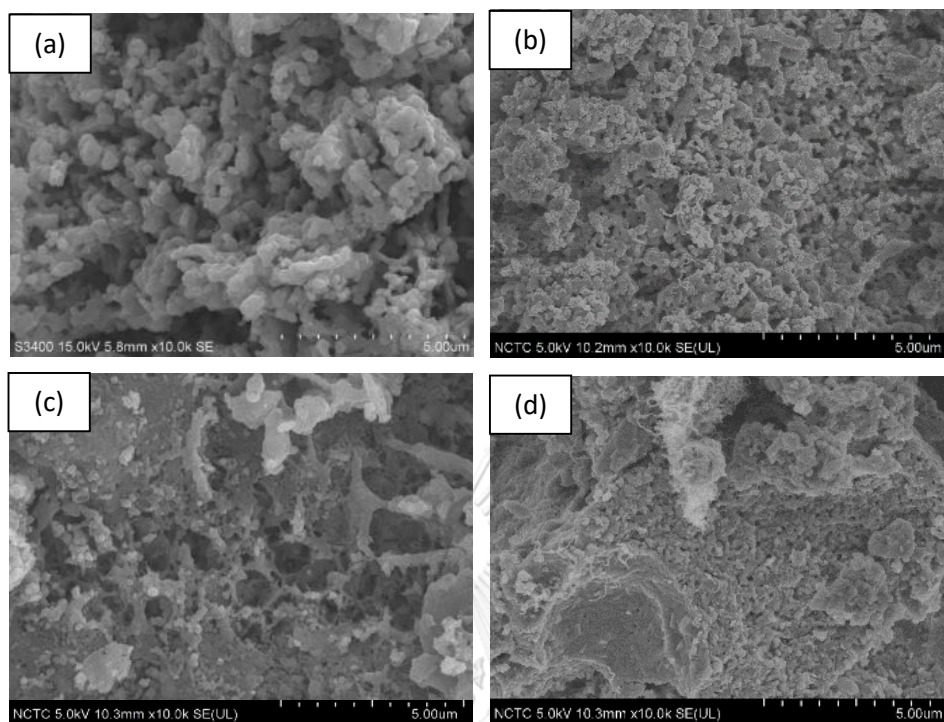


Figure 5.26 SEM image of multifunctional catalyst a) Cu/(Ni-CA) (fresh) b) Cu/(Ni-CA) (used) c) Ni-Cu-CA (fresh) d) Ni-Cu-CA (used)

**Table 5.8** XPS analysis results of the multifunctional catalysts

Sample	Binding Energy of Ni (eV)	Binding Energy of Cu (eV)	Atomic concentration of elements on surface (%)				
			Ni 2p	Cu 2p	O 1s	Ca 2p	Al 2p
Cu-(Ni-CA) (Fresh)	861.9	965.3	3.40	7.48	71.3	6.23	11.5
Cu-(Ni-CA) Used (5 <sup>th</sup> cycle)	858.9	965.4	2.22	4.47	76.29	6.35	10.67
Ni-Cu-CA (Fresh)	857.6	963.5	8.06	2.70	68.31	11.56	9.37
Ni-Cu-CA Used (5 <sup>th</sup> cycle)	851.0	964.0	7.49	1.47	71.73	10.53	8.78

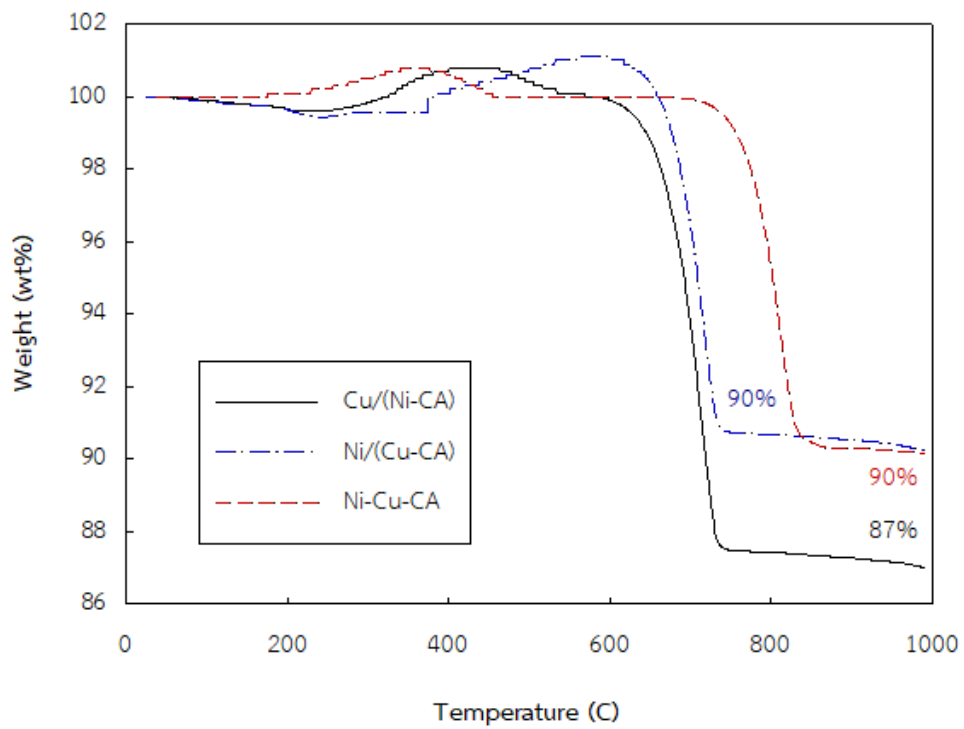


Figure 5.27 TGA analysis of Cu/(Ni-CA), Ni/(Cu-CA) and Ni-Cu-CA



## CHAPTER 6

### CONCLUSION AND RECOMMENDATIONS

#### 6.1 Conclusion

In this work the multifunctional catalyst (catalyst-oxygen carrier/sorbent) was investigated the effect for hydrogen production including the effect of CaO sorbent precursor, the effect of preparation synthesis method and the effect of addition Cu as oxygen carrier. The result was summarized as follows.

- Different CaO precursors from calcium acetate ( $\text{Ca}_2\text{Ac}$ ) and calcium chloride ( $\text{CaCl}_2$ ) as calcium precursor, sodium carbonate ( $\text{Na}_2\text{CO}_3$ ) and urea ( $\text{CO}(\text{NH}_2)_2$ ) as carbonate precursor were tested for hydrogen production from sorption enhanced steam ethanol reforming at steam to ethanol molar ratio (S/E) of 4:1, temperature of 600 °C, and pressure of 1 atm. The results showed 90% hydrogen purity can be maintained for 60 min in pre-breakthrough period with 10 repeated cycles of reaction. This observation is due to due to Ac-Urea multifunctional catalyst exhibited high surface area of 28.07  $\text{m}^2/\text{g}$  and well dispersed Al in catalyst. Our results demonstrated that different CaO precursors provided different hydrogen production performances due to the physical properties and morphology of catalyst.
- The effect of multifunctional material preparation method on hydrogen production showed that the catalyst from sol-gel synthesis method demonstrated good textural properties and high sorption capacity for hydrogen production than the catalyst prepared from sol-mixing method. The results showed 91% hydrogen purity during 45 min for sorption enhanced ethanol steam reforming. The sol-gel method showed low energy consumption than sol-mixing because the sol-mixing had to be calcined twice and required high amount of precursor. Therefore, the catalyst prepared from sol-gel method is likely suitable for industrial applications than sol-mixing method.



- The effect of addition of Cu as co-oxygen carrier on hydrogen production via sorption enhanced chemical looping steam ethanol reforming was studied with different preparation methods. One-pot Ni-Cu-CA multifunctional catalyst by sol-gel method showed the highest hydrogen purity of 94% for 60 min. The Cu/(Ni-CA) catalyst shows hydrogen purity of 89% for 45 min and Ni/(Cu-CA) exhibits the lower hydrogen purity of 83% for 30 min. The Cu/(Ni-CA) can convert  $\text{CaCO}_3$  to CaO in the calcination step at lower temperature of 800 °C while Ni/(Cu-CA) and Ni-Cu-CA can convert  $\text{CaCO}_3$  to CaO at temperature of 850 °C. Because the oxidation of Ni into NiO is high exothermic reaction and the sorbent and oxygen carrier molecule of Cu/(Ni-CA) were contact closer than Ni/(Cu-CA) and Ni-Cu-CA multifunctional catalyst. The stability of Cu/(Ni-CA) can be maintained at ca. 88%, whereas hydrogen purity of Ni-Cu-CA slightly decreased from 93% to 87% after 5 cycles.

## 6.2 Recommendations

1. The regeneration of  $\text{CaCO}_3$  at low temperature is favorable and it can be developed by optimizing CuO/CaO ratio and NiO/CaO ratio.
2. The oxygen capacity of CuO and NiO as oxygen carrier should be investigated in TGA cycle analysis for studying oxygen storage of oxygen carrier.
3. The support for hydrogen such as  $\text{SiO}_2$ , SBA-15, lanthanum, and zeolite are alternative supports to improve the surface area and metal dispersion that may offer a good stability.
4. The long catalyst preparation time for sol-gel method is of concern for industrial applications. It should be an interesting topic to shorten the preparation time of the sol-gel method or other preparation methods may be proposed.

## REFERENCES



จุฬาลงกรณ์มหาวิทยาลัย  
**CHULALONGKORN UNIVERSITY**

## REFERENCES

- [1] Gunduz, S. and Dogu, T. Sorption-enhanced reforming of ethanol over Ni-and Co-incorporated MCM-41 type catalysts. Industrial & Engineering Chemistry Research 51(26) (2011): 8796-8805.
- [2] Kalamaras, C.M. and Efstathiou, A.M. Hydrogen production technologies: current state and future developments. in Conference papers in science: Hindawi, 2013.
- [3] Sharma, A. and Arya, S.K. Hydrogen from Algal Biomass: A review of Production process. Biotechnology Reports 15 (2017): 63-69.
- [4] Ragauskas, A.J., Williams, C.K., Davison, B.H., Britovsek, G., Cairney, J., Eckert, C.A., Frederick, W.J., Hallett, J.P., Leak, D.J., and Liotta, C.L. The path forward for biofuels and biomaterials. Science 311(5760) (2006): 484-489.
- [5] Song, C. Overview of hydrogen production options for hydrogen energy development, fuel-cell fuel processing and mitigation of CO<sub>2</sub> emissions. in Proceedings of 20th International Pittsburgh Coal Conference, pp. 15-19, 2003.
- [6] Nikolaidis, P. and Poullikkas, A. A comparative overview of hydrogen production processes. Renewable and Sustainable Energy Reviews 67 (2017): 597-611.
- [7] Liu, W., Farrington, G., Chaput, F., and Dunn, B. Synthesis and electrochemical studies of spinel phase LiMn<sub>2</sub>O<sub>4</sub> cathode materials prepared by the Pechini process. Journal of The Electrochemical Society 143(3) (1996): 879-884.
- [8] Ptasinski, K.J. Efficiency analysis of hydrogen production methods from biomass. International Journal of Alternative Propulsion 2(1) (2008): 39-49.
- [9] Yang, S.-T., Liu, X., and Zhang, Y. Metabolic engineering–applications, methods, and challenges. in Bioprocessing for Value-Added Products from Renewable Resources, pp. 73-118: Elsevier, 2007.
- [10] Yang, S.-T. Bioprocessing–from biotechnology to biorefinery. in Bioprocessing for value-added products from renewable resources, pp. 1-24: Elsevier, 2007.
- [11] Zhou, Z., Qi, Y., Xie, M., Cheng, Z., and Yuan, W. Synthesis of CaO-based sorbents through incorporation of alumina/aluminate and their CO<sub>2</sub> capture performance. Chemical Engineering Science 74 (2012): 172-180.

- [12] Cunha, A.F., Wu, Y.-J., Li, P., Yu, J.-G., and Rodrigues, A.E. Sorption-enhanced steam reforming of ethanol on a novel K–Ni–Cu–hydrotalcite hybrid material. Industrial & Engineering Chemistry Research 53(10) (2014): 3842-3853.
- [13] Wu, G., Zhang, C., Li, S., Huang, Z., Yan, S., Wang, S., Ma, X., and Gong, J. Sorption enhanced steam reforming of ethanol on Ni–CaO–Al<sub>2</sub>O<sub>3</sub> multifunctional catalysts derived from hydrotalcite-like compounds. Energy & Environmental Science 5(10) (2012): 8942-8949.
- [14] Kirtay, E. Recent advances in production of hydrogen from biomass. Energy Conversion and Management 52(4) (2011): 1778-1789.
- [15] Phromprasit, J., Powell, J., and Assabumrungrat, S. Metals (Mg, Sr and Al) modified CaO based sorbent for CO<sub>2</sub> sorption/desorption stability in fixed bed reactor for high temperature application. Chemical Engineering Journal 284 (2016): 1212-1223.
- [16] Xue, X. and Wu, S. The microstructure and stability of a Ni-nano-CaO/Al<sub>2</sub>O<sub>3</sub> reforming catalyst under carbonation–calcination cycling conditions. International Journal of Hydrogen Energy 40(16) (2015): 5617-5623.
- [17] Wang, F. Hydrogen production from steam reforming of ethanol over an Ir/ceria-based catalyst: catalyst ageing analysis and performance improvement upon ceria doping. Université Claude Bernard-Lyon I, 2012.
- [18] Roh, H.-S., Wang, Y., King, D.L., Platon, A., and Chin, Y.-H. Low temperature and H<sub>2</sub> selective catalysts for ethanol steam reforming. Catalysis Letters 108(1-2) (2006): 15-19.
- [19] Cavallaro, S. Ethanol steam reforming on Rh/Al<sub>2</sub>O<sub>3</sub> catalysts. Energy & Fuels 14(6) (2000): 1195-1199.
- [20] Peela, N.R. and Kunzru, D. Oxidative steam reforming of ethanol over Rh based catalysts in a micro-channel reactor. International Journal of Hydrogen Energy 36(5) (2011): 3384-3396.
- [21] Frusteri, F., Freni, S., Spadaro, L., Chiodo, V., Bonura, G., Donato, S., and Cavallaro, S. H<sub>2</sub> production for MC fuel cell by steam reforming of ethanol over MgO supported Pd, Rh, Ni and Co catalysts. Catalysis Communications 5(10) (2004): 611-615.

- [22] Breen, J., Burch, R., and Coleman, H. Metal-catalysed steam reforming of ethanol in the production of hydrogen for fuel cell applications. Applied Catalysis B: Environmental 39(1) (2002): 65-74.
- [23] He, Z., Yang, M., Wang, X., Zhao, Z., and Duan, A. Effect of the transition metal oxide supports on hydrogen production from bio-ethanol reforming. Catalysis Today 194(1) (2012): 2-8.
- [24] Goula, M.A., Kontou, S.K., and Tsiakaras, P.E. Hydrogen production by ethanol steam reforming over a commercial Pd/V-Al<sub>2</sub>O<sub>3</sub> catalyst. Applied Catalysis B: Environmental 49(2) (2004): 135-144.
- [25] Aprêtre, F., Descorme, C., and Duprez, D. Bio-ethanol catalytic steam reforming over supported metal catalysts. Catalysis Communications 3(6) (2002): 263-267.
- [26] Ochoa-Fernández, E., Rønning, M., Grande, T., and Chen, D. Synthesis and CO<sub>2</sub> capture properties of nanocrystalline lithium zirconate. Chemistry of Materials 18(25) (2006): 6037-6046.
- [27] Radfarnia, H.R. and Iliuta, M.C. Application of surfactant-template technique for preparation of sodium zirconate as high temperature CO<sub>2</sub> sorbent. Separation and Purification Technology 93 (2012): 98-106.
- [28] Martínez-dlCruz, L. and Pfeiffer, H. Microstructural thermal evolution of the Na<sub>2</sub>CO<sub>3</sub> phase produced during a Na<sub>2</sub>ZrO<sub>3</sub>-CO<sub>2</sub> chemisorption process. The Journal of Physical Chemistry C 116(17) (2012): 9675-9680.
- [29] Li, Z.-s., Cai, N.-s., and Yang, J.-b. Continuous production of hydrogen from sorption-enhanced steam methane reforming in two parallel fixed-bed reactors operated in a cyclic manner. Industrial & Engineering Chemistry Research 45(26) (2006): 8788-8793.
- [30] Kim, J.-N., Ko, C.H., and Yi, K.B. Sorption enhanced hydrogen production using one-body CaO-Ca<sub>12</sub>Al<sub>14</sub>O<sub>33</sub>-Ni composite as catalytic absorbent. International Journal of Hydrogen Energy 38(14) (2013): 6072-6078.
- [31] Hu, Y., Liu, W., Peng, Y., Yang, Y., Sun, J., Chen, H., Zhou, Z., and Xu, M. One-step synthesis of highly efficient CaO-based CO<sub>2</sub> sorbent pellets via gel-casting technique. Fuel Processing Technology 160 (2017): 70-77.

- [32] Dewoolkar, K.D. and Vaidya, P.D. Tailored hydrotalcite-based hybrid materials for hydrogen production via sorption-enhanced steam reforming of ethanol. International Journal of Hydrogen Energy 41(14) (2016): 6094-6106.
- [33] Wu, Y. Sorption-Enhanced Steam Reforming of Ethanol for Hydrogen Production. Universidade do Porto (Portugal), 2014.
- [34] Lu, H., Reddy, E.P., and Smirniotis, P.G. Calcium oxide based sorbents for capture of carbon dioxide at high temperatures. Industrial & Engineering Chemistry Research 45(11) (2006): 3944-3949.
- [35] Santos, E., Alfonsín, C., Chambel, A., Fernandes, A., Dias, A.S., Pinheiro, C., and Ribeiro, M. Investigation of a stable synthetic sol-gel CaO sorbent for CO<sub>2</sub> capture. Fuel 94 (2012): 624-628.
- [36] Lu, H., Khan, A., Pratsinis, S.E., and Smirniotis, P.G. Flame-made durable doped-CaO nanosorbents for CO<sub>2</sub> capture. Energy & Fuels 23(2) (2008): 1093-1100.
- [37] Radfarnia, H.R. and Iliuta, M.C. Metal oxide-stabilized calcium oxide CO<sub>2</sub> sorbent for multicycle operation. Chemical Engineering Journal 232 (2013): 280-289.
- [38] Luo, C., Zheng, Y., Ding, N., Wu, Q., Bian, G., and Zheng, C. Development and performance of CaO/La<sub>2</sub>O<sub>3</sub> sorbents during calcium looping cycles for CO<sub>2</sub> capture. Industrial & Engineering Chemistry Research 49(22) (2010): 11778-11784.
- [39] Xu, P., Xie, M., Cheng, Z., and Zhou, Z. CO<sub>2</sub> Capture performance of CaO-based sorbents prepared by a sol-gel method. Industrial & Engineering Chemistry Research 52(34) (2013): 12161-12169.
- [40] Dietrich, W., Lawrence, P.S., Grünewald, M., and Agar, D.W. Theoretical studies on multifunctional catalysts with integrated adsorption sites. Chemical Engineering Journal 107(1-3) (2005): 103-111.
- [41] Pecharaumporn, P., Wongsakulphasatch, S., Glinrun, T., Maneedaeng, A., Hassan, Z., and Assabumrungrat, S. Synthetic CaO-based sorbent for high-temperature CO<sub>2</sub> capture in sorption-enhanced hydrogen production. International Journal of Hydrogen Energy (2018).
- [42] Hench, L.L. and West, J.K. The sol-gel process. Chemical Reviews 90(1) (1990): 33-72.

- [43] Rao, B.G., Mukherjee, D., and Reddy, B.M. Novel approaches for preparation of nanoparticles. in Nanostructures for Novel Therapy, pp. 1-36: Elsevier, 2017.
- [44] Yao, D., Yang, H., Chen, H., and Williams, P.T. Co-precipitation, impregnation and so-gel preparation of Ni catalysts for pyrolysis-catalytic steam reforming of waste plastics. Applied Catalysis B: Environmental 239 (2018): 565-577.
- [45] Zhao, C., Zhou, Z., Cheng, Z., and Fang, X. Sol-gel-derived, CaZrO<sub>3</sub>-stabilized Ni/CaO-CaZrO<sub>3</sub> bifunctional catalyst for sorption-enhanced steam methane reforming. Applied Catalysis B: Environmental 196 (2016): 16-26.
- [46] Rydén, M. and Ramos, P. H<sub>2</sub> production with CO<sub>2</sub> capture by sorption enhanced chemical-looping reforming using NiO as oxygen carrier and CaO as CO<sub>2</sub> sorbent. Fuel Processing Technology 96 (2012): 27-36.
- [47] Wang, K., Dou, B., Jiang, B., Song, Y., Zhang, C., Zhang, Q., Chen, H., and Xu, Y. Renewable hydrogen production from chemical looping steam reforming of ethanol using xCeNi/SBA-15 oxygen carriers in a fixed-bed reactor. International Journal of Hydrogen Energy 41(30) (2016): 12899-12909.
- [48] Dou, B., Zhang, H., Cui, G., Wang, Z., Jiang, B., Wang, K., Chen, H., and Xu, Y. Hydrogen production by sorption-enhanced chemical looping steam reforming of ethanol in an alternating fixed-bed reactor: Sorbent to catalyst ratio dependencies. Energy Conversion and Management 155 (2018): 243-252.
- [49] Dou, B., Zhang, H., Cui, G., Wang, Z., Jiang, B., Wang, K., Chen, H., and Xu, Y. Hydrogen production and reduction of Ni-based oxygen carriers during chemical looping steam reforming of ethanol in a fixed-bed reactor. International Journal of Hydrogen Energy 42(42) (2017): 26217-26230.
- [50] Chiu, P.-C. and Ku, Y. Chemical looping process-a novel technology for inherent CO<sub>2</sub> capture. Aerosol Air Qual. Res 12 (2012): 1421-1432.
- [51] Fernández, J., Abanades, J., Murillo, R., and Grasa, G. Conceptual design of a hydrogen production process from natural gas with CO<sub>2</sub> capture using a Ca-Cu chemical loop. International Journal of Greenhouse Gas Control 6 (2012): 126-141.

- [52] Chen, L.-C. and Lin, S.D. The ethanol steam reforming over Cu-Ni/SiO<sub>2</sub> catalysts: Effect of Cu/Ni ratio. Applied Catalysis B: Environmental 106(3-4) (2011): 639-649.
- [53] Zheng, Z., Sun, C., Dai, R., Wang, S., Wu, X., An, X., Wu, Z., and Xie, X. Ethanol steam reforming on Ni-based catalysts: effect of Cu and Fe addition on the catalytic activity and resistance to deactivation. Energy & Fuels 31(3) (2017): 3091-3100.
- [54] Westbye, A., Aranda, A., Dietzel, P., and Di Felice, L. The effect of Copper (II) oxide loading and precursor on the cyclic stability of combined mayenite based materials for calciumcopper looping technology. International Journal of Hydrogen Energy 44(25) (2019): 12604-12616.
- [55] Suryanarayana, C. and Norton, M.G. X-ray diffraction: A practical approach. Springer Science & Business Media, 2013.
- [56] Sowinska, M. In-operando hard X-ray photoelectron spectroscopy study on the resistive switching physics of H<sub>2</sub>O-based RRAM. BTU Cottbus-Senftenberg, 2014.
- [57] Wang, S., Shen, H., Fan, S., Zhao, Y., Ma, X., and Gong, J. CaO-based meshed hollow spheres for CO<sub>2</sub> capture. Chemical Engineering Science 135 (2015): 532-539.
- [58] Sayyah, M., Ito, B.R., Rostam-Abadi, M., Lu, Y., and Suslick, K.S. CaO-based sorbents for CO<sub>2</sub> capture prepared by ultrasonic spray pyrolysis. RSC Advances 3(43) (2013): 19872-19875.
- [59] Papageridis, K.N., Siakavelas, G., Charisiou, N.D., Avraam, D.G., Tzounis, L., Kousi, K., and Goula, M.A. Comparative study of Ni, Co, Cu supported on  $\gamma$ -alumina catalysts for hydrogen production via the glycerol steam reforming reaction. Fuel Processing Technology 152 (2016): 156-175.
- [60] Pirondini, L. and Dalcanale, E. Molecular recognition at the gas–solid interface: a powerful tool for chemical sensing. Chemical Society Reviews 36(5) (2007): 695-706.





## APPENDIX A

## WEIGHT HOURLY SPACE VELOCITY (WHSV)

In this part, the general definition of weight hourly space velocity (WHSV) was shown in equation (A1).

$$\text{WHSV} = \text{Gas volumetric flow rate} / \text{catalyst weight} \text{ (h}^{-1}\text{)} \quad (\text{A1})$$

Sample calculate

Total feed flow rate = 50 cm<sup>3</sup>/min

The amount of catalyst = 2 g

$$\begin{aligned} \text{WHSV} &= \frac{50 \text{ cm}^3/\text{min}}{2 \text{ g}} \times \frac{60 \text{ min}}{1 \text{ h}} \times \frac{1000 \text{ g}}{1 \text{ kg}} \times \frac{1 \text{ m}^3}{1000000 \text{ cm}^3} \times \frac{781 \text{ kg}}{\text{m}^3} \\ &= 117.15 \text{ h}^{-1} \end{aligned}$$

## APPENDIX B

## CALCULATION FOR CATALYST PREPARATION

## B.1 Calculation of metal precursor

Ni 3%wt

Ni 58.7 in  $\text{Ni}(\text{NO}_3)_2 \cdot 6\text{H}_2\text{O}$  290.81 g/molNi 0.3 in  $\text{Ni}(\text{NO}_3)_2 \cdot 6\text{H}_2\text{O}$   $\frac{0.3 \times 290.81}{58.7} = 5.124 \times 10^{-3}$  mol

## B.2 Calculation of citric acid

molar ratio of metal : citric acid equal 1.2

Citric acid =  $5.124 \times 10^{-3} \times 1.2 \times 210.14 = 1.292$  g

## B.3 Calculation of DI water

=  $\frac{6.15 \times 10^{-3} \times 50 \times 18}{0.997}$ 

= 5.55 ml

**APPENDIX C**  
**CALIBRATION CURVES**

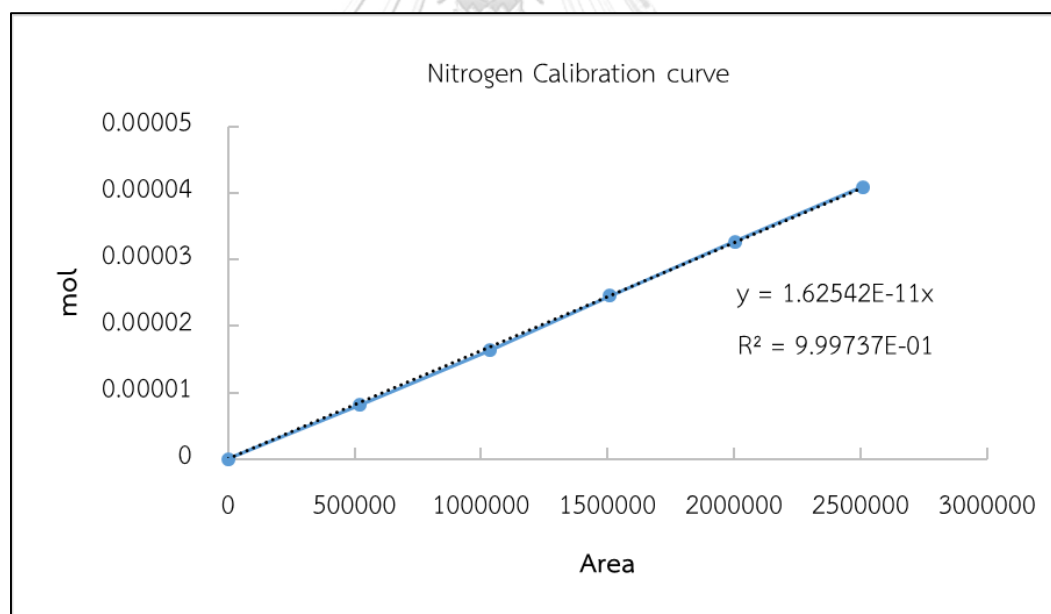
Calibration curve is done from gas chromatography (GC-8A) equipped with two columns that are Molecular Sieve and Porapak column. Table C.1 shows the operating conditions for thermal conductivity detector chromatography and table C.2 shows operating conditions of Flame ionisation detector.

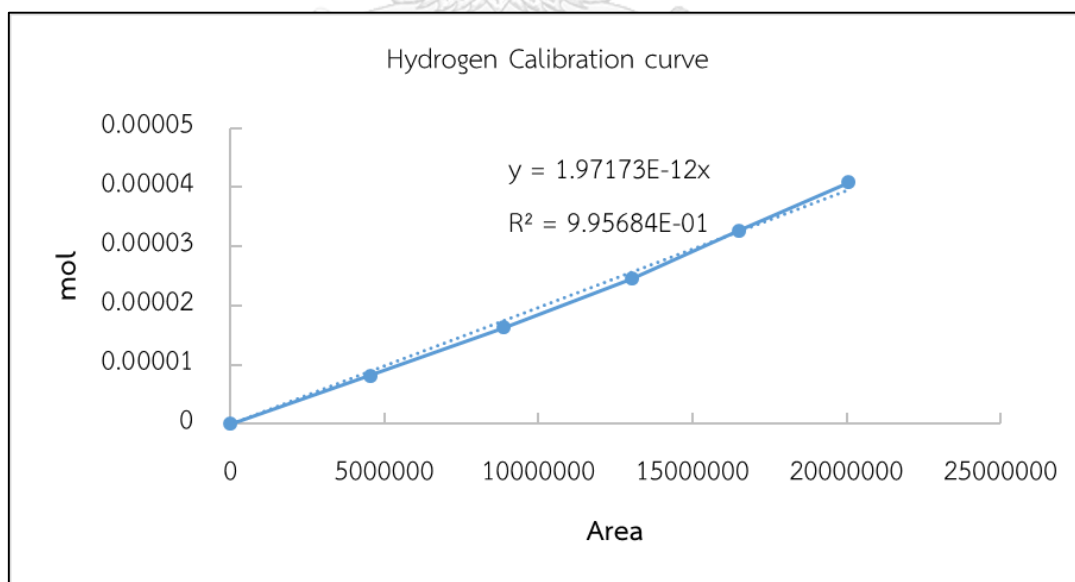
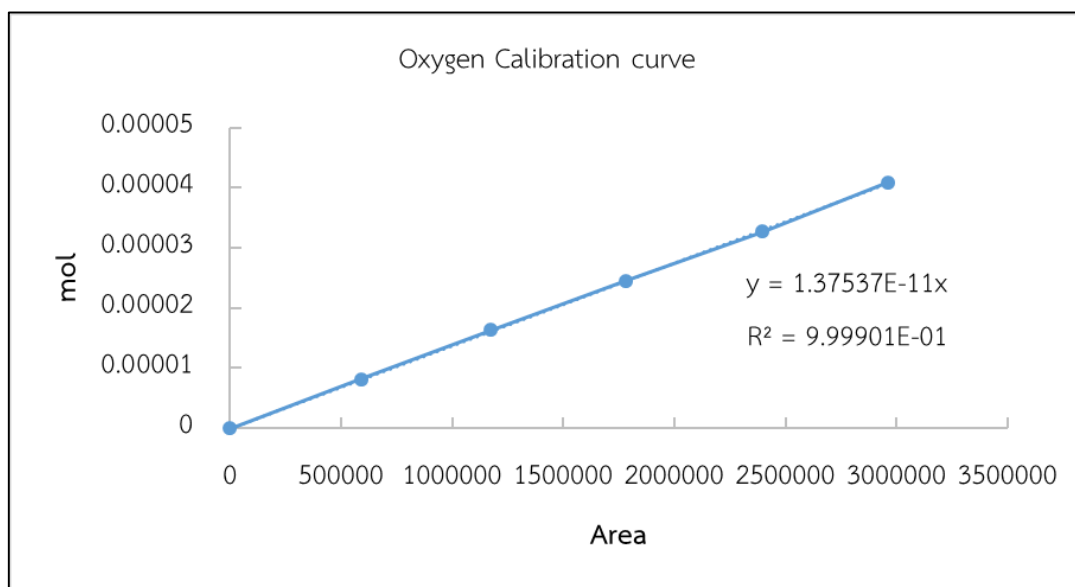
**Table C.1** Operating conditions for thermal conductivity detector chromatography

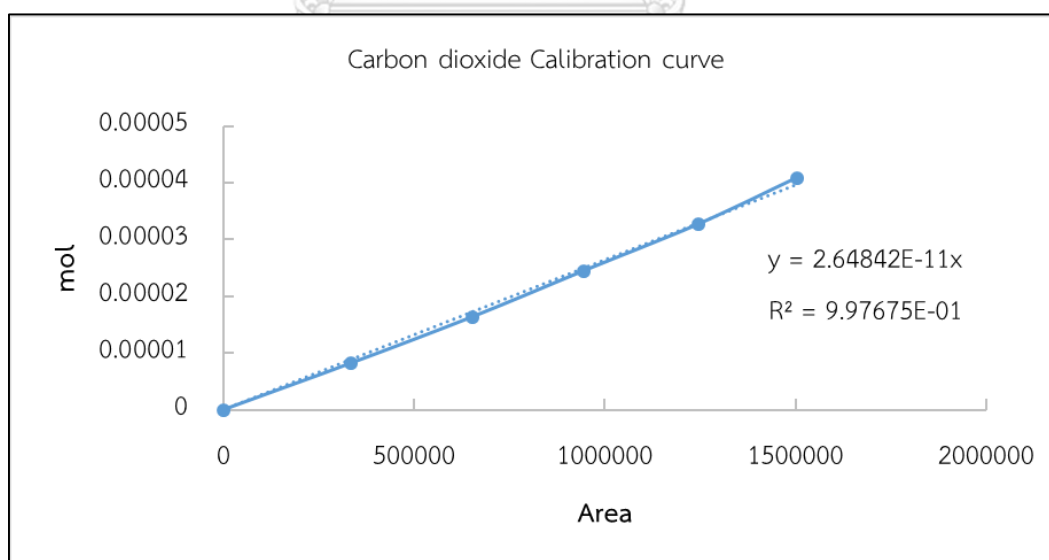
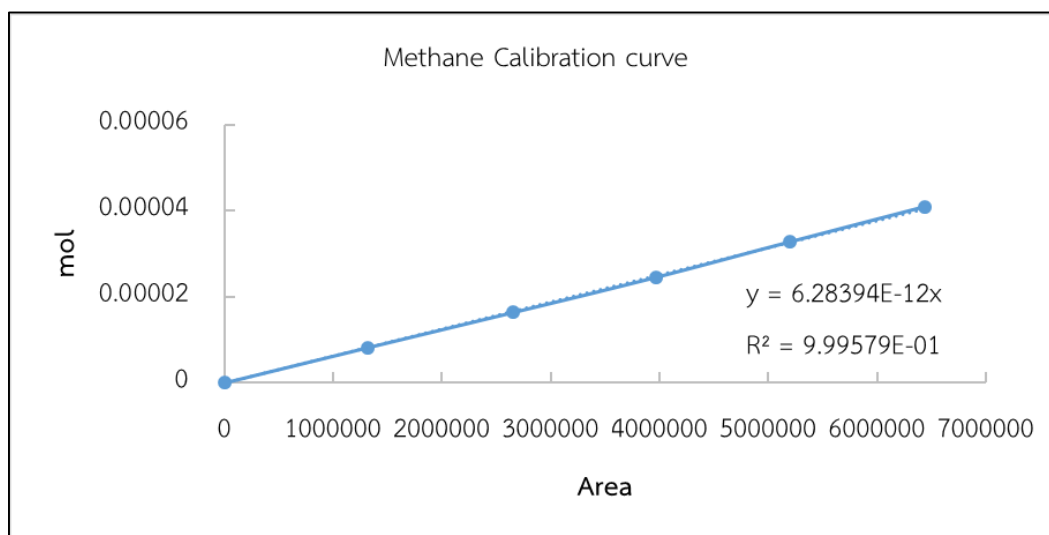
Gas Chromatography	Shimadzu GC-8A	
Detector	TCD	
Column	Molecular sieve 5A	Porapak-Q
- Column material	SUS	SUS
- Length (m)	2	2
- Outer diameter (mm)	4	4
- Inner diameter (mm)	3	3
- Mesh range	60/80	60/80
- Maximum temperature (°C)	350	350
Carrier gas	Ar (99.999%)	Ar (99.999%)
Column temperature		
- initial (°C)	50	50
- final (°C)	50	50
Injector temperature (°C)	70	70
Detector temperature (°C)	150	150
Current (mA)	70	70
Analyzed gas	N <sub>2</sub> , H <sub>2</sub> , CO, CH <sub>4</sub>	CO <sub>2</sub>

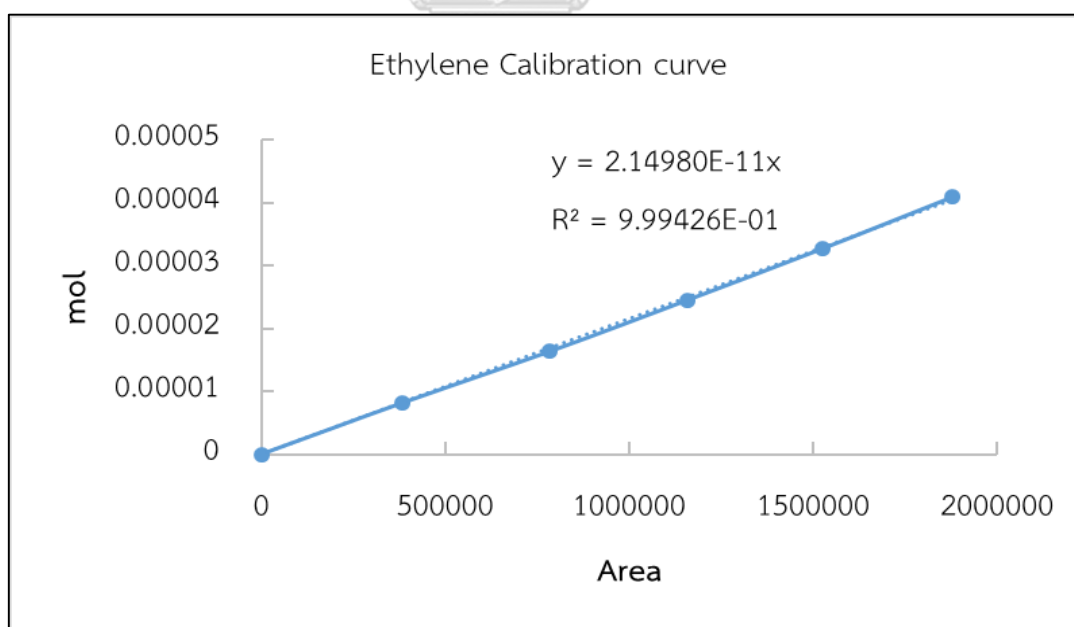
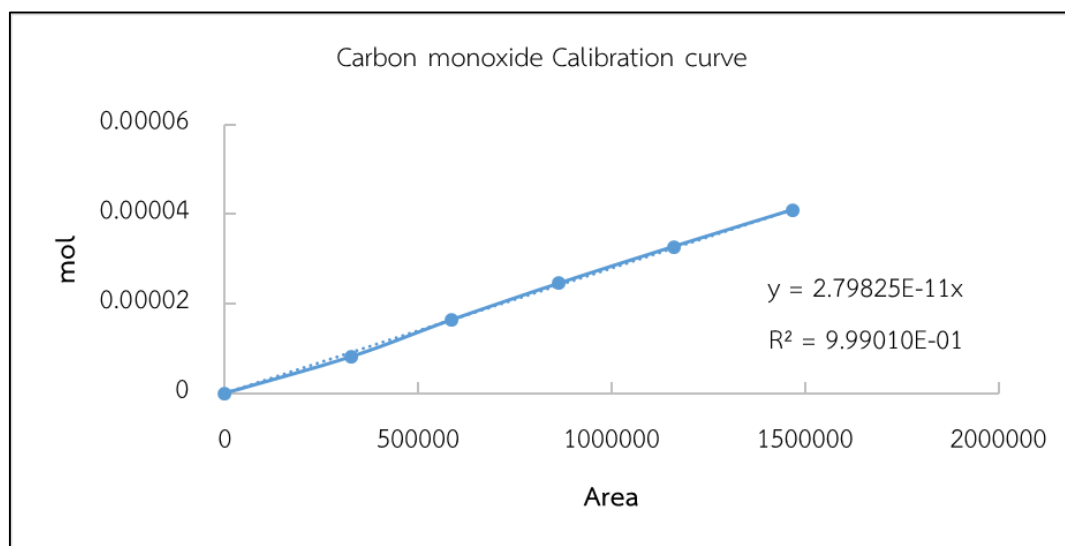
**Table C.1** Operating conditions for flame ionisation detector

Gas Chromatography	Shimadzu GC-8A
Detector	FID
Column	Inert cap WAX
- Length (m)	60
- Outer diameter (mm)	0.32
- Inner diameter (um)	1
- Maximum temperature (°C)	260
Injector temperature (°C)	180
Detector temperature (°C)	50
Analyzed gas	Ethanol

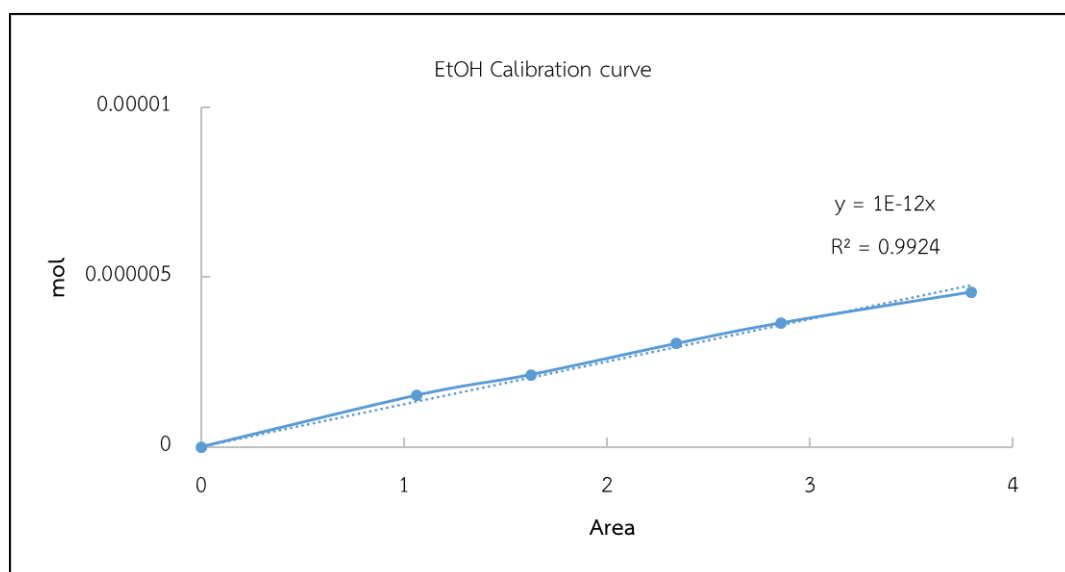












## VITA

**NAME** Talita Nimmas

**DATE OF BIRTH** 26 August 1993

**PLACE OF BIRTH** Bangkok

**INSTITUTIONS ATTENDED** Chonrasodsadornumrung School  
Khon Kaen University

**HOME ADDRESS** Chonburi

**PUBLICATION** Influence of CaO precursor on carbon dioxide capture performance and sorption-enhanced steam ethanol reforming, International Journal of Hydrogen Energy, DOI10.1016/j.ijhydene.2018.07.095